Intelligent Sliding-Mode Control for Five-DOF Active Magnetic Bearing Control System

Prof. Faa-Jeng Lin

Electric Machinery and Control Laboratory
Department of Electrical Engineering
National Central University

Outline

- Abstract
- Introduction
- System Dissection, Dynamic Analyses, and Experimental Designs of Five-DOF AMB System
  - TAMB System
  - Five-DOF AMB System
- Precise Tracking Control of TAMB System
  - Using Model-Free Control Methods
  - Using Adaptive Complementary Sliding-Mode Control
  - Using Robust Non-Singular Terminal Sliding-Mode Control
- Robust Control of Fully Suspended Five-DOF AMB System
  - Using Decentralized PID Neural Network Control
  - Using Decentralized Intelligent Double Integral Sliding-Mode Control
- Discussions and Conclusions

Abstract

- In this dissertation, a fully suspended five degree-of-freedom (DOF) AMB control system, which is composed of two radial AMBs (RAMBs) and one thrust AMB (TAMB), is developed to fulfill the requirements of the practical applications.
- The motivations of this dissertation are:

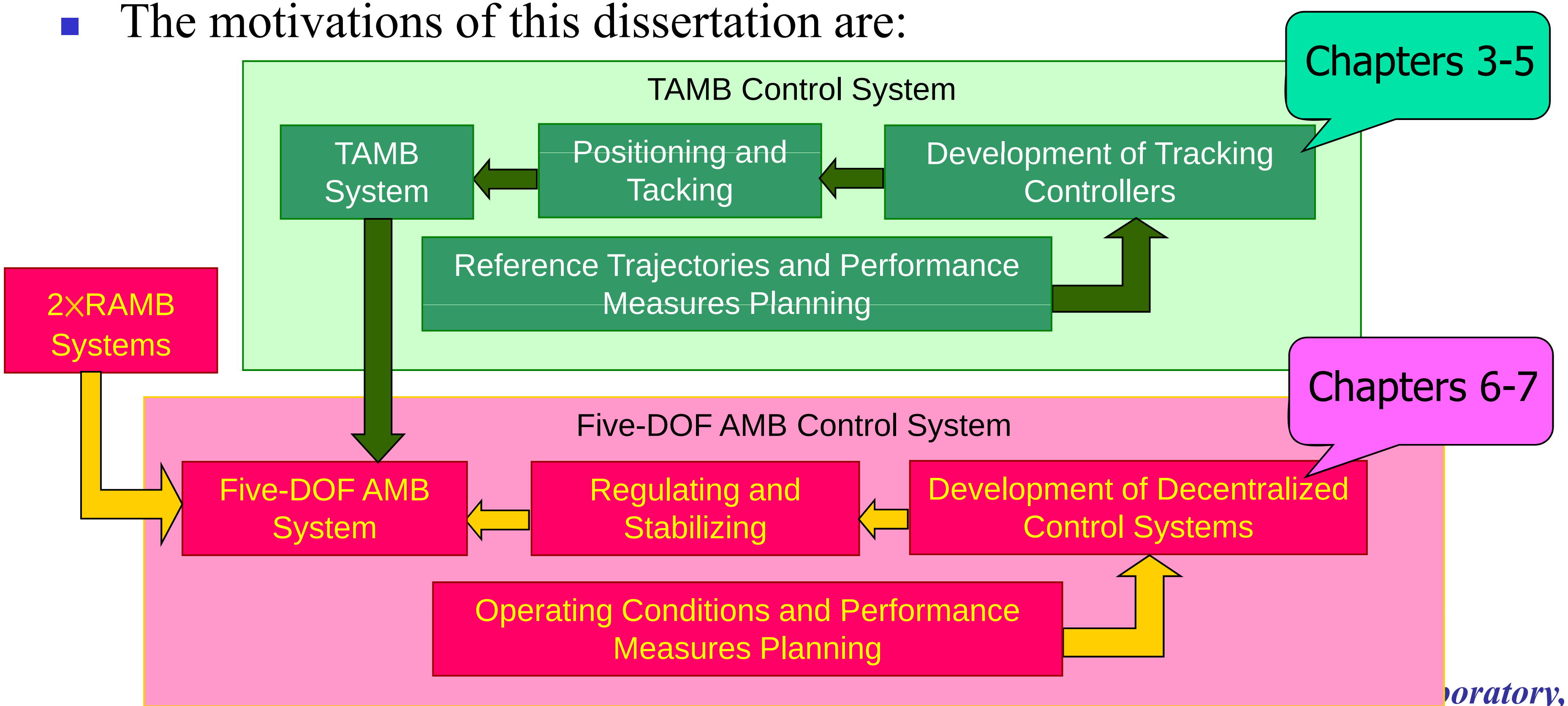

Outline

- Abstract
- Introduction
- System Dissection, Dynamic Analyses, and Experimental Designs of Five-DOF AMB System
  - TAMB System
  - Five-DOF AMB System
- Precise Tracking Control of TAMB System
  - Using Model-Free Control Methods
  - Using Adaptive Complementary Sliding-Mode Control
  - Using Robust Non-Singular Terminal Sliding-Mode Control
- Robust Control of Fully Suspended Five-DOF AMB System
  - Using Decentralized PID Neural Network Control
  - Using Decentralized Intelligent Double Integral Sliding-Mode Control
- Discussions and Conclusions

Introduction

- Magnetic suspension systems have attracted increasing attentions for many applications such as
  - Vibration isolation device
  - High-speed maglev train
  - Fast-tool servo system
  - Precision motion platform
  - Biomedical engineering

- For several kinds of the magnetic suspension systems, magnetic bearing (MB) is used to suspend and move the rotor to the predefined positions functionally by the controlled electromagnetic force *without mechanical contact and friction*.

Introduction

- MB offers many features over conventional bearings such as

Advantages:

- Contact-free, frtionless
- Elimination of the lubrication
- Ideal for clean-room operation
- Low losses and longer life
- Higher rotational speed
- Low vibration and noise
- Tolerable against heat, cold, vacuum

Disadvantages:

- High control complexity
- High initial cost

Minimum Equipments for fully suspended AMB	
Electromagnets	**10**
Position Sensors	**5**
Control Core (with 5 AD and 5 DA converters)	**1**
Power Amplifiers	**5**
Constant Current Sources	**5**

- MB can be divided into the passive MB (PMB), i.e. permanent MB, and the active MB (AMB), i.e., electromagnetic MB, mainly.
  - The term "passive" of PMB covers MBs that do not require any external current feed to the bearing.
  - The term "active" of AMB implies that bearing forces are actively controlled by means of electromagnets through a well-designed closed control loop.

Introduction

- The elements of AMB:
  - Electromagnet
  - Rotor
  - Sensor
  - Controller
  - Power Amplifier

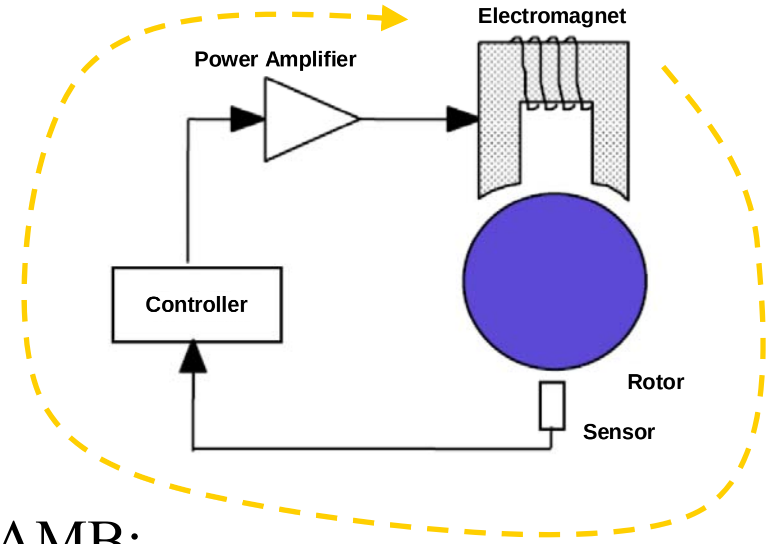

- According to its structure and usage of AMB:
  - Radial AMB (RAMB)
  - Thrust AMB (TAMB), i.e. Axial AMB
  - Combination

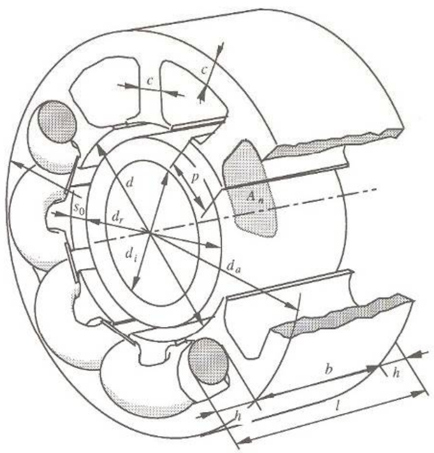

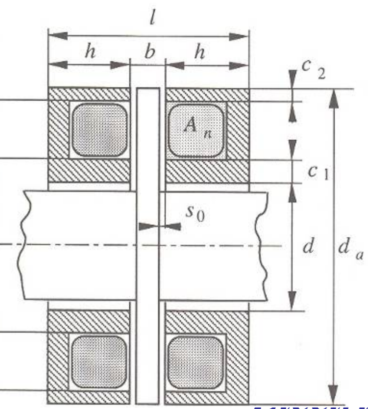

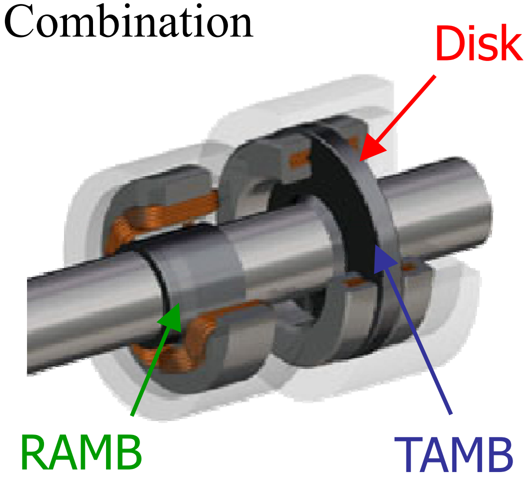

Source: Schweitzer, Waukesha

Introduction

- Various applications of AMBs:

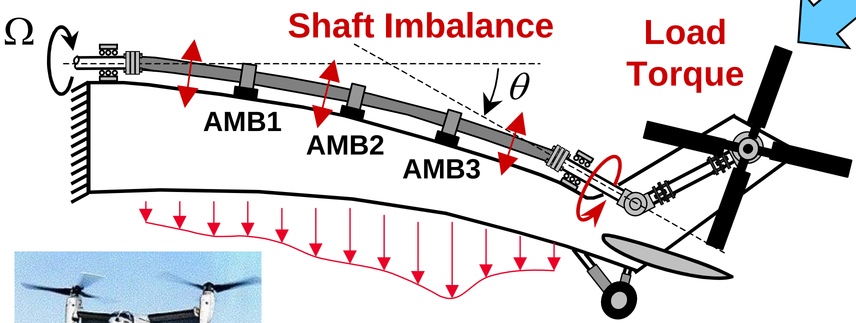

Helicopter and Tiltrotor

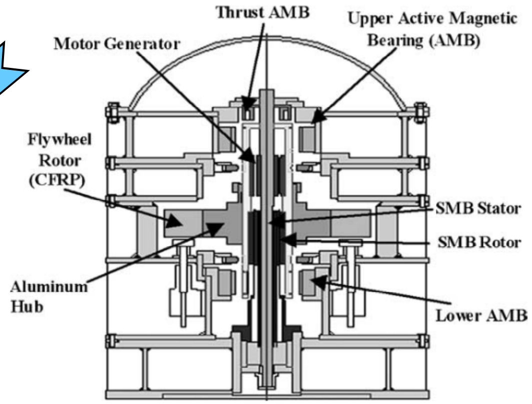

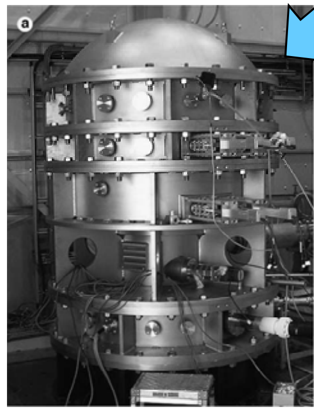

Flywheels

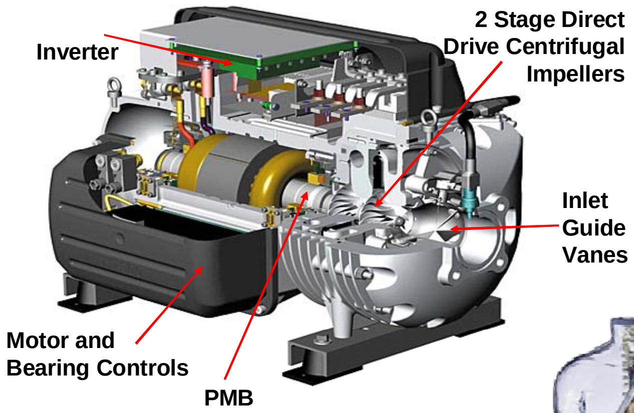

Compressor

Turbomolecular Pumps

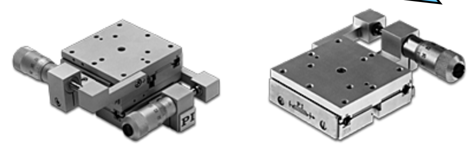

Magnetic Bearing Stage

Bearingless Motor

Hard Drive

High-Speed Spindle

Heart Pump

Vacuum Vessel

Blood Pump

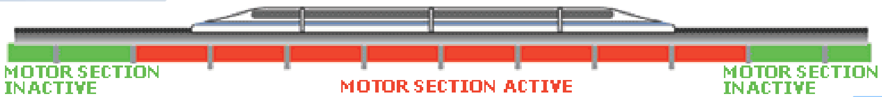

Maglev Trains

Introduction

- In the AMB system:
  - A fixed current is supplied to each electromagnet and can be referred as the ***bias current*** $\boldsymbol{i_b}$. $\boxed{(i_b \Rightarrow x_0)}$
  - A variable current is superimposed on the bias current, which is obtained by the designed controller and can be referred as the ***control current*** $\boldsymbol{i_c}$. $\boxed{(i_c \Rightarrow \triangle x)}$
- The purpose of the bias setting is to improve the linearity of the force-current relationships around the operating point ($\boldsymbol{i_b, x_0}$).
- The operating modes of the drive system which supply the currents to the electromagnets can be classified into three classes:
  - Class-A driving mode (differential driving mode, DDM);
  - Class-B driving mode;
  - Class-C driving mode.

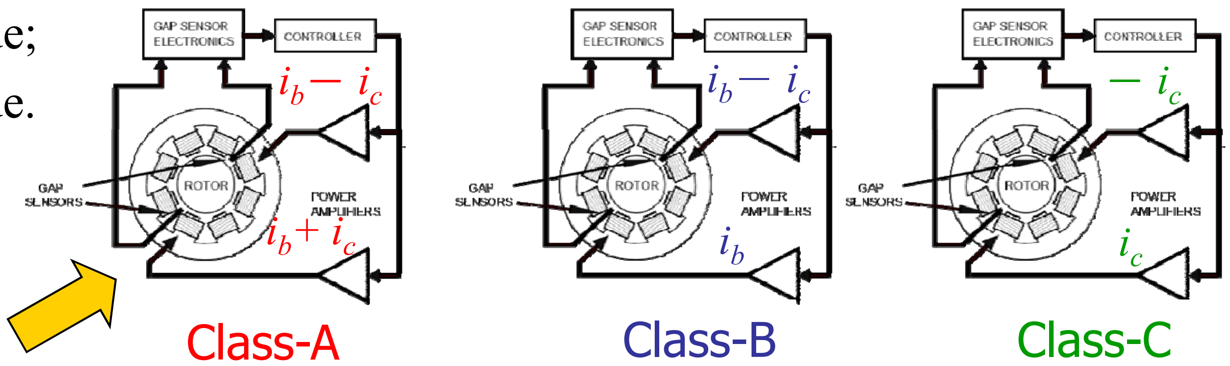

Introduction

- Comparisons of various developed AMB systems:

Refer.	System Structure	DOF	Rotor Specifics Length (mm)	Rotor Specifics Diamet. (mm)	Rotor Specifics Weight (kg)	Nominal Air Gap (mm)	Development Environment	Highest Speed (RPM)	Publication (Year)
[58]	RAMB×1 (three poles)	2	180	15	0.55	0.945	dSPACE/ MATLAB	570	IEEE Trans. Magn. (2005)
[61]	RAMB×1	2	—	—	0.125	1.6	DSP+EZLAB™ C Language	1800	Mechatronics (2003)
[63]	RAMB×2	4	442.3	—	10.78	0.5	TMS320C6701	3000	IET Contr. Theory Appl. (2007)
[68]	RAMB×2	4	—	—	1.541	—	dSPACE/ MATLAB	3200	IEEE Trans. Magn. (2005)
[69]	RAMB×2	4	625	10	1.54	0.5	Host PC×1 Target PC×1 MATLAB xPC Target	10000	Control Eng. Practice (2008)
[70]	RAMB×2 TAMB×1	5	304.8	9.5	0.98	RAMB: 0.525 TAMB: 0.783	dSPACE/ MATLAB	14000	Control Eng. Practice (2007)
[71]	RAMB×1	2	—	—	—	—	—	4800	Expert Syst. Appl. (2009)
	RAMB×2 TAMB×1	**5**	**500**	**16.6**	**Rotor: 2.565 Disk:0.5**	**RAMB: 0.4 TAMB: 0.5**	**PC×1 Visual Basic 6.0**	**4800**	**This Study (2009)**

Outline

- Abstract
- Introduction
- System Dissection, Dynamic Analyses, and Experimental Designs of Five-DOF AMB System
  - TAMB System
  - Five-DOF AMB System
- Precise Tracking Control of TAMB System
  - Using Model-Free Control Methods
  - Using Adaptive Complementary Sliding-Mode Control
  - Using Robust Non-Singular Terminal Sliding-Mode Control
- Robust Control of Fully Suspended Five-DOF AMB System
  - Using Decentralized PID Neural Network Control
  - Using Decentralized Intelligent Double Integral Sliding-Mode Control
- Discussions and Conclusions

System Dissection, Dynamic Analyses, and Experimental Designs of Five-DOF AMB System

- The fully suspended five-DOF AMB system is composed of four radial DOF controlled by two identical RAMBs and one axial DOF controlled by a TAMB.

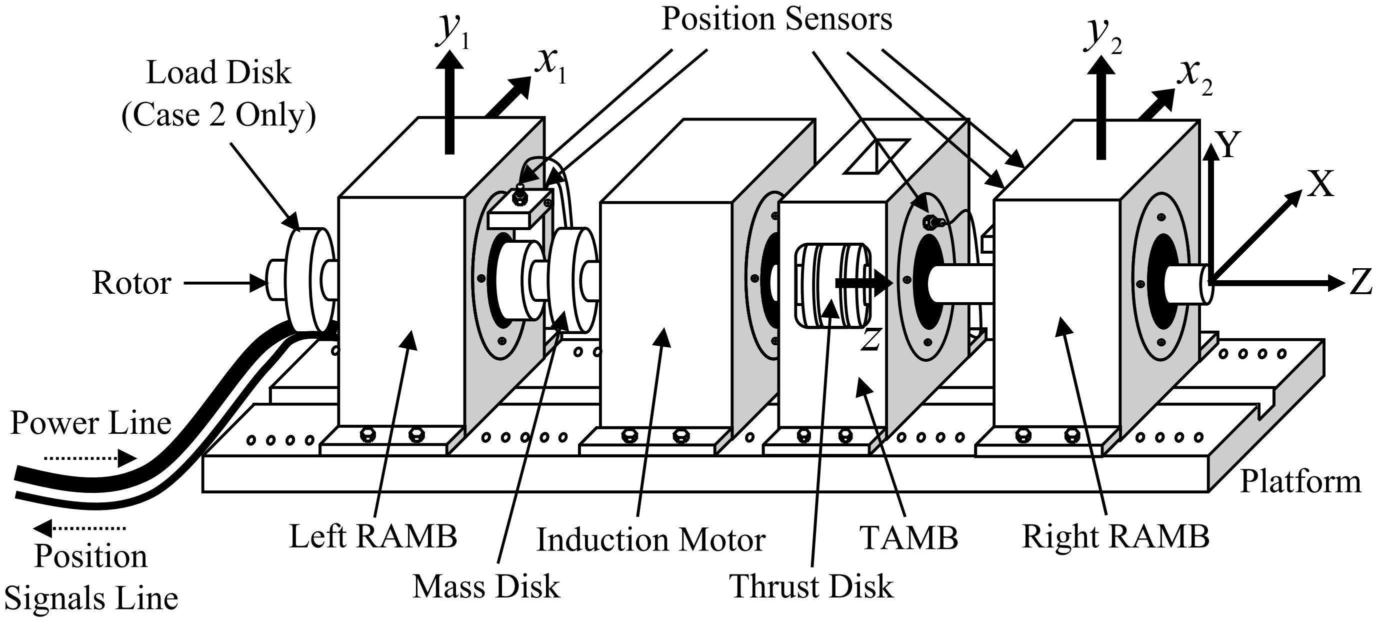

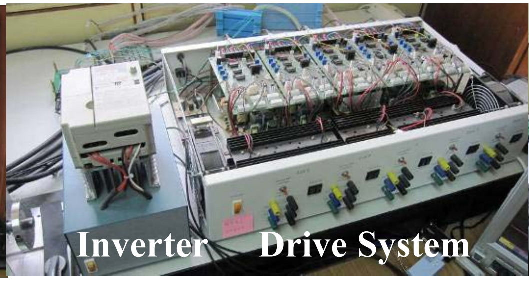

System Dissection, Dynamic Analyses, and Experimental Designs of Five-DOF AMB System

- In the case of an AMB, where iron is used in the stator and the rotor, electromagnets cause a flux Φ to circulate a magnetic loop.
- The relation of flux Φ and cross-sections A_s and A_0 can be stated as

$$\Phi = B_s A_s = B_0 A_0$$

- One can obtain the following result

$$B_0 = \frac{\Phi_0}{A} = \frac{Ni}{\left(\cancelto{0}{\frac{l_s}{\mu_s}} + \cancelto{0}{\frac{l_r}{\mu_r}} + \frac{2l_0}{\mu_0}\right)} \cong \frac{\mu_0 Ni}{2l_0}$$

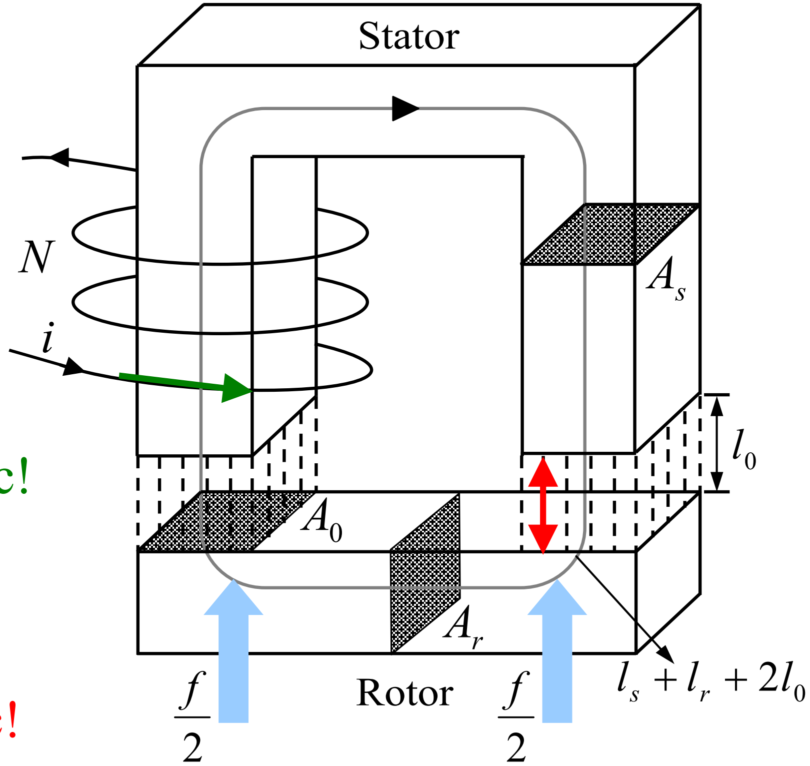

- Consider the Maxwell force

$$f = \frac{B_0^2 A_0}{\mu_0} = \frac{\mu_0 A_0 N^2 i^2}{4l_0^2} = k\frac{i^2}{l_0^2}$$

quadratic!

inversely quadratic!

where $k = \dfrac{\mu_0 A_0 N^2}{4}$

Outline

- Abstract
- Introduction
- System Dissection, Dynamic Analyses, and Experimental Designs of Five-DOF AMB System
  - TAMB System
  - Five-DOF AMB System
- Precise Tracking Control of TAMB System
  - Using Model-Free Control Methods
  - Using Adaptive Complementary Sliding-Mode Control
  - Using Robust Non-Singular Terminal Sliding-Mode Control
- Robust Control of Fully Suspended Five-DOF AMB System
  - Using Decentralized PID Neural Network Control
  - Using Decentralized Intelligent Double Integral Sliding-Mode Control
- Discussions and Conclusions

TAMB System

- A typically structure of the TAMB system is shown in Fig. 2.5. In the TAMB system, a thrust disk is embedded on the rotor and used to carry out the rotor position control on the defined axial direction practically.

How does it work?

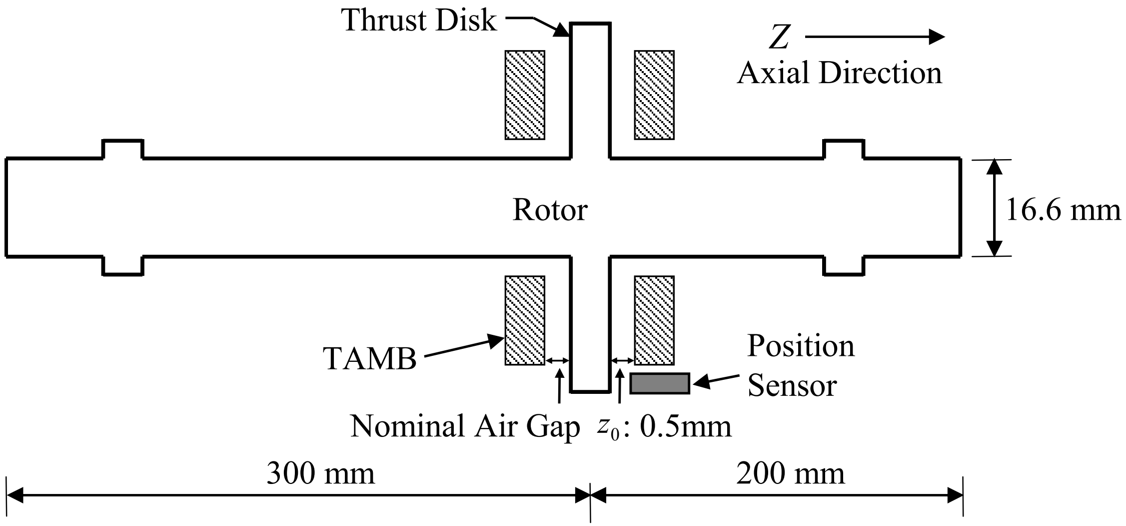

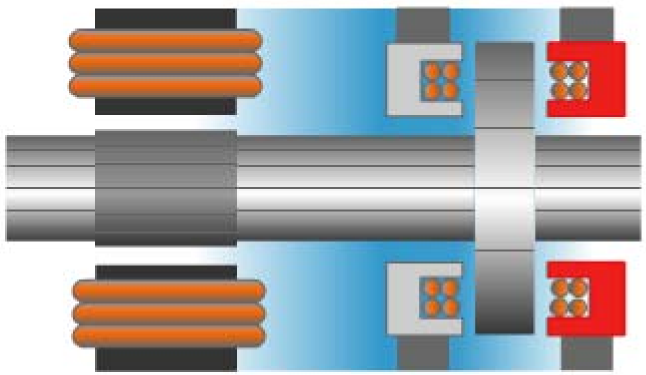

Source: S2M

Thus, it's important to develop tracking controllers for TAMB in practical applications.

TAMB System

- Drive System for TAMB System
  - A drive system including DDM and power amplifiers of TAMB is shown in Fig. 2.6 in which the dotted line or solid line of the thrust disk means that the thrust disk is centered in the air gap or deviated from the center in Z-axis, respectively.
  - The total nonlinear attractive electromagnetic forces for Z-axis is modeled as:

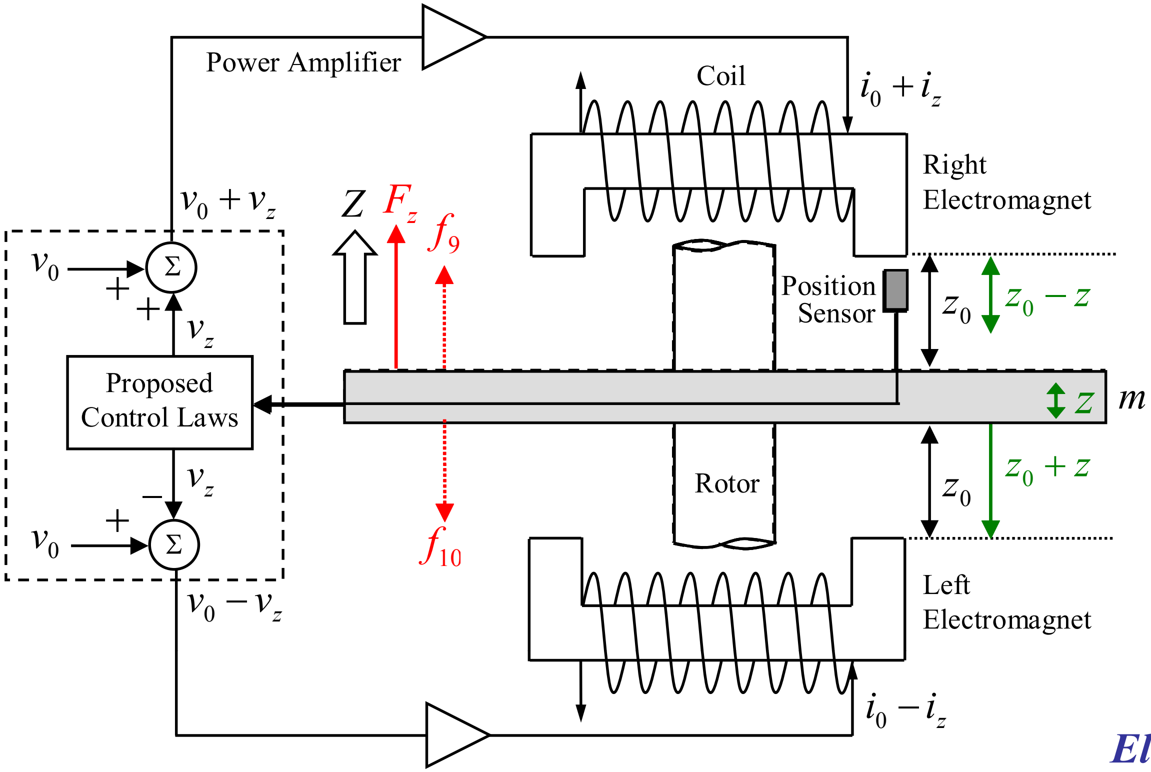

$$F_z = f_9 - f_{10}$$

$$= k_a \left[\frac{(i_0 + i_z)^2}{(z_0 - z)^2} - \frac{(i_0 - i_z)^2}{(z_0 + z)^2} \right]$$

where:

k_a: electromagnet constant of TAMB

i_0: bias current

i_b: control current

z_o: nominal air gap

z: rotor position in Z-axis

TAMB System

- Dynamic Model of TAMB System
  - Using the Newton's law, the dynamic model of the TAMB control system as shown in Fig. 2.5 can be described as follows:

    $$m\ddot{z} + c\dot{z} - f_{dz} = F_z$$

  - By taking the Taylor's expansion with respect to the nominal operating position ($z = 0,\ i_z = 0$), the nonlinear electromagnetic force can be represented by the following linearized electromagnetic force model:

    $$F_z \cong k_{ap} z + k_{ai} i_z$$

    where

    $$k_{ap} \equiv \left. \frac{\partial F_z(z, i_z)}{\partial z} \right|_{z=0,\, i_z=0} = 4k_a \frac{i_0^2}{z_0^3}$$

    $$k_{ai} \equiv \left. \frac{\partial F_z(z, i_z)}{\partial i_z} \right|_{z=0,\, i_z=0} = 4k_a \frac{i_0}{z_0^2}$$

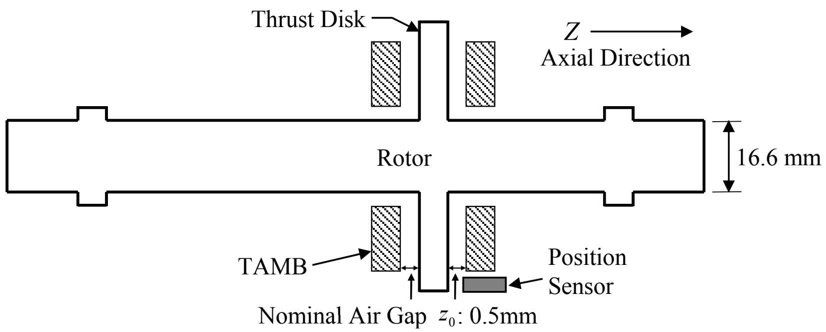

  - Now, the dynamic model of the TAMB system using the linearized electromagnetic force model can be described as follows:

    $$m\ddot{z} = -c\dot{z} + k_{ap} z + k_{ai} i_z + f_{dz}$$

TAMB System

- Experimental Design for TAMB Control System

  A. Experimental Setup

  - The experimental setup for the TAMB control system including the TAMB system, eddy-current position sensor, drive system with DDM and power amplifiers, and PC is shown in Fig. 2.10.

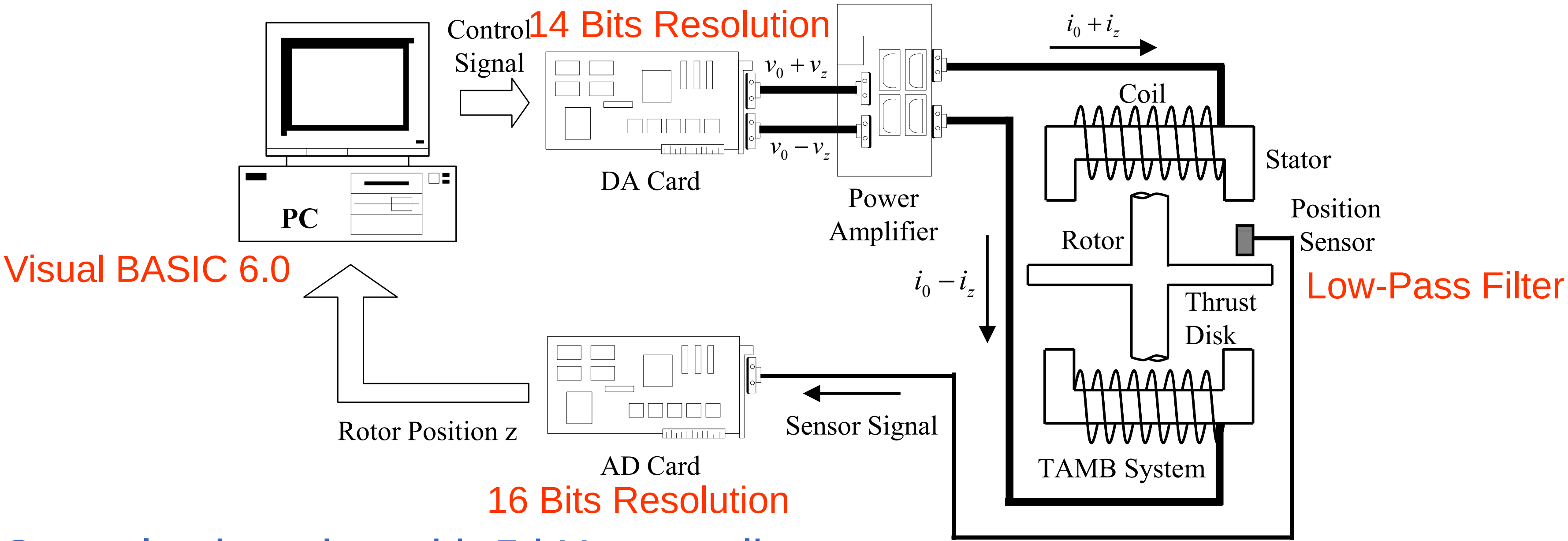

Control subroutine with 5 kHz sampling rate.

One controlled DOF requires 2 DACs.

TAMB System

B. Reference Trajectories Planning

- The designed periodic sinusoidal command can examine the smoothness of tracking responses. Moreover, the designed non-periodic trapezoidal command can verify the effectiveness of the instant and stable tracking responses.
- Two test conditions are provided which are the nominal Case (Case 1) and the parameter variation Case (Case 2). In Case 2, two stainless steel disks with respective 0.38 kg weights are added to the left and right side of the rotor.

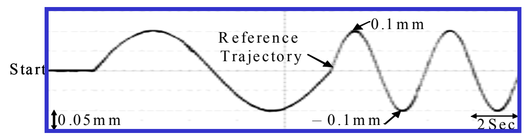

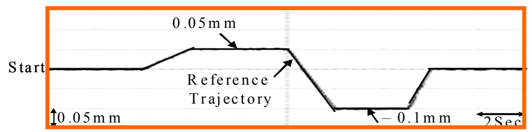

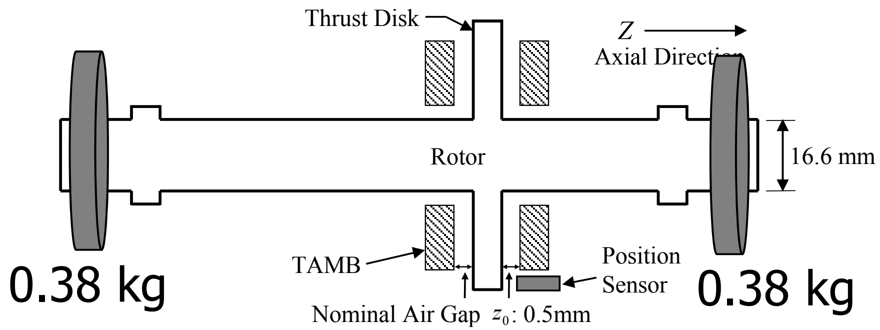

C. Performance Measures and Comparisons

- The *maximum tracking error T_M*, the average tracking error T_A and the standard deviation of the tracking error T_S for the trajectory tracking are adopted:

$$T_M = \max_n (T_e(N)), \quad \text{where} \quad T_e(N) = |z_m(N) - z(N)| \qquad T_A = \frac{\sum_{N=1}^{n} (T_e(N))}{n} \qquad T_S = \sqrt{\sum_{N=1}^{n} \frac{(T_e(N) - T_A)^2}{n}}$$

Outline

- Abstract
- Introduction
- System Dissection, Dynamic Analyses, and Experimental Designs of Five-DOF AMB System
  - TAMB System
  - Five-DOF AMB System
- Precise Tracking Control of TAMB System
  - Using Model-Free Control Methods
  - Using Adaptive Complementary Sliding-Mode Control
  - Using Robust Non-Singular Terminal Sliding-Mode Control
- Robust Control of Fully Suspended Five-DOF AMB System
  - Using Decentralized PID Neural Network Control
  - Using Decentralized Intelligent Double Integral Sliding-Mode Control
- Discussions and Conclusions

Five-DOF AMB System

- Two pairs of the U-shaped drive coils are installed perpendicularly on the stator and used to produce the perpendicular attractive electromagnetic forces.

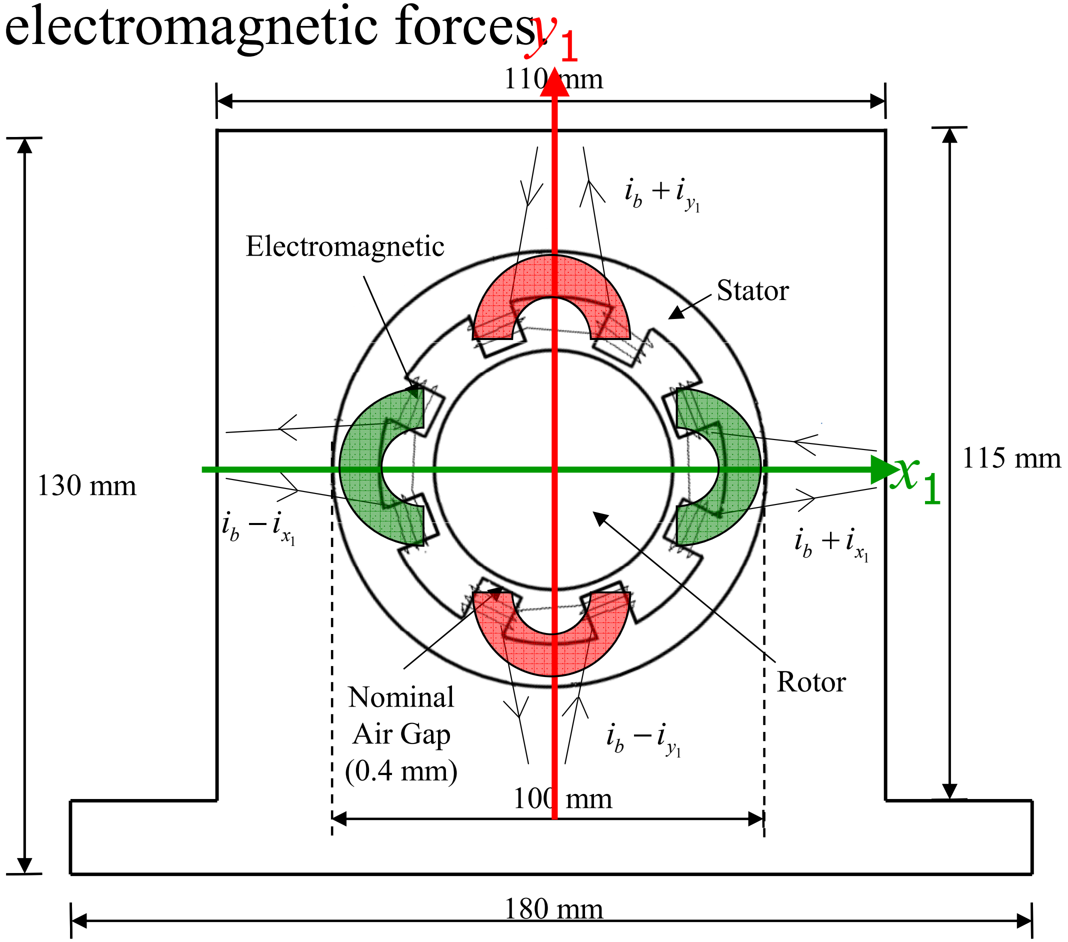

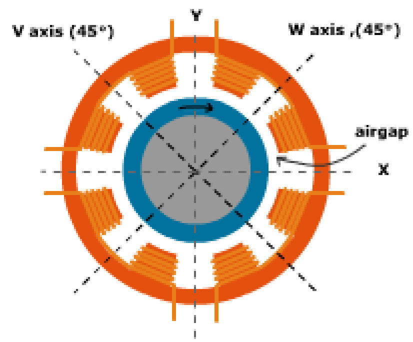

Five-DOF AMB System

- Drive System for Left RAMB
  - A drive system including DDM and power amplifiers of left RAMB is shown in Fig. 2.8 in which the dotted line or solid line of the rotor means that the rotor is centered in the aperture or deviated from the center in X-Y axes, respectively.
  - The total nonlinear attractive electromagnetic forces for X-axis and Y-axis are:

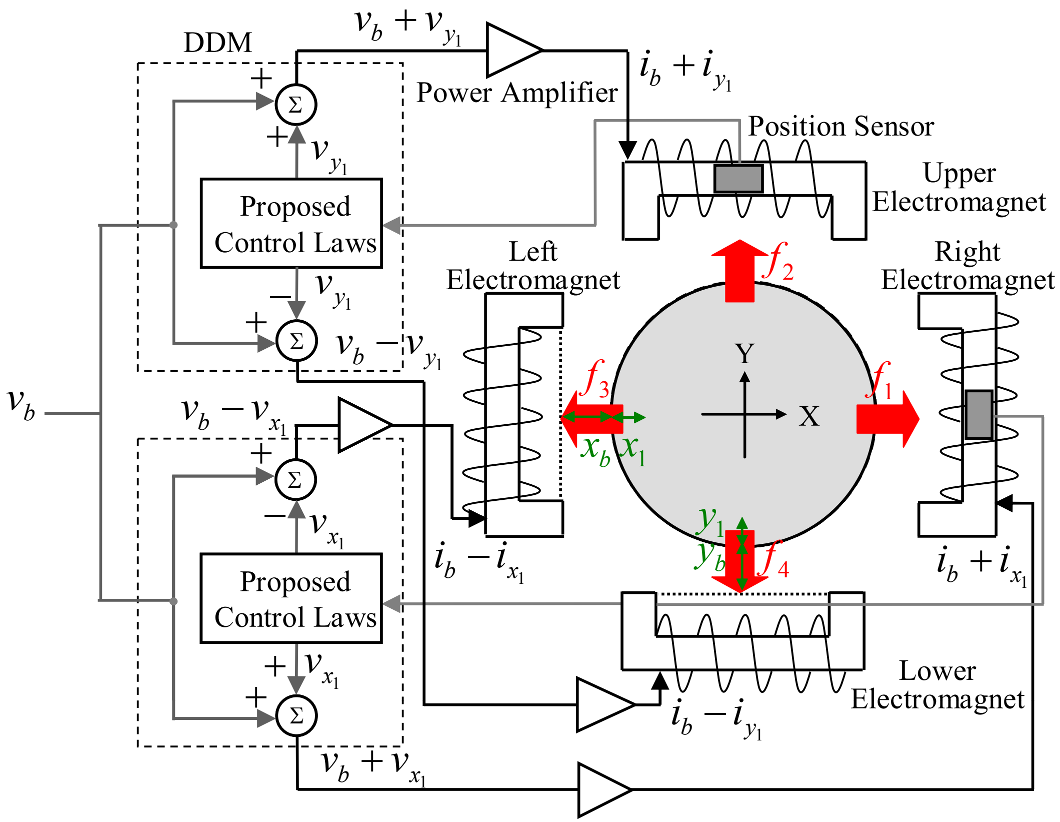

$$F_{x_1} \equiv f_1 - f_3 = k_r \left[\frac{(i_b + i_{x_1})^2}{(x_b - x_1)^2} - \frac{(i_b - i_{x_1})^2}{(x_b + x_1)^2} \right]$$

$$F_{y_1} \equiv f_2 - f_4 = k_r \left[\frac{(i_b + i_{y_1})^2}{(y_b - y_1)^2} - \frac{(i_b - i_{y_1})^2}{(y_b + y_1)^2} \right]$$

where:

k_r: electromagnet constant of RAMB

i_{x_b}, i_{y_b}: bias currents in X-Y axes

i_{x_1}, i_{y_1}: control currents in X-Y axes

x_b, y_b: nominal air gaps in X-Y axes

x_1, y_1: rotor positions in X-Y axes

Five-DOF AMB System

- Dynamic Model for Five-DOF AMB System
  - Assuming the rotor is a rigid and symmetric body, the relationship between the center of gravity (CG) of the rotor and the five-DOF AMB is shown in Fig. 2.9.
  - The linearized electromagnetic force models and the relationships between the rotor positions and the CG coordinates are approximated as:

$$
\begin{cases}
m\ddot{x}_c = F_{x_1} + F_{x_2} + f_{dx} \\
m\ddot{y}_c = F_{y_1} + F_{y_2} - mg + f_{dy} \\
m\ddot{z}_c = F_z + f_{dz} \\
J\ddot{\theta}_y - J_z\omega\dot{\theta}_x = -aF_{x_1} + bF_{x_2} + cf_{dx} \\
J\ddot{\theta}_x + J_z\omega\dot{\theta}_y = aF_{y_1} - bF_{y_2} - cf_{dy}
\end{cases}
$$

$$F_{y_2} = f_6 - f_8 \cong k_{rp}y_2 + k_{ri}i_{y_2}$$

$$F_{x_2} = f_5 - f_7 \cong k_{rp}x_2 + k_{ri}i_{x_2}$$

$$F_{y_1} = f_2 - f_4 \cong k_{rp}y_1 + k_{ri}i_{y_1}$$

$$F_{x_1} = f_1 - f_3 \cong k_{rp}x_1 + k_{ri}i_{x_1}$$

$$F_z = f_9 - f_{10} \cong k_{ap}z + k_{ai}i_z$$

the rotor is rigid and the displacements are small

$$x_c = \frac{bx_1 + ax_2}{a+b} = \frac{bx_1 + ax_2}{l}$$

$$y_c = \frac{by_1 + ay_2}{a+b} = \frac{by_1 + ay_2}{l}$$

$$\theta_x = \frac{y_1 - y_2}{a+b} = \frac{y_1 - y_2}{l}$$

$$\theta_y = \frac{x_2 - x_1}{a+b} = \frac{x_2 - x_1}{l}$$

Five-DOF AMB System

- The dynamic model describing the motion of the rotor of the five-DOF AMB system about the CG can be represented as follows

$$\begin{cases} m\ddot{x}_c = F_{x_1} + F_{x_2} + f_{dx} \\ m\ddot{y}_c = F_{y_1} + F_{y_2} - mg + f_{dy} \\ m\ddot{z}_c = F_z + f_{dz} \\ J\ddot{\theta}_y - J_z\omega\dot{\theta}_x = -aF_{x_1} + bF_{x_2} + cf_{dx} \\ J\ddot{\theta}_x + J_z\omega\dot{\theta}_y = aF_{y_1} - bF_{y_2} - cf_{dy} \end{cases}$$

the rotor is rigid and the displacements are small

$$x_c = \frac{bx_1 + ax_2}{a+b} = \frac{bx_1 + ax_2}{l} \qquad \theta_x = \frac{y_1 - y_2}{a+b} = \frac{y_1 - y_2}{l}$$

$$y_c = \frac{by_1 + ay_2}{a+b} = \frac{by_1 + ay_2}{l} \qquad \theta_y = \frac{x_2 - x_1}{a+b} = \frac{x_2 - x_1}{l}$$

- Substituting above equalities into the dynamic model of the five-DOF AMB system, the dynamic model can be represented as:

$$\begin{cases} \ddot{x}_1 + \frac{aJ_z\omega}{Jl}(\dot{y}_1 - \dot{y}_2) = \left(\frac{1}{m} + \frac{a^2}{J}\right)F_{x_1} + \left(\frac{1}{m} - \frac{ab}{J}\right)F_{x_2} + \left(\frac{1}{m} - \frac{ac}{J}\right)f_{dx} \\ \ddot{x}_2 - \frac{bJ_z\omega}{Jl}(\dot{y}_1 - \dot{y}_2) = \left(\frac{1}{m} - \frac{ab}{J}\right)F_{x_1} + \left(\frac{1}{m} + \frac{b^2}{J}\right)F_{x_2} + \left(\frac{1}{m} + \frac{bc}{J}\right)f_{dx} \\ \ddot{y}_1 + \frac{aJ_z\omega}{Jl}(\dot{x}_2 - \dot{x}_1) = \left(\frac{1}{m} + \frac{a^2}{J}\right)F_{y_1} + \left(\frac{1}{m} - \frac{ab}{J}\right)F_{y_2} + \left(\frac{1}{m} - \frac{ac}{J}\right)f_{dy} - g \\ \ddot{y}_2 - \frac{bJ_z\omega}{Jl}(\dot{x}_2 - \dot{x}_1) = \left(\frac{1}{m} - \frac{ab}{J}\right)F_{y_1} + \left(\frac{1}{m} + \frac{b^2}{J}\right)F_{y_2} + \left(\frac{1}{m} + \frac{bc}{J}\right)f_{dy} - g \\ \ddot{z} = \frac{1}{m}F_z + \frac{1}{m}f_{dz} \end{cases}$$

Five-DOF AMB System

$$F=\begin{bmatrix}F_{x_1}\\F_{x_2}\\F_{y_1}\\F_{y_2}\\F_z\end{bmatrix}=\begin{bmatrix}f_1-f_3\\f_2-f_4\\f_5-f_7\\f_6-f_8\\f_9-f_{10}\end{bmatrix}\approx\begin{bmatrix}k_{rp}x_1+k_{ri}i_{x_1}\\k_{rp}y_1+k_{ri}i_{y_1}\\k_{rp}x_2+k_{ri}i_{x_2}\\k_{rp}y_2+k_{ri}i_{y_2}\\k_{ap}z+k_{ai}i_z\end{bmatrix}$$

- The dynamic model of the five-DOF AMB system can be rearranged using the matrix form as follows:

$$\underline{M}\ddot{X}+\underline{G}\dot{X}=\underline{K}F+\underline{E}D+Cg$$

where $X=[x_1\ \ x_2\ \ y_1\ \ y_2\ \ z]^T$ is the state vector; $F=[F_{x_1}\ \ F_{x_2}\ \ F_{y_1}\ \ F_{y_2}\ \ F_z]^T$ is the electromagnetic force vector; $D=[f_{dx}\ \ f_{dy}\ \ f_{dz}]^T$ is the external disturbance vector; $C=[0\ \ 0\ \ -1\ \ -1\ \ 0]^T$ is the gravity vector; $\underline{M}$, $\underline{G}$, $\underline{K}$, and $\underline{E}$ are the mass, gyroscope, electromagnetic force, and external disturbance matrixes, respectively, and defined as follows:

$$\underline{M}=\begin{bmatrix}1&0&0&0&0\\0&1&0&0&0\\0&0&1&0&0\\0&0&0&1&0\\0&0&0&0&1\end{bmatrix}\quad \underline{G}=\begin{bmatrix}0&0&\alpha_1&-\alpha_1&0\\0&0&-\alpha_2&\alpha_2&0\\-\alpha_1&\alpha_1&0&0&0\\\alpha_2&-\alpha_2&0&0&0\\0&0&0&0&0\end{bmatrix}\quad \underline{K}=\begin{bmatrix}\beta_1&\beta_2&0&0&0\\\beta_2&\beta_3&0&0&0\\0&0&\beta_1&\beta_2&0\\0&0&\beta_2&\beta_3&0\\0&0&0&0&\beta_4\end{bmatrix}\quad \underline{E}=\begin{bmatrix}\gamma_1&0&0\\\gamma_2&0&0\\0&\gamma_1&0\\0&\gamma_2&0\\0&0&\gamma_3\end{bmatrix}$$

where $\alpha_1=\dfrac{aJ_z\omega}{Jl}$, $\alpha_2=\dfrac{bJ_z\omega}{Jl}$, $\beta_1=\dfrac{1}{m}+\dfrac{a^2}{J}$, $\beta_2=\dfrac{1}{m}-\dfrac{ab}{J}$, $\beta_3=\dfrac{1}{m}+\dfrac{b^2}{J}$, $\beta_4=\dfrac{1}{m}$,

$\gamma_1=\dfrac{1}{m}-\dfrac{ac}{J}$, $\gamma_2=\dfrac{1}{m}+\dfrac{bc}{J}$, $\gamma_3=\dfrac{1}{m}$.

- Observing the matrixes $\underline{G}$ and $\underline{K}$, the coupling effects in the five-DOF AMB system are serious apparently.

Five-DOF AMB System

- To decouple the original coupled dynamic model as five independent subsystems for the purpose of decentralized control, the dynamic model can be further rewritten as

$$\underline{M}\ddot{X} = \underline{A}X + \underline{B}U + \underline{M}H$$

where $U = \begin{bmatrix} i_{x_1} & i_{x_2} & i_{y_1} & i_{y_2} & i_z \end{bmatrix}^T$ is the control current vector; $H = \begin{bmatrix} h_{x_1} & h_{x_2} & h_{y_1} & h_{y_2} & h_z \end{bmatrix}^T$ is the decoupled term vector; $\underline{A}$ and $\underline{B}$ are the stiffness, and control gain matrixes, respectively, and defined as follows:

$$\underline{A} = \begin{bmatrix} k_{rp}\beta_1 & 0 & 0 & 0 & 0 \\ 0 & k_{rp}\beta_3 & 0 & 0 & 0 \\ 0 & 0 & k_{rp}\beta_1 & 0 & 0 \\ 0 & 0 & 0 & k_{rp}\beta_3 & 0 \\ 0 & 0 & 0 & 0 & k_{ap}\beta_4 \end{bmatrix} \quad \underline{B} = \begin{bmatrix} k_{ri}\beta_1 & 0 & 0 & 0 & 0 \\ 0 & k_{ri}\beta_3 & 0 & 0 & 0 \\ 0 & 0 & k_{ri}\beta_1 & 0 & 0 \\ 0 & 0 & 0 & k_{ri}\beta_3 & 0 \\ 0 & 0 & 0 & 0 & k_{ai}\beta_4 \end{bmatrix}$$

$$H = \begin{bmatrix} h_{x_1} \\ h_{x_2} \\ h_{y_1} \\ h_{y_2} \\ h_z \end{bmatrix} = \begin{bmatrix} -\alpha_1\dot{y}_1 + \alpha_1\dot{y}_2 + 2k_{rp}\beta_2 x_2 + 2k_{ri}\beta_2 i_{x_2} + \gamma_1 f_{dx} \\ \alpha_2\dot{y}_1 - \alpha_2\dot{y}_2 + 2k_{rp}\beta_2 x_1 + 2k_{ri}\beta_2 i_{x_1} + \gamma_2 f_{dx} \\ \alpha_1\dot{x}_1 - \alpha_1\dot{x}_2 + 2k_{rp}\beta_2 y_2 + 2k_{ri}\beta_2 i_{y_2} + \gamma_1 f_{dy} - g \\ -\alpha_2\dot{x}_1 + \alpha_2\dot{x}_2 + 2k_{rp}\beta_2 y_1 + 2k_{ri}\beta_2 i_{y_1} + \gamma_2 f_{dy} - g \\ \gamma_3 f_{dz} \end{bmatrix}$$

- Hence, the states of the dynamic model are completely decoupled. Therefore the developed decentralized model-based control systems can be easily applied

Five-DOF AMB System

- Experimental Design for Five-DOF AMB Control System

A. Experimental Setup

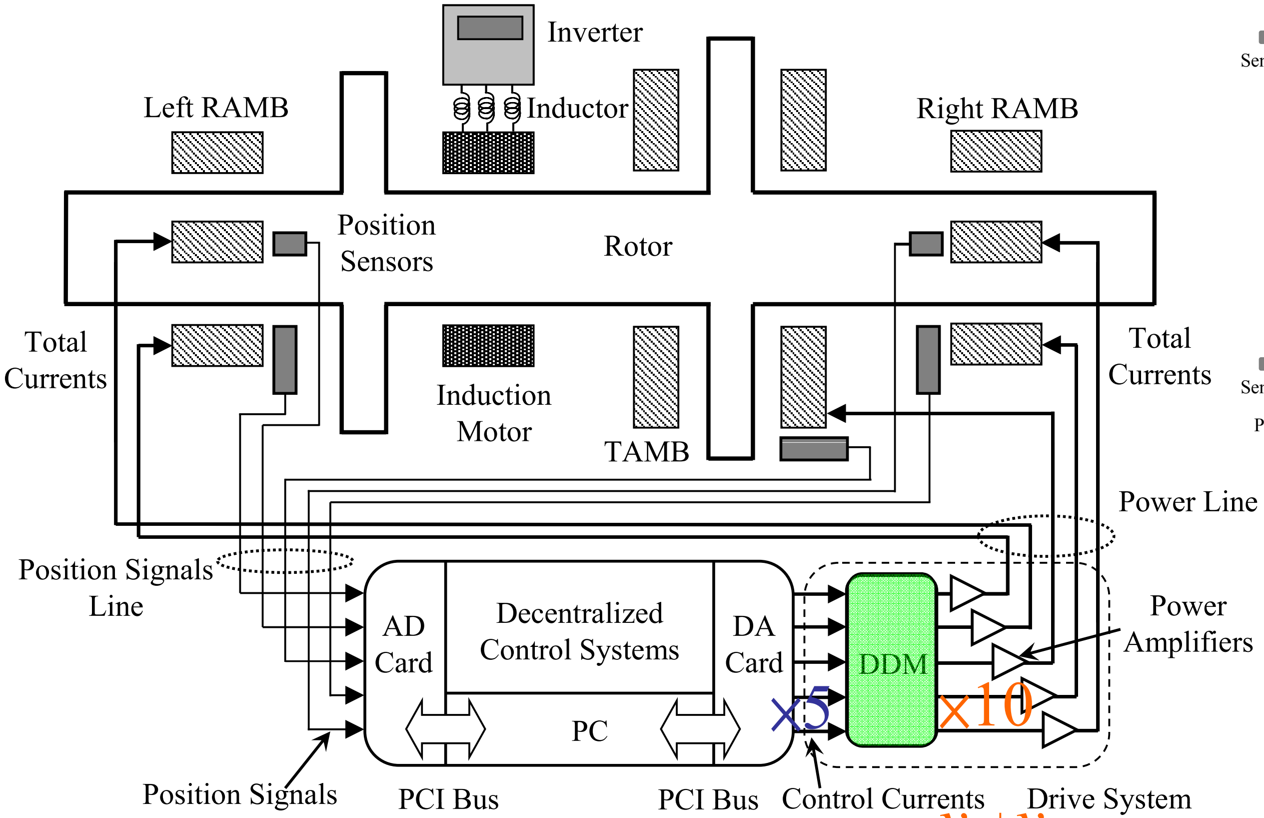

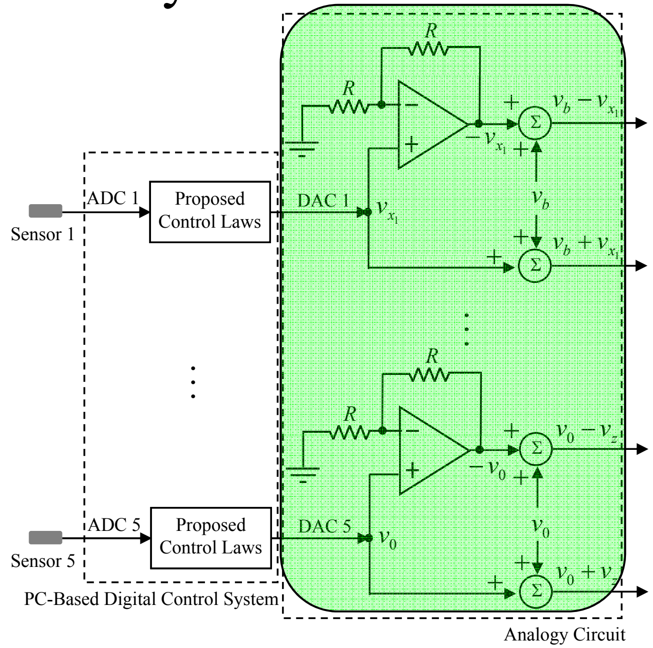

v_{x1} $\quad$ v_b+v_{x1}

v_b-v_{x1}

Control subroutine with 4 kHz sampling rate

Five-DOF AMB System

- Five-DOF Control with Independent Loops:

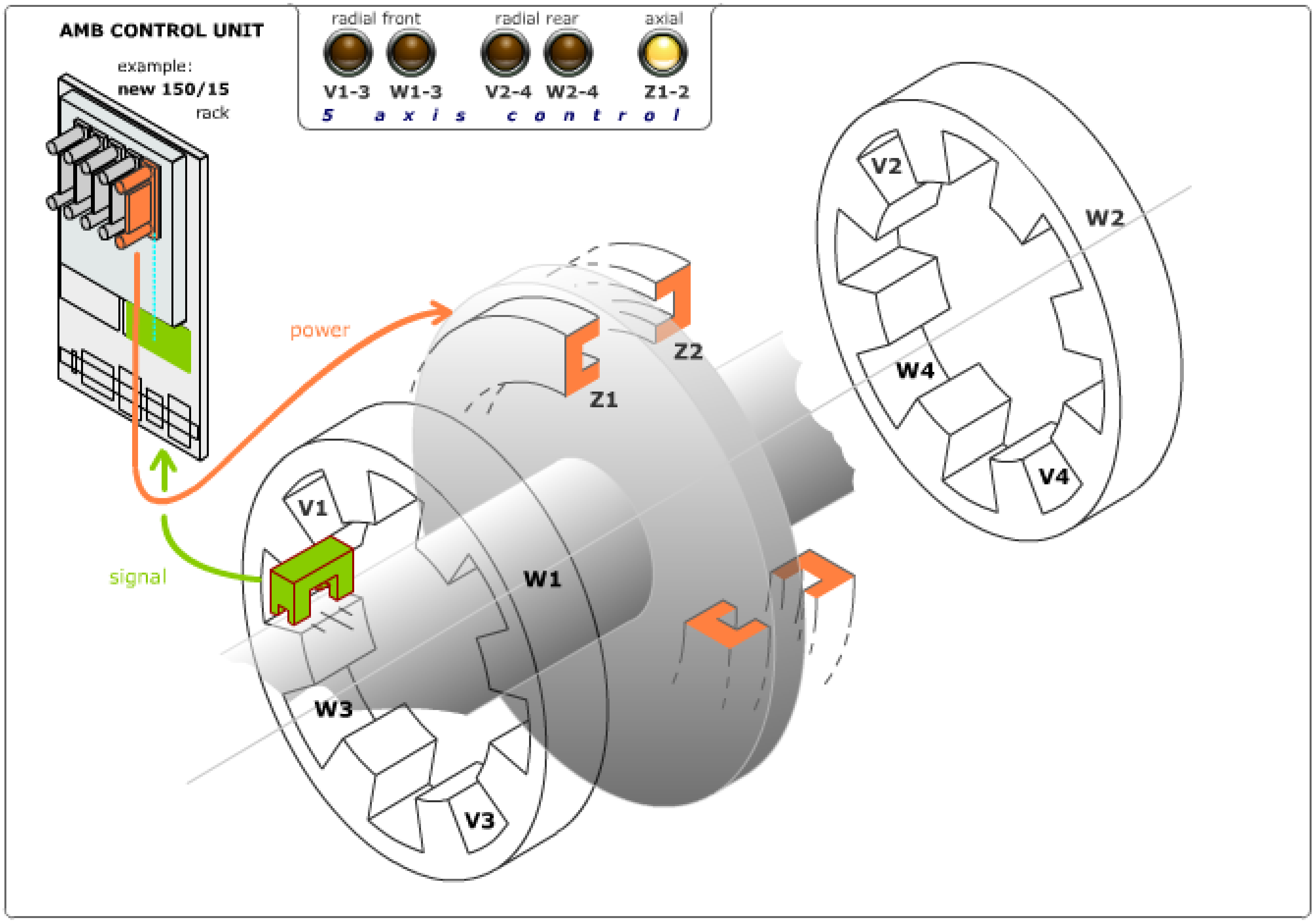

Source: S2M

Five-DOF AMB System

B. Operating Conditions Planning

	Rotating Speed (RPM)	Load (kg)
Case 1: General Operating Condition	2400	none
Case 2: Parameter Variation Condition	2400	0.38
Case 3: High Rotating Speed Condition	4800	none

- It is noted that since the adopted rotor are relative large-scale size with longer length and heavier weight comparing with the others, the rotor speed 4800RPM is a relative high speed especially that five-DOF are controlled simultaneously.

C. Performance Measures and Comparisons

- To measure the control performances, the root mean square (RMS) value $T_{R\Phi}$ and peak to peak value $T_{P\Phi}$ of regulating errors are defined as follows:

$$T_{R\phi} = \sqrt{\frac{\sum_{N=1}^{n} [\phi(N)]^2}{n}} \;;$$

$$T_{P\phi} = m_\phi - s_\phi \text{ where } m_\phi = \max_N(\phi(N)), \; s_\phi = \min_N(\phi(N));$$

Φ can be x_1, x_2, y_1, y_2, and z.

Outline

- Abstract
- Introduction
- System Dissection, Dynamic Analyses, and Experimental Designs of Five-DOF AMB System
  - TAMB System
  - Five-DOF AMB System
- Precise Tracking Control of TAMB System
  - Using Model-Free Control Methods
  - Using Adaptive Complementary Sliding-Mode Control
  - Using Robust Non-Singular Terminal Sliding-Mode Control
- Robust Control of Fully Suspended Five-DOF AMB System
  - Using Decentralized PID Neural Network Control
  - Using Decentralized Intelligent Double Integral Sliding-Mode Control
- Discussions and Conclusions

Precise Tracking Control of TAMB System— Using PID and RNN controls

- According to the regulation of control currents, the rotor position on the axial direction of a TAMB system can be controlled for the tracking of various reference trajectories.

A. PID Control

$$u(t) = K_P e(t) + K_I \int_0^{\tau} e(t) d\tau + K_D \dot{e}(t)$$

B. RNN Control

$$\Delta W_{ij}^1 = -\eta_{W^1}^R \frac{\partial E}{\partial y_o} \frac{\partial y_o}{\partial net_o^3} \frac{\partial net_o^3}{\partial W_{ij}^1}$$

$$= \eta_{W^1}^R \delta_o W_j^2 \Gamma_j [1 - \Gamma_j] x_i$$

$$\Delta W_j^2 = -\eta_{W^2}^R \frac{\partial E}{\partial y_o} \frac{\partial y_o}{\partial net_o^3} \frac{\partial net_o^3}{\partial W_j^2}$$

$$= \eta_{W^2}^R \delta_o \Gamma_j$$

$$\delta_o \cong (z_m - z) + (\dot{z}_m - \dot{z}) = e + \dot{e}$$

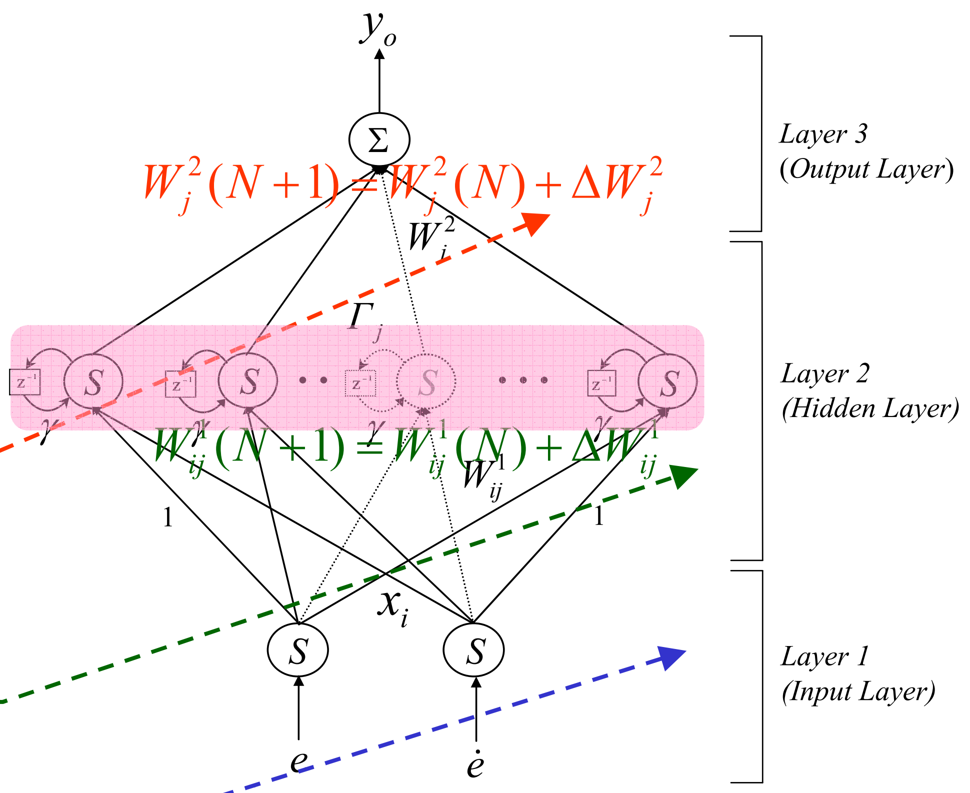

Supervised Control

C. HPBRNN Control

- All the activation functions of hidden neurons use different orthonormal Hermite polynomial basis function (OHPBF).
- The feedback of the output layer with self-connections is added to improve the convergence speed and precision.

$$H_1(t) = 1$$
$$H_2(t) = 2t$$
$$\vdots$$
$$H_n(t) = 2tH_{n-1}(t) - 2(n-1)H_{n-2}(t),\ n \geq 3$$

$$h_j(t) = \frac{1}{\sqrt{2^j j! \sqrt{\pi}}} e^{-\frac{t^2}{2}} H_j(t)$$

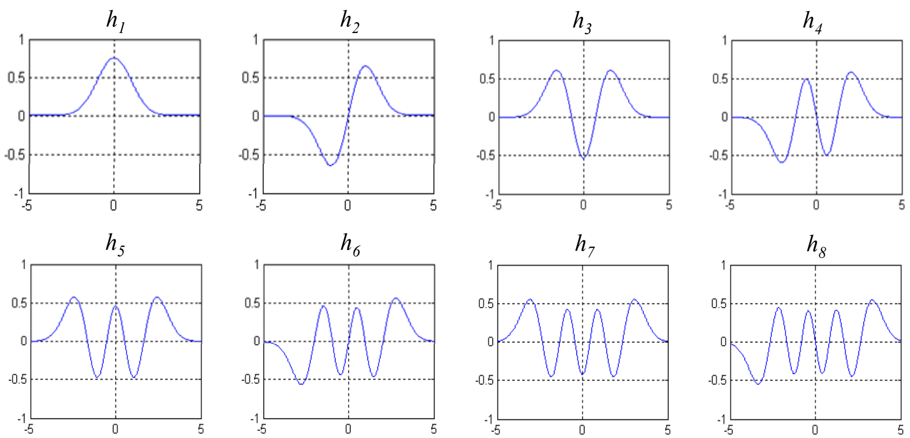

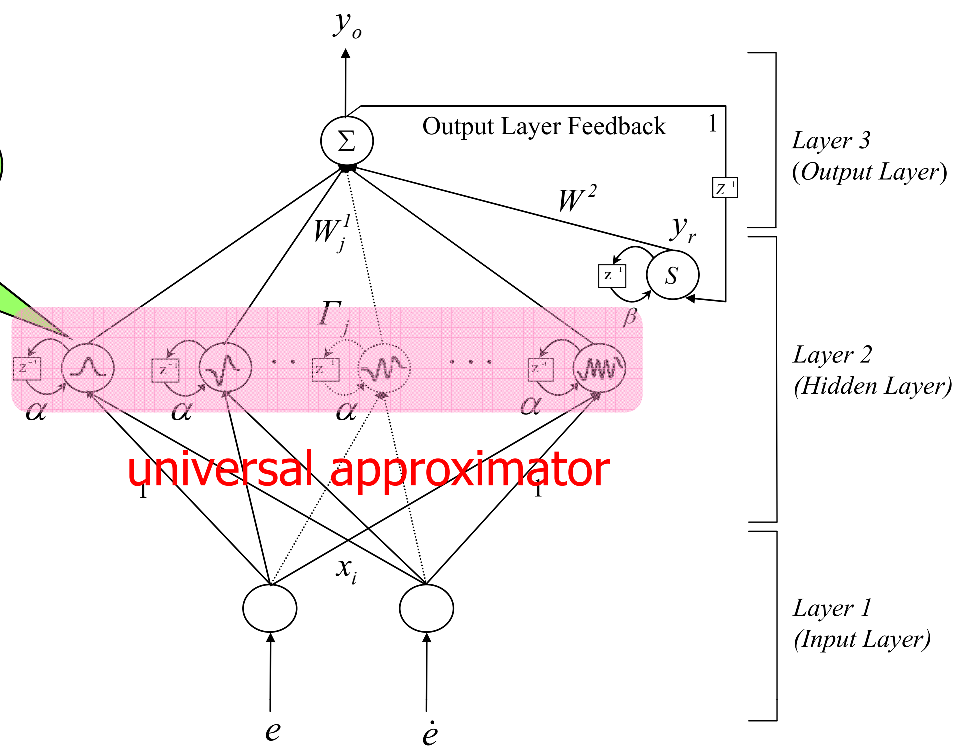

Precise Tracking Control of TAMB System—Using HPBRNN Control

- To obtain the leaning algorithm for the HPBRNN, the BP learning rule is also adopted here.

$$\Delta W_j^1 = -\eta_{W^1}^H \frac{\partial E}{\partial W_j^1} = -\eta_{W^1}^H \frac{\partial E}{\partial y_o} \frac{\partial y_o}{\partial net_o^3} \frac{\partial net_o^3}{\partial W_j^1} = \eta_{W^1}^H \delta_o \Gamma_j$$

$$E(N+1) < E(N)$$

$$\Delta W^2 = -\eta_{W^2}^H \frac{\partial E}{\partial W^2} = -\eta_{W^2}^H \frac{\partial E}{\partial y_o} \frac{\partial y_o}{\partial net_o^3} \frac{\partial net_o^3}{\partial W^2} = \eta_{W^2}^H \delta_o y_r$$

- The varied learning rates, which guarantee the convergence of the tracking error based on the analyses of a discrete-type Lyapunov function, are derived as follows:

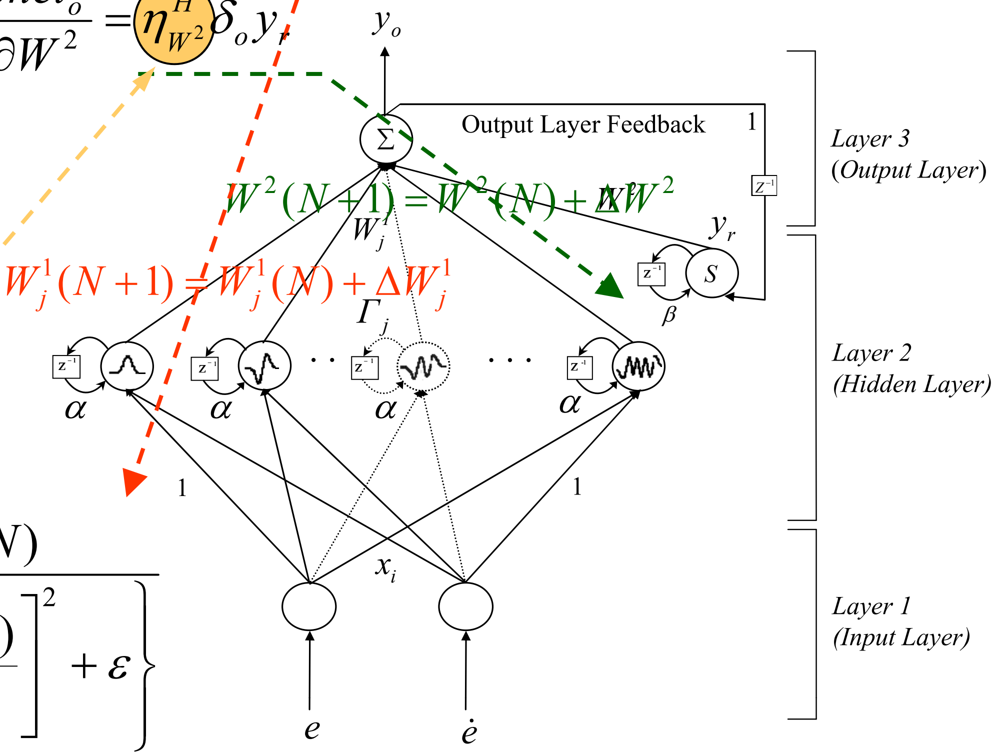

$$\eta_{W^1}^H = \frac{E(N)}{2\left\{\sum_{j=1}^{n}\left[\frac{\partial E(N)}{\partial W_j^1}\right]^2 + \varepsilon\right\}} \qquad \eta_{W^2}^H = \frac{E(N)}{2\left\{\left[\frac{\partial E(N)}{\partial W^2}\right]^2 + \varepsilon\right\}}$$

Precise Tracking Control of TAMB System—Using HPBRNN Control

D. Comparison of RNN and HPBRNN

- The proposed HPBRNN can perform better function approximation due to its activation functions with different OHPBFs.

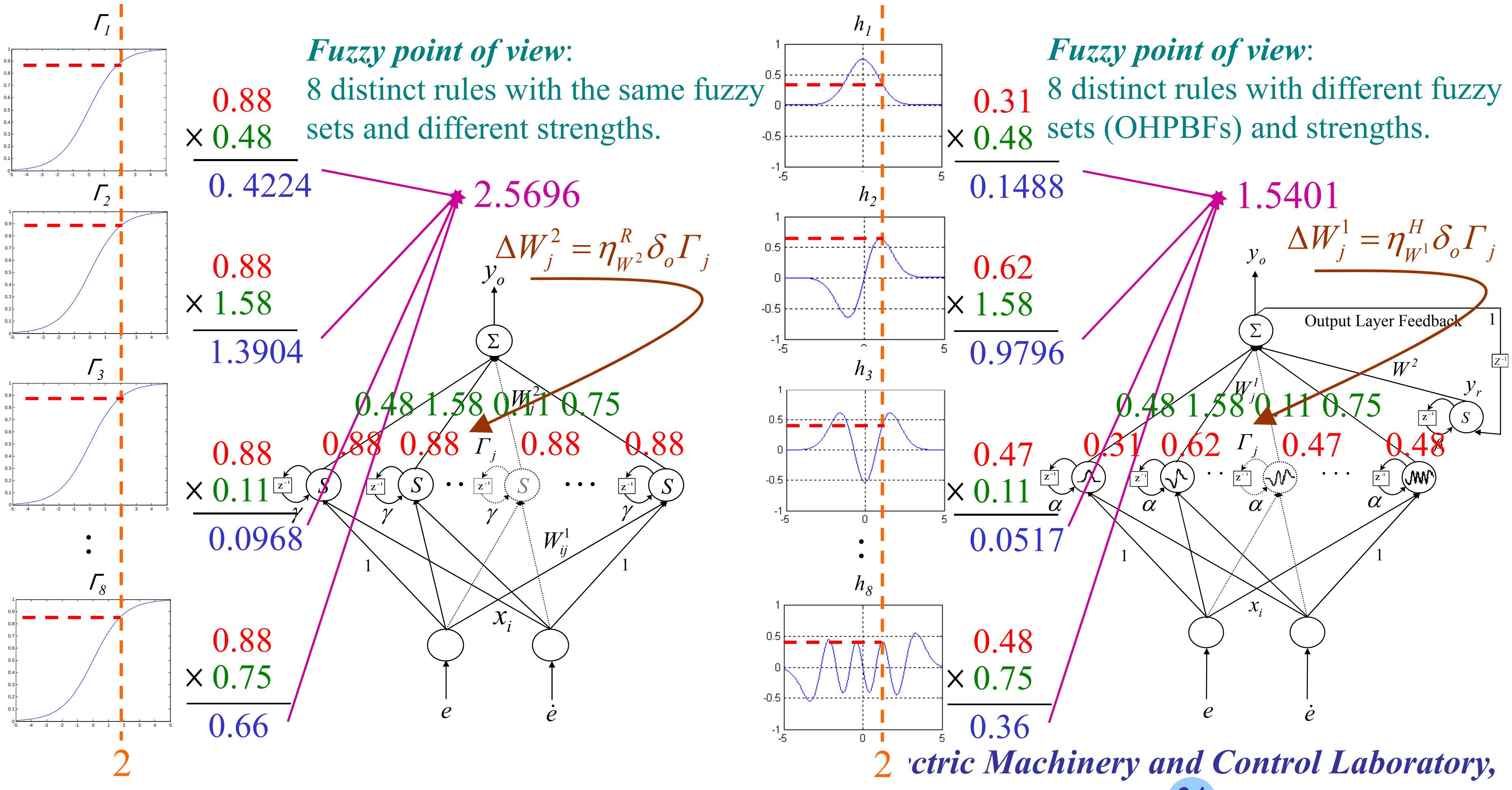

Precise Tracking Control of TAMB System—Using HPBRNN Control

- The configuration of the TAMB control system using HPBRNN with on-line learning algorithm and adaptive learning rates is shown as follows:

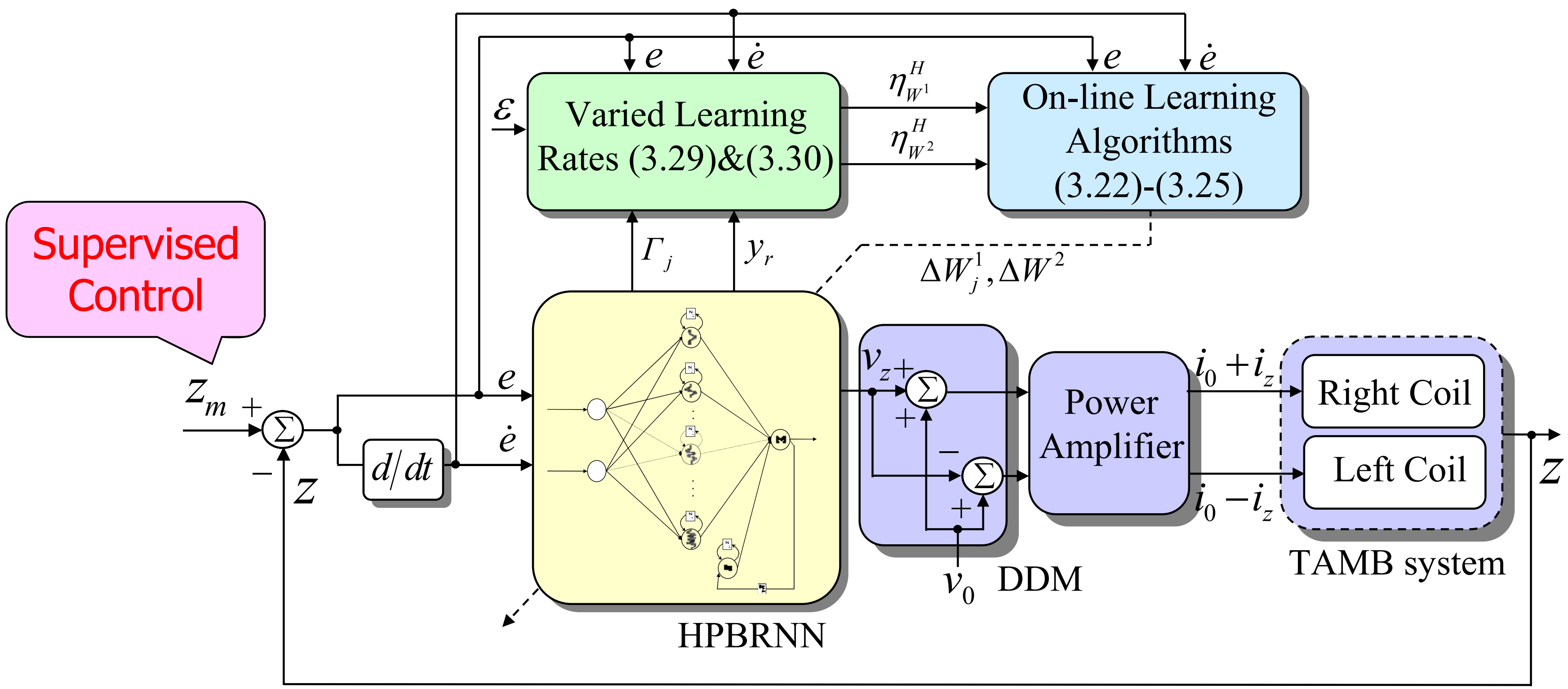

Precise Tracking Control of TAMB System—Using Model-Free Control Methods

- *A. Experimental results of TAMB control system using PID controller*
  - From the experimental results as shown in Figs. 3.5(a), (d) and 3.6(a), (d), poor tracking responses are obtained under both conditions at Case 1 and Case 2 owing to the fixed-gains PID controller is unable of dealing with the uncertainties in practical TAMB control system.

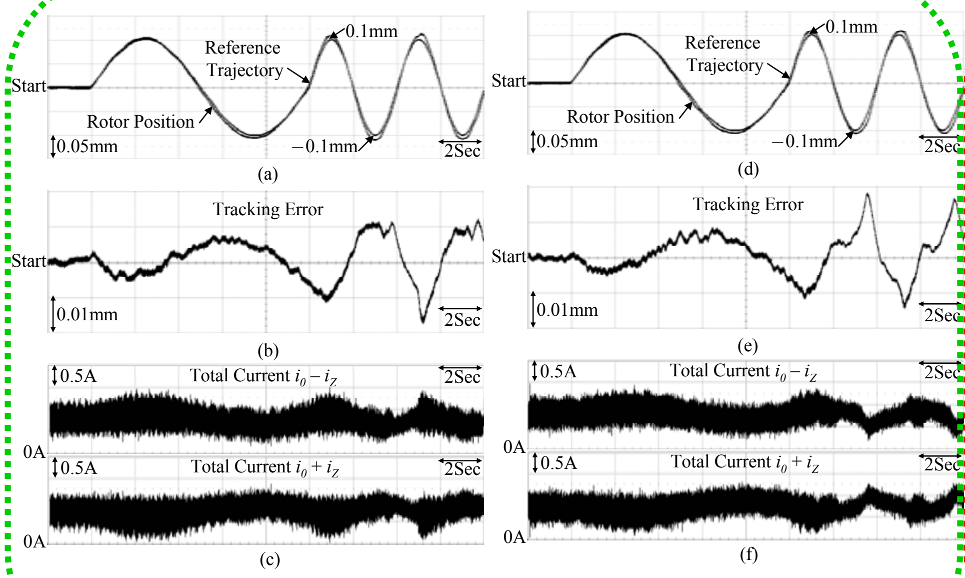

Case 1 Case2

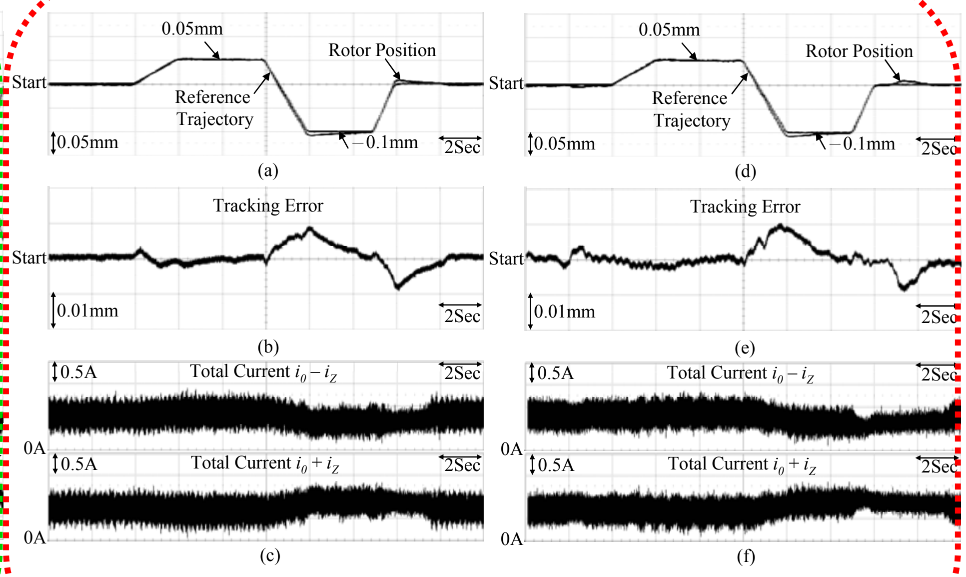

Case 1 Case 2

Precise Tracking Control of TAMB System—Using Model-Free Control Methods

- *B. Experimental results of TAMB control system using RNN controller*
  - Though the tracking responses have been improved, the tracking errors are unavoidable due to the limitation of the approximated ability of RNN.
  - The possible solutions may increase the number of hidden neurons or change the learning rates. However, the increased neurons will result in heavy computational burden and inappropriate rates can cause the system unstable.

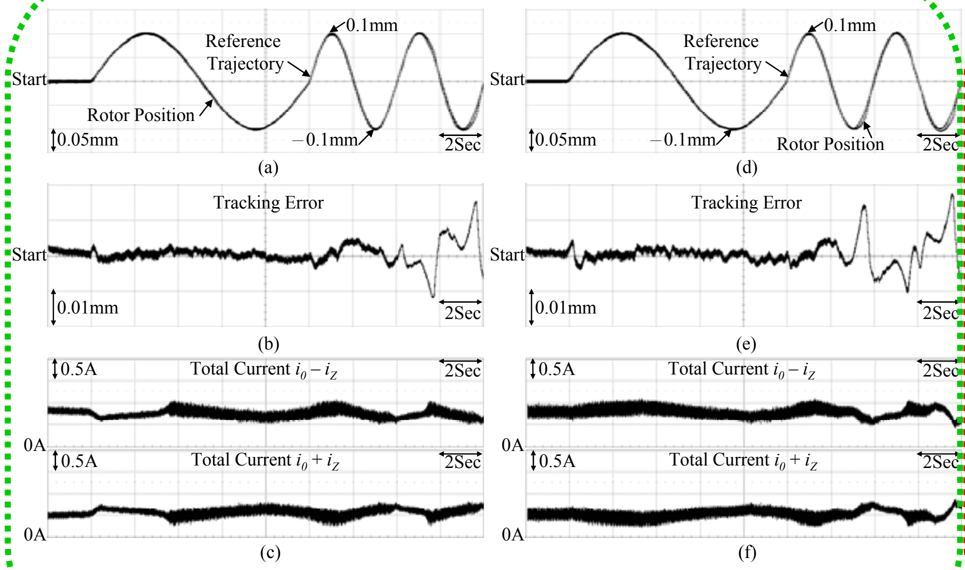

Case 1 Case2

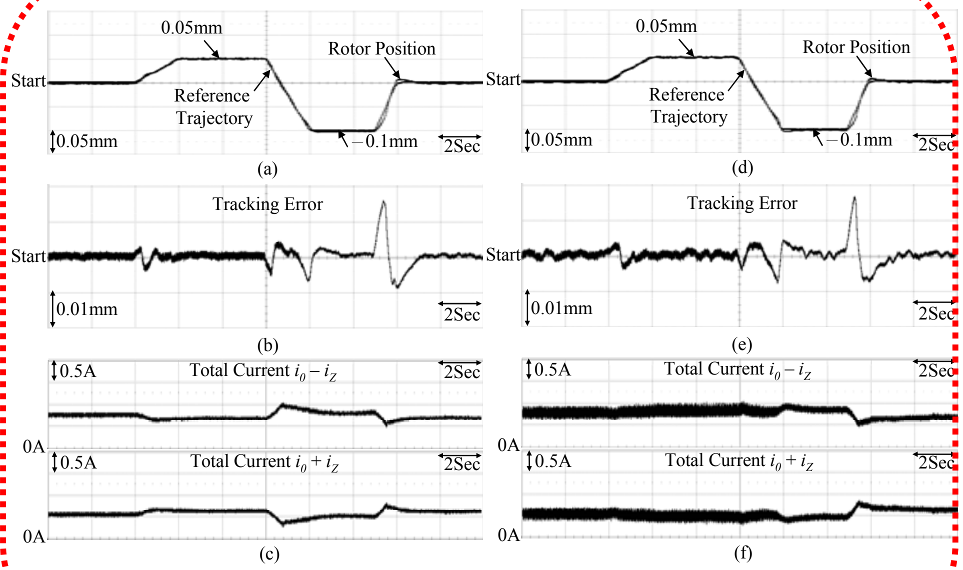

Case 1 Case 2

Precise Tracking Control of TAMB System—Using Model-Free Control Methods

- *C. Experimental results of TAMB control system using HPBRNN controller*
  - From the experimental results, the tracking performances are much improved, and the required total currents are also successfully reduced.
  - Consequently, the robustness of the TAMB control system using HPBRNN under the occurrence of uncertainties for both test conditions can be clearly observed.

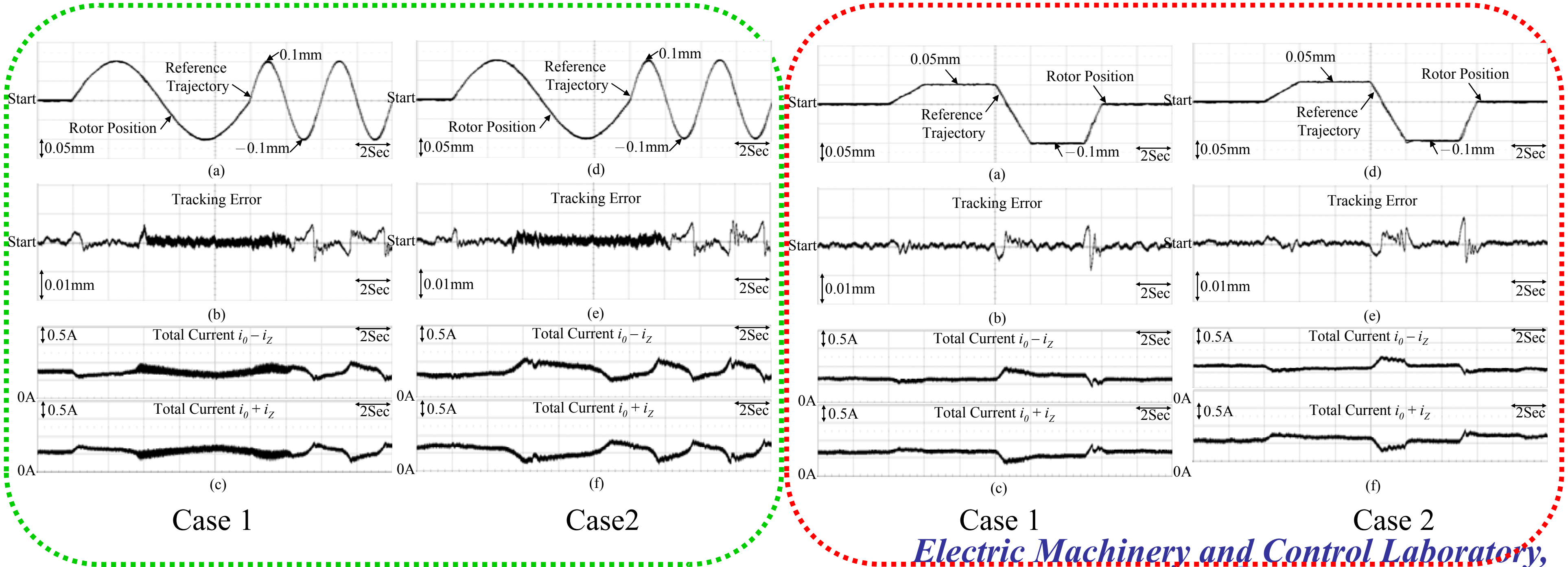

Precise Tracking Control of TAMB System—Using Model-Free Control Methods

- The performance measures of the PID, RNN and HPBRNN controllers are shown in Table 3.1 and Table 3.2, respectively.
- Obviously, the proposed HPBRNN possesses the best robust control performance and can control the TAMB system effectively.

Table 3.1 Performance measures of TAMB control system using model-free control methods at Case 1.

Tracking Errors, μm	PID		RNN		HPBRNN	
	Sinusoid	Trapezoid	Sinusoid	Trapezoid	Sinusoid	Trapezoid
Maximum	17.277	9.264	14.787	15.614	7.633	8.489
Average	4.625	2.428	2.074	2.153	1.874	1.678
Standard Deviation	3.138	2.134	1.804	1.909	1.323	1.263

Table 3.2 Performance measures of TAMB control system using model-free control methods at Case 2.

Tracking Errors, μm	PID		RNN		HPBRNN	
	Sinusoid	Trapezoid	Sinusoid	Trapezoid	Sinusoid	Trapezoid
Maximum	18.655	10.042	17.816	17.134	8.077	9.975
Average	4.962	2.808	2.401	2.451	2.043	1.860
Standard Deviation	3.606	2.530	1.979	1.898	1.402	1.332

Outline

- Abstract
- Introduction
- System Dissection, Dynamic Analyses, and Experimental Designs of Five-DOF AMB System
  - TAMB System
  - Five-DOF AMB System
- Precise Tracking Control of TAMB System
  - Using Model-Free Control Methods
  - Using Adaptive Complementary Sliding-Mode Control
  - Using Robust Non-Singular Terminal Sliding-Mode Control
- Robust Control of Fully Suspended Five-DOF AMB System
  - Using Decentralized PID Neural Network Control
  - Using Decentralized Intelligent Double Integral Sliding-Mode Control
- Discussions and Conclusions

Precise Tracking Control of TAMB System—Using Adaptive Complementary SMC

- To obtain a standard second order state equation for the controller design, the dynamic model of the TAMB system shown in (2.19) is rewritten as follows:

$$\ddot{z}(t) = A(z;t)\dot{z}(t) + B(z;t)z(t) + G(z;t)U(t) + d(z;t) \quad \Longleftarrow \quad \boxed{m\ddot{z} = -c\dot{z} + k_{ap}z + k_{ai}i_z + f_{dz}}$$

- The above dynamic model is rewritten considering the separation of nominal system parameters and system parameter variations as

$$\begin{aligned}\ddot{z}(t) &= [A_n + \Delta A(z;t)]\dot{z}(t) + [B_n + \Delta B(z;t)]z(t) + [G_n + \Delta G(z;t)]U(t) + d(z;t) \\ &= A_n\dot{z}(t) + B_n z(t) + G_n U(t) + \boxed{L(z;t)}\end{aligned}$$

where $L(z;t)$ is called the lumped uncertainty and defined as

$$\boxed{L(z;t) = \Delta A(z;t)\dot{z}(t) + \Delta B(z;t)z(t) + \Delta G(z;t)U(t) + d(z;t)}$$

- Here, the bound of the lumped uncertainty is necessary to be known in advance and satisfies the inequality as follows:

$$\delta = |L(z;t)| + \xi$$

Precise Tracking Control of TAMB System—Using SMC

- *A. Sliding-Mode Control (SMC)*
  - SMC has gained a lot of attentions in recent years for its insensitivity to system parameter variations and external disturbance once the system trajectory reaches and stays on the sliding surface.
  - First, a conventional sliding surface is defined as follows:

$$s(t) = \left(\frac{d}{dt} + \lambda\right)e(t)$$

  - Differentiating $S(t)$ with respect to time:

$$\dot{s}(t) = \ddot{e}(t) + \lambda\dot{e}(t)$$
$$= \ddot{z}_m(t) - A_n\dot{z}(t) - B_n z(t) - G_n U(t) - L(\mathbf{z};t) + \lambda\dot{e}(t)$$

  - The *globally uniformly ultimate boundedness (GUUB) stability* is guaranteed if the control effort uses the SMC control law U_{SMC} designed as:

$$U_{SMC}(t) = G_n^{-1}\left[\ddot{z}_m(t) - A_n\dot{z}(t) - B_n z(t) + \lambda\dot{e}(t) + \delta\,\mathrm{sat}\left(\frac{s(t)}{\Phi}\right)\right]$$

where $\mathrm{sat}(\cdot)$ and Φ are the saturation function and the boundary layer thickness, respectively.

Precise Tracking Control of TAMB System—Using SMC

- The saturation function is adopted in SMC to reduce the chattering as follows:

$$\operatorname{sat}\left(\frac{s(t)}{\Phi}\right)=\begin{cases}\operatorname{sgn}(s(t)), & |s(t)|>\Phi\\ s/\Phi, & |s(t)|\le\Phi\end{cases}$$

- Therefore, the SMC control law ensures that any initial states outside the boundary layer ($s(0)>\Phi$) will reach the boundary layer in finite time and remain inside thereafter ($s(t)\leqq\Phi$).

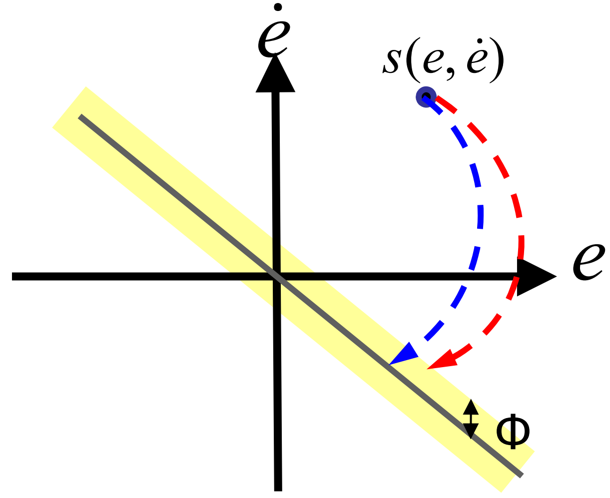

Hitting control gain δ

Good insensitivity to uncertainty, but cause system unstable easily.

Stable control effort, but weak robustness.

Boundary layer thickness Φ

Reduce chattering, but increase steady-state errors.

Precise tracking response, but high chattering control effort.

Therefore, a trade-off problem between chattering and control accuracy arises.

Precise Tracking Control of TAMB System—Using CSMC

- *B. Complementary Sliding-Mode Control (CSMC)*
  - The CSMC can efficiently *reduce the guaranteed ultimate bounds* by half while using saturation function compared with SMC.
  - Moreover, *faster transient response* of the tracking error during the reaching phase also can be obtained.
  - The control object of the CSMC is to let $\dot{e}$, e and $\int_0^{\tau} e d\tau$ move toward the neighborhood of the intersection of the integral and complementary sliding surfaces.
  - Define the integral sliding surface s_g and complementary sliding surface s_c as:

$$s_g(t) = \left(\frac{d}{dt} + \lambda\right)^2 \Lambda(t) \quad \text{where} \quad \Lambda(t) = \int_0^t e(\tau) d\tau$$

$$s_c(t) = \left(\frac{d}{dt} + \lambda\right)\left(\frac{d}{dt} - \lambda\right)\Lambda(t)$$

  - Then, define the sliding surfaces summation variable σ as follows:

$$\begin{aligned} \sigma(t) &= s_g(t) + s_c(t) \\ &= 2\left[\dot{e}(t) + \lambda e(t)\right] \\ &= 2\left[s(t)\right] \end{aligned}$$

Precise Tracking Control of TAMB System—Using CSMC

- ***Theorem 4.1***: Considering the TAMB system represented by (4.2), if the proposed CSMC control law U_{CSMC}, which is composed of an equivalent control law U_{eq} and a hitting control law U_{hit}, is adopted as the control effort , then the GUUB stability of the proposed CSMC system can be guaranteed.

$$U_{CSMC}(t) = U_{eq}(t) + U_{hit}(t)$$

$$U_{eq}(t) = G_n^{-1} \times \left[\ddot{z}_m(t) - A_n\dot{z}(t) - B_n z(t) + 2\lambda\dot{e}(t) + \lambda^2 e(t) + \lambda s_g(t)\right]$$

$$U_{hit}(t) = G_n^{-1} \times \left[\delta \text{sat}\left(\frac{\boxed{\sigma(t)}}{\Phi}\right)\right]$$

- ***Proof***: Choose the Lyapunov function candidate V_{CSMC} as

$$V_{CSMC}(s_g(t), s_c(t)) = \frac{1}{2}\left[s_g^2(t) + s_c^2(t)\right]$$

- Taking the time derivative of the first Lyapunov function, and using above equations, then

$$\dot{V}_{CSMC}(s_g(t), s_c(t)) = s_g(t)\dot{s}_g(t) + s_c(t)\dot{s}_c(t)$$

$$\vdots$$

$$\leq -\xi\left|\sigma(t)\right| \leq 0$$

whenever $\left|\sigma(t)\right| > \Phi$.

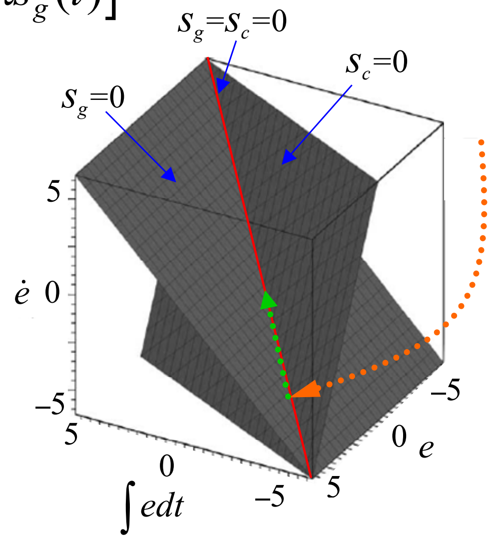

SMC	CSMC
$s(t) \leqq \Phi$	$\sigma(t) \leqq \Phi$ =>2 $s(t) \leqq \Phi$
CSMC owns half guaranteed ultimate bounds compared with SMC.	

Only the GUUB stability is guaranteed.

Precise Tracking Control of TAMB System—Using ACSMC

- *C. MIMO RHNN Estimator*
  - In the ACSMC system, two complicated dynamic functions are estimated by two outputs of the MIMO recurrent Hermite neural network (RHNN) estimator directly.
  - Here, the output vector of the MIMO RHNN is $[y_1 \;\; y_2] = [\hat{P} \;\; \hat{Q}]$
  - For ease of discussion, the outputs of the RHNN are rewritten as follows:

$$y_1 = \hat{P}(e \mid \hat{\boldsymbol{\alpha}}) = \hat{\boldsymbol{\alpha}}^{T}\boldsymbol{\Gamma}$$

$$y_2 = \hat{Q}(e \mid \hat{\boldsymbol{\beta}}) = \hat{\boldsymbol{\beta}}^{T}\boldsymbol{\Gamma}$$

where $\boldsymbol{\Gamma} = [\Gamma_1 \;\; \Gamma_2 \; \cdots \Gamma_n]^T$,

$$\hat{\boldsymbol{\alpha}} = [w_{11} \; w_{21} \; \cdots \; w_{n1}]^T, \; \hat{\boldsymbol{\beta}} = [w_{12} \; w_{22} \; \cdots \; w_{n2}]^T.$$

  - By universal approximation theorem,

$$P = P^*(e \mid \boldsymbol{\alpha}^*) + \varepsilon_p = \boldsymbol{\alpha}^{*T}\boldsymbol{\Gamma} + \varepsilon_p$$

$$Q = Q^*(e \mid \boldsymbol{\beta}^*) + \varepsilon_q = \boldsymbol{\beta}^{*T}\boldsymbol{\Gamma} + \varepsilon_q$$

optimal weighting vectors minimum approximated errors

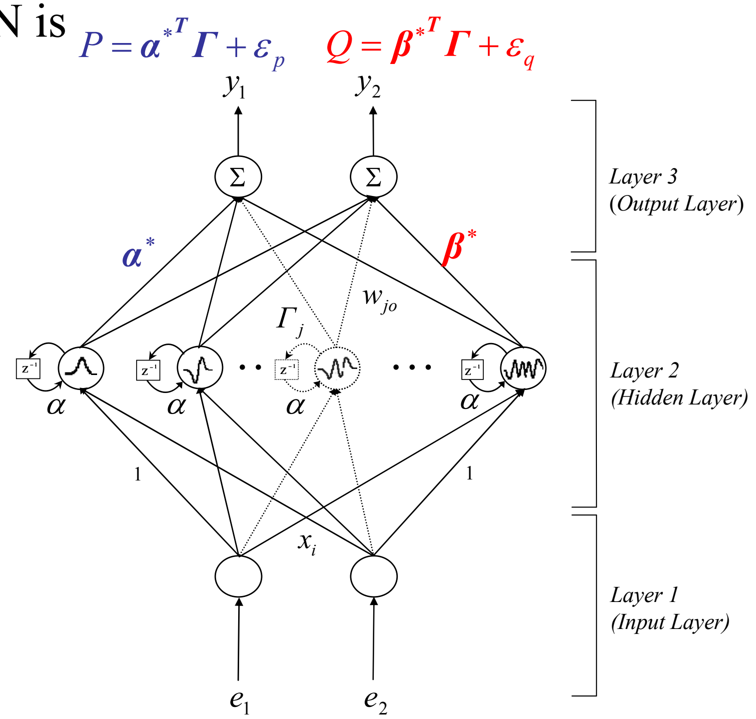

Precise Tracking Control of TAMB System—Using ACSMC

- *D. Adaptive Complementary Sliding-Mode Control (ACSMC)*
  - The proposed ACSMC with the MIMO RHNN estimator promotes the control system from GUUB to asymptotic stability without the uncertainty bound.
  - First, reformulate the term $s_g - \lambda s_c$ as follows:

$$\begin{aligned}\dot{s}_g(t) - \lambda s_c(t) &= \ddot{z}_m(t) - A_n\dot{z}(t) - B_n z(t) - G_n U(t) - L(\boldsymbol{z};t) + 2\lambda\dot{e}(t) + \lambda^2 e(t) - \lambda s_c(t)\\ &= H(\boldsymbol{z};t) - G_n U(t) + \lambda\Xi(\boldsymbol{z};t) - \lambda G_n s_c(t)\\ &= G_n\left[G_n^{-1}H(\boldsymbol{z};t) - U(t) + G_n^{-1}\lambda\Xi(\boldsymbol{z};t) - \lambda s_c(t)\right]\\ &= G_n\Big[\underbrace{\boxed{P(t)}}_{y_1} - U(t) + \lambda\underbrace{\boxed{Q(t)}}_{y_2} - \lambda s_c(t)\Big]\end{aligned}$$

where $H(\boldsymbol{z};t) = \ddot{z}_m(t) - A_n\dot{z}(t) - B_n z(t) - L(\boldsymbol{z};t)$, $\boxed{P(t) = G_n^{-1}H(\boldsymbol{z};t)}$, $\boxed{Q(t) = G_n^{-1}\Xi(\boldsymbol{z};t)}$, $\Xi(\boldsymbol{z};t) = 2\dot{e}(t) + \lambda e(t) - s_c(t) + G_n s_c(t)$.

  - The MIMO RHNN estimator is proposed to estimate the two complicated dynamic functions $P(t)$ and $Q(t)$ directly including the lumped uncertainty to further improve the control performance.

Precise Tracking Control of TAMB System—Using ACSMC

- ***Theorem 4.2***: Considering the TAMB system represented by (4.2), if the proposed ACSMC control law U_{ACSMC}, which is composed of the MIMO RHNN estimator designed as U_e with estimation laws for the two dynamic functions $P(t)$ and $Q(t)$, the robust compensator designed as U_c with adaptive laws, is adopted as the control effort U, then the asymptotic stability of the proposed ACSMC system can be guaranteed.

$$U_{ACSMC}(t) = U_e(t) + U_c(t)$$

$$U_e(t) = \hat{P}(e \mid \hat{\boldsymbol{\alpha}}) + \lambda \hat{Q}(e \mid \hat{\boldsymbol{\beta}}) \text{ using estimation laws } \begin{cases} \dot{\hat{\boldsymbol{\alpha}}} = \eta_\alpha \sigma(t) \boldsymbol{\Gamma} \\ \dot{\hat{\boldsymbol{\beta}}} = \eta_\beta \lambda \sigma(t) \boldsymbol{\Gamma} \end{cases}$$

$$U_c(t) = \hat{\varepsilon}_p + \lambda \left[\hat{\varepsilon}_q + s_g(t) \right] \text{ using adaptive laws } \begin{cases} \dot{\hat{\varepsilon}}_p = \eta_p \sigma(t) \\ \dot{\hat{\varepsilon}}_q = \eta_q \lambda \sigma(t) \end{cases}$$

- ***Proof***: Choose the Lyapunov function candidate V_{ACSMC} as

$$V_{ACSMC}(s_g(t), s_c(t), \tilde{\boldsymbol{\alpha}}, \tilde{\boldsymbol{\beta}}, \tilde{\varepsilon}_p, \tilde{\varepsilon}_q) = \frac{1}{2}\left[s_g^2(t) + s_c^2(t) \right] + \frac{G_n}{2\eta_\alpha} \tilde{\boldsymbol{\alpha}}^T \tilde{\boldsymbol{\alpha}} + \frac{G_n}{2\eta_\beta} \tilde{\boldsymbol{\beta}}^T \tilde{\boldsymbol{\beta}} + \frac{G_n}{2\eta_p} \tilde{\varepsilon}_p^{\,2} + \frac{G_n}{2\eta_q} \tilde{\varepsilon}_q^{\,2}$$

where $\tilde{\boldsymbol{\alpha}} = \boldsymbol{\alpha}^* - \hat{\boldsymbol{\alpha}}$, $\tilde{\boldsymbol{\beta}} = \boldsymbol{\beta}^* - \hat{\boldsymbol{\beta}}$, $\tilde{\varepsilon}_p = \varepsilon_p - \hat{\varepsilon}_p$, and $\tilde{\varepsilon}_q = \varepsilon_q - \hat{\varepsilon}_q$.

- Taking the time derivative of V_{ACSMC}, and using Barbalat's Lemma. Then,

$$\dot{V}_{ACSMC} = -\lambda G_n \sigma^2(t) \le 0 \quad \lim_{t \to \infty} \sigma^2(t) = 0$$ asymptotic stability is guaranteed

Precise Tracking Control of TAMB System—Using ACSMC

- The configuration of the TAMB control system using ACSMC system with MIMO RHNN estimator is shown as follows:

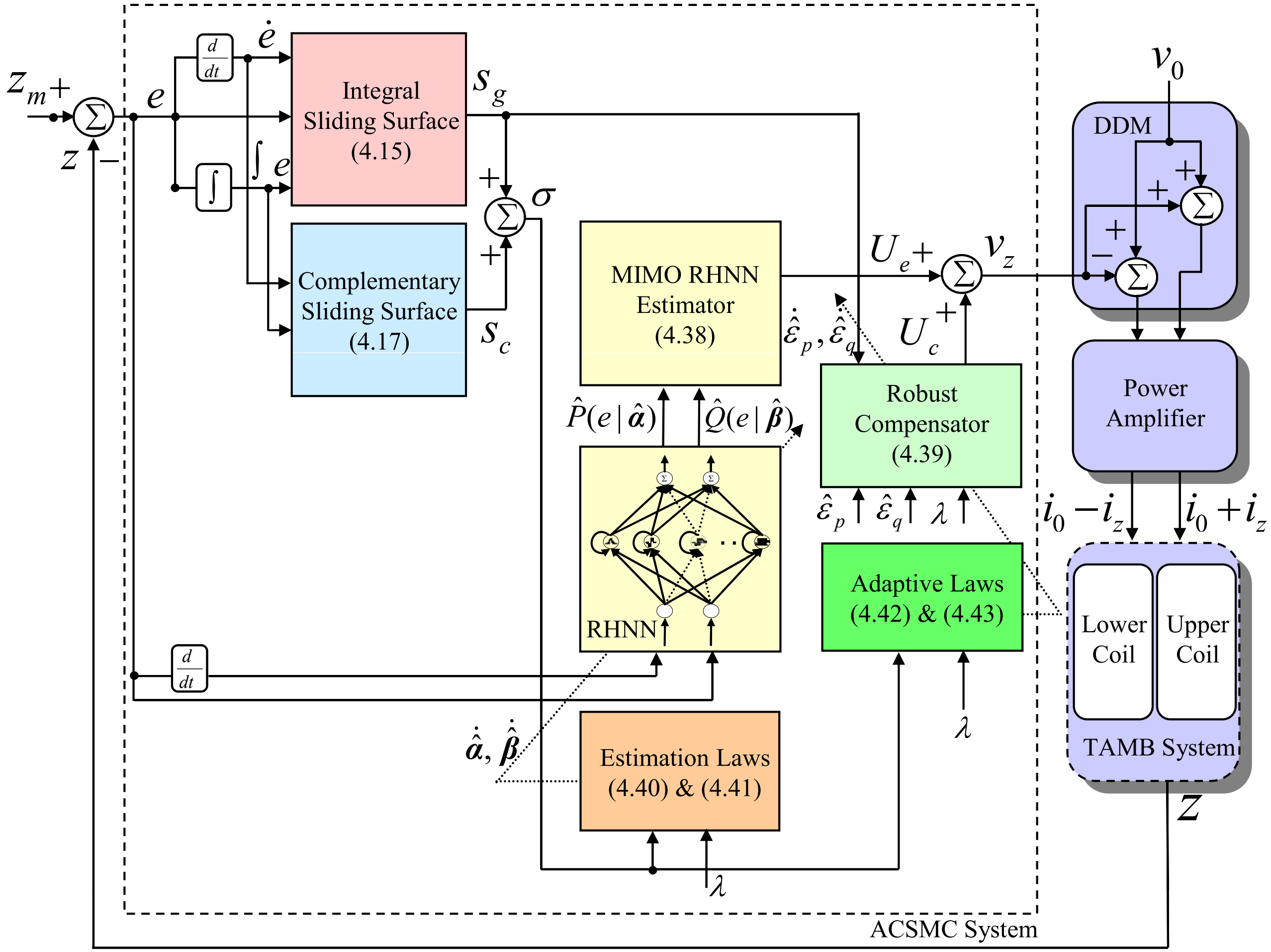

Precise Tracking Control of TAMB System—Using Adaptive Complementary SMC

- *A. Experimental results of TAMB control system using SMC system*
  - Poor tracking responses are obtained due to the saturation function is used.
  - Though the tracking response can be improved with larger δ or smaller Φ, the chattering will be more serious, and the control effort will be saturated easily.

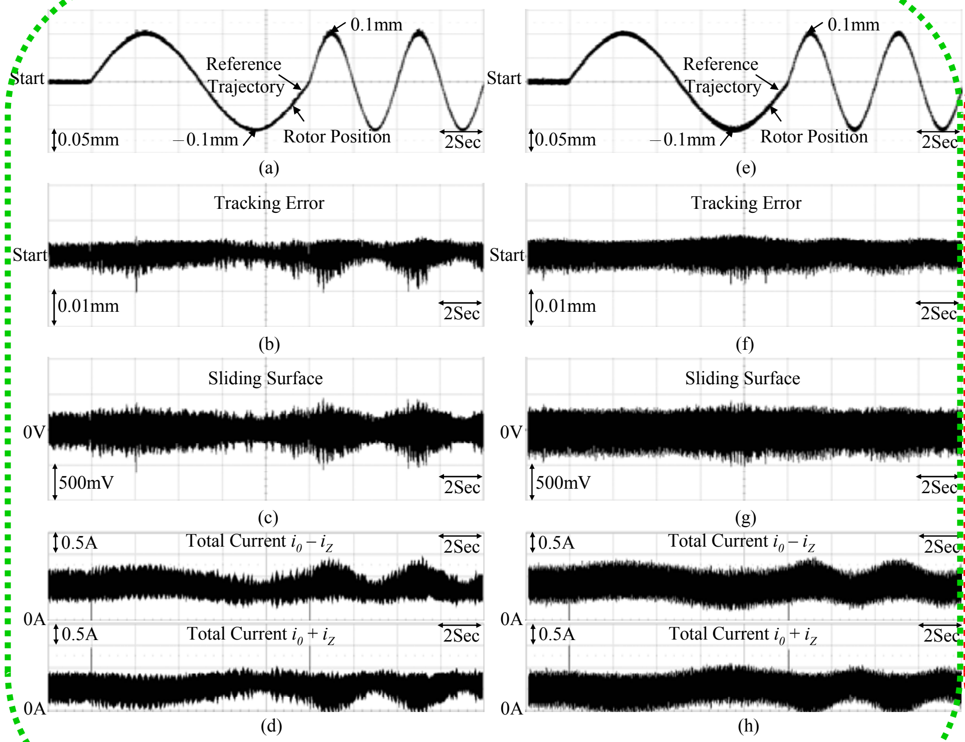

Case 1 Case2

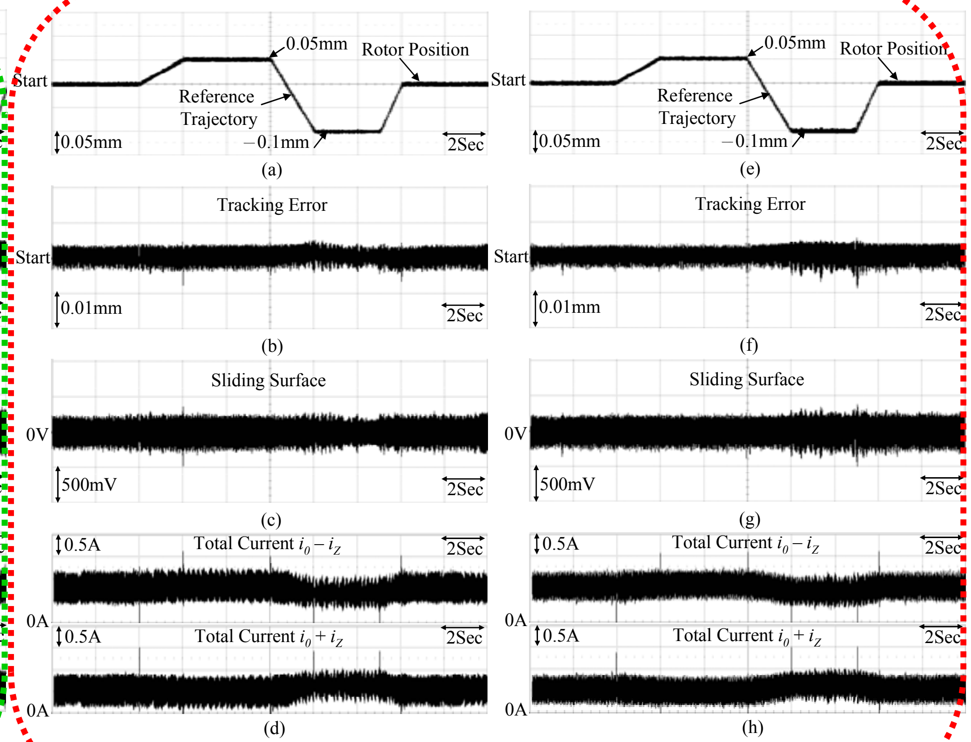

Case 1 Case 2

Precise Tracking Control of TAMB System—Using Adaptive Complementary SMC

- *B.Experimental results of TAMB control system using CSMC system*
  - Both the integral and complementary sliding surfaces are approach zero nearly.
  - The tracking responses at Case 2 are unacceptable due to the CSMC with small δ and large Φ is not robust enough to deal with the uncertainty in terms of the additional load disk.

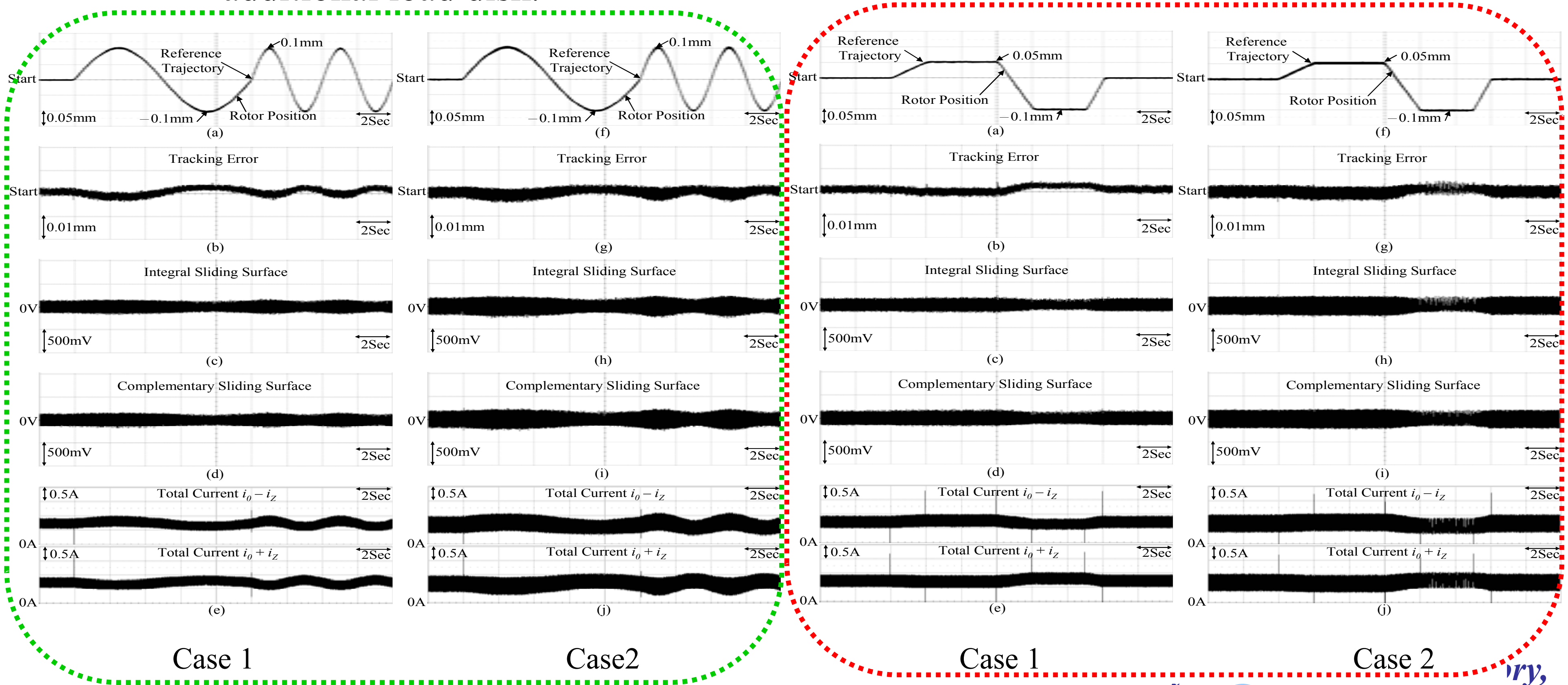

Precise Tracking Control of TAMB System—Using Adaptive Complementary SMC

- *C.Experimental results of TAMB control system using ACSMC system*
  - From the experimental results, the tracking performances are improved greatly due to the on-line tuning of the control parameters.
  - Since the control efforts are obtained by the MIMO RHNN majorly and exquisitely, the required total currents are also reduced effectively.

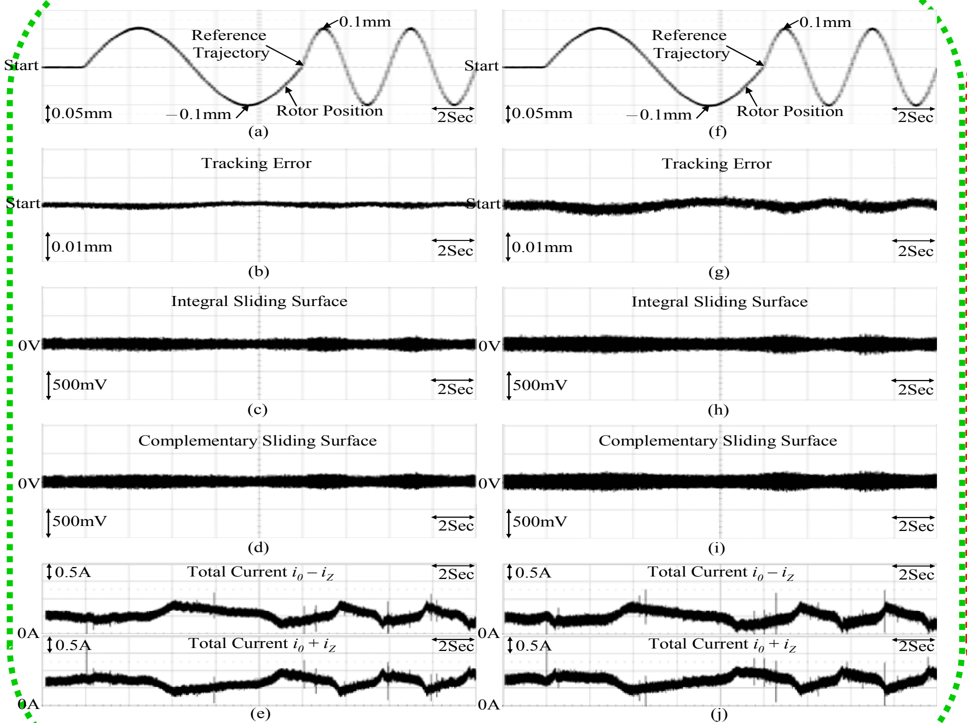

Case 1 Case2

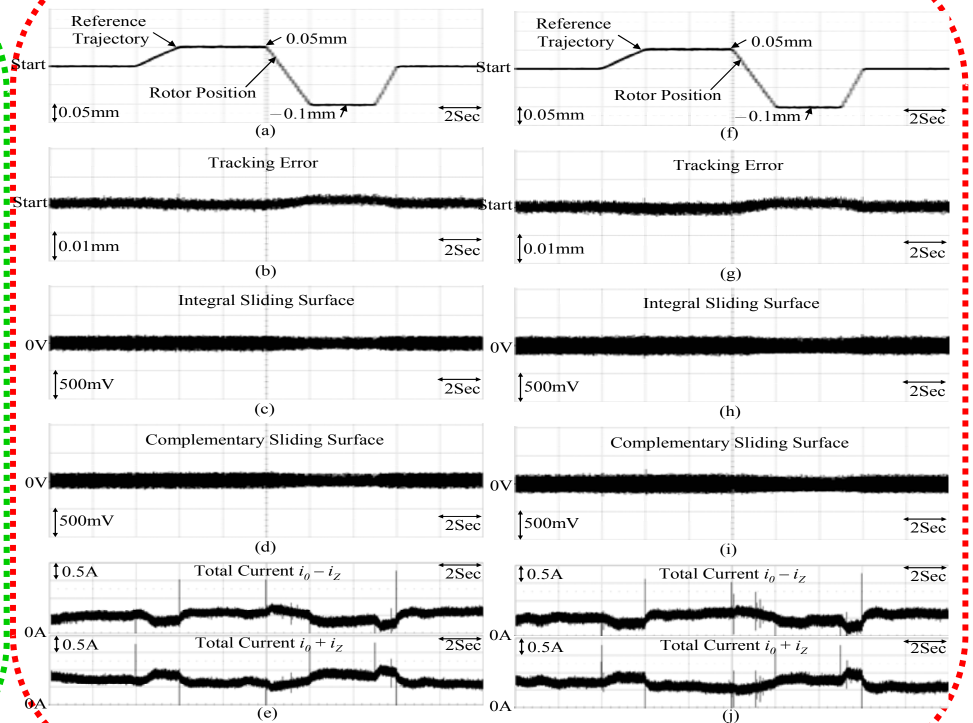

Case 1 Case 2

Precise Tracking Control of TAMB System—Using Adaptive Complementary SMC

- The performance measures of the SMC, CSMC and ACSMC systems are shown in Table 4.1 and Table 4.2, respectively.
- Obviously, the proposed ACSMC possesses the best robust control performance and can control the TAMB system effectively.

Table 4.1 Performance measures of TAMB control system using SMC, CSMC, and ACSMC systems at Case 1.

Tracking Errors, μm	SMC		CSMC		ACSMC	
	Sinusoid	Trapezoid	Sinusoid	Trapezoid	Sinusoid	Trapezoid
Maximum	10.081	8.115	3.957	4.174	3.324	3.563
Average	4.388	2.819	1.634	1.556	1.054	1.110
Standard Deviation	3.360	2.375	1.275	1.205	1.066	1.075

Table 4.2 Performance measures of TAMB control system using SMC, CSMC, and ACSMC systems at Case 2.

Tracking Errors, μm	SMC		CSMC		ACSMC	
	Sinusoid	Trapezoid	Sinusoid	Trapezoid	Sinusoid	Trapezoid
Maximum	11.161	9.259	4.421	4.759	3.971	3.655
Average	4.812	3.095	1.702	1.786	1.204	1.319
Standard Deviation	3.772	2.652	1.475	1.395	1.172	1.192

Outline

- Abstract
- Introduction
- System Dissection, Dynamic Analyses, and Experimental Designs of Five-DOF AMB System
  - TAMB System
  - Five-DOF AMB System
- Precise Tracking Control of TAMB System
  - Using Model-Free Control Methods
  - Using Adaptive Complementary Sliding-Mode Control
  - Using Robust Non-Singular Terminal Sliding-Mode Control
- Robust Control of Fully Suspended Five-DOF AMB System
  - Using Decentralized PID Neural Network Control
  - Using Decentralized Intelligent Double Integral Sliding-Mode Control
- Discussions and Conclusions

Precise Tracking Control of TAMB System—Using TSMC

- *A. Terminal Sliding-Mode Control (TSMC)*
  - First, define the terminal sliding surface s_m to achieve *finite time tracking control (FTTC)* as follows

    $$s_m(t) = \dot{e}(t) + \lambda e(t)^{\frac{q}{p}}$$

    where λ is a designed positive constant; p and q are both positive odd integers which should satisfy the following condition $p>q$.
  - If the control effort $U(t)$ of the TSMC control law $U_{TSMC}(t)$ is designed as:

    $$U_{TSMC}(t) = G_n^{-1}\left[\ddot{z}_m(t) - A_n\dot{z}(t) - B_n z(t) + \lambda\frac{q}{p}e(t)^{\frac{q}{p}-1}\dot{e}(t) + \delta\,\mathrm{sgn}(s_m(t))\right]$$

  - Then, the following stability result can be obtained:

    $$\boxed{\frac{1}{2}\frac{d}{dt}s_m(t)^2 < -\xi\left|s_m(t)\right|}$$

  - Thus, the tracking error e will reach the terminal sliding surface s_m in finite time t_r as shown in the following

    $$t_r \le \frac{\left|s_m(0)\right|}{\xi}$$

Precise Tracking Control of TAMB System—Using TSMC

- On the other hand, when the terminal sliding surface s_m=0 is reached, the system dynamic $\dot{e}(t)$ is

$$\dot{e}(t) = -\lambda e(t)^{\frac{q}{p}} \Leftarrow \boxed{s_m(t) = \dot{e}(t) + \lambda e(t)^{\frac{q}{p}} = 0}$$

- A finite time t_s, which is taken to travel from $e(t_r)\neq 0$ to $e(t_r+t_s)=0$, can be obtained

$$t_s = -\frac{1}{\lambda}\int_{e(t_r)}^{0} e^{-\frac{q}{p}} de = \frac{p}{\lambda(p-q)} \left|e(t_r)\right|^{1-\frac{q}{p}}$$

- Therefore, both the tracking error e and its derivative $\dot{e}$ will converge to zero in finite time by using the TSMC system as shown in Fig. 5.1.

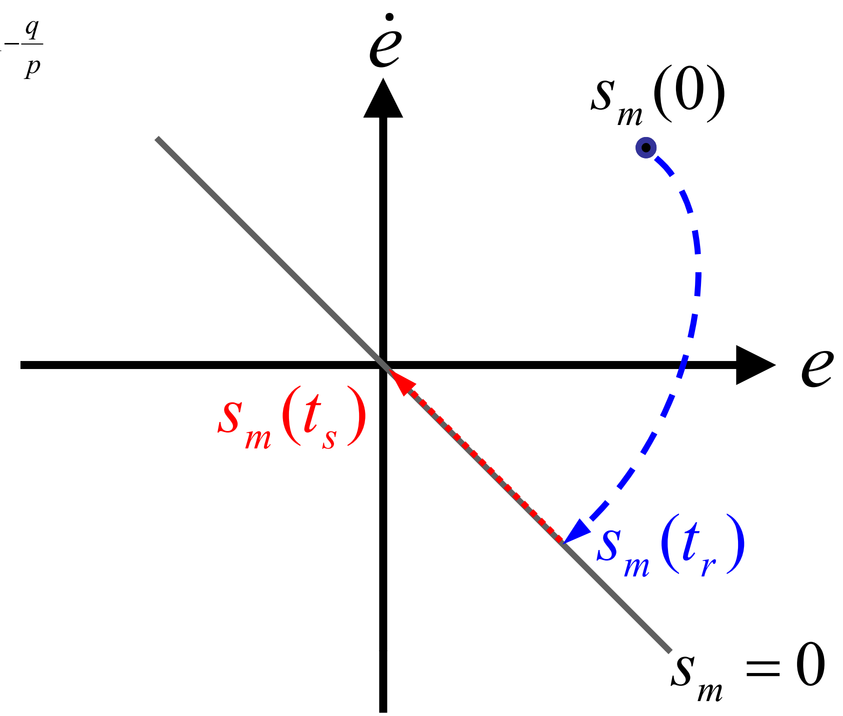

Precise Tracking Control of TAMB System—Using TSMC

- Now, considering the TSMC control law, the forth term containing $e(t)^{\frac{q}{p}-1}\dot{e}(t)$ may occur a singularity problem if $\dot{e}(t)\neq 0$ when $e(t)=0$ due to the power of $e(t)$ is negative.

ex: p=5, q=3

$$U_{TSMC}(t)=G_n^{-1}\left[\ddot{z}_m(t)-A_n\dot{z}(t)-B_n z(t)+\lambda\frac{q}{p}e(t)^{\frac{q}{p}-1}\dot{e}(t)+\delta\operatorname{sgn}(s_m(t))\right]$$

$$\frac{1}{\sqrt[5]{e^2(t)}}\dot{e}(t)$$

- Therefore, the TSMC can not guarantee a bounded control effort if $\dot{e}(t)\neq 0$ when $e(t)=0$.
- Though the singularity problem only occurs in the reaching phase when the condition $q<p<2q$ holds, it is noted that the singularity problem may also occur even after the terminal sliding surface $s_m(t_r+t_s)$ is reached due to the computational errors and uncertain factors.
- $\because\ \dot{e}(t)=-\lambda e(t)^{q/p}$

  $\therefore\ e(t)^{q/p-1}\dot{e}(t)=-\lambda e(t)^{\frac{2q-p}{p}}$ >0

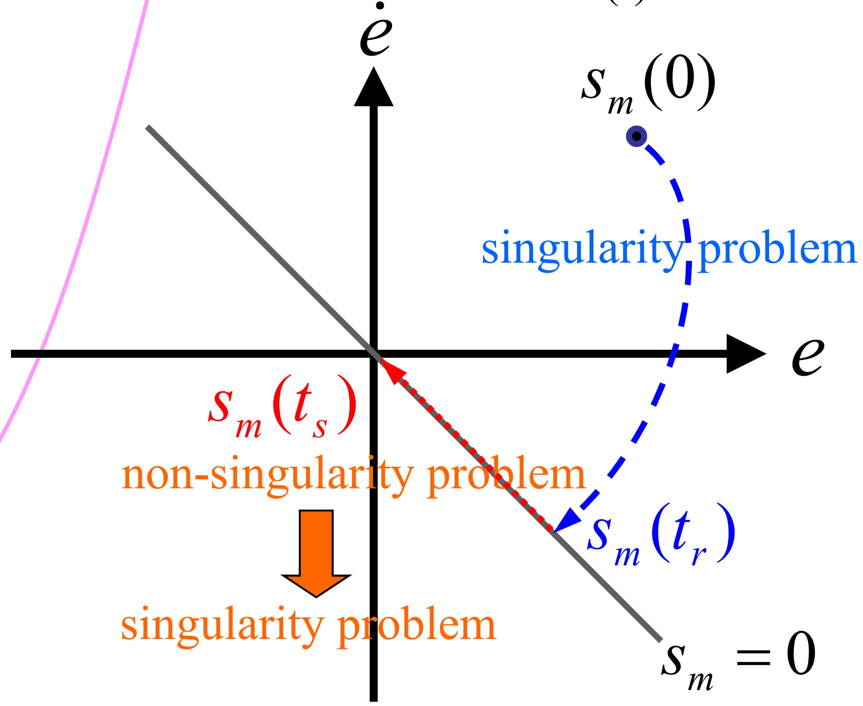

Precise Tracking Control of TAMB System—Using NTSMC

- *B. Non-Singular Terminal Sliding-Mode Control (NTSMC)*
  - Now, the NTSMC is further proposed to overcome the singularity problem of the TSMC. Define the non-singular terminal sliding surface s_n as

$$s_n(t) = e(t) + \frac{1}{\lambda}\dot{e}(t)^{\frac{p}{q}}$$

  - Considering the non-singular terminal sliding surface s_n, the TAMB system is stable if the control effort $U(t)$ uses NTSMC control law $U_{NTSMC}(t)$ designed as:

$$U_{NTSMC}(t) = G_n^{-1}\left[\ddot{z}_m(t) - A_n\dot{z}(t) - B_n z(t) + \lambda\frac{q}{p}\dot{e}(t)^{\frac{2q-p}{q}} + \delta\,\mathrm{sgn}(s_n(t))\right]$$

  - It is obvious that the forth term of the NTSMC control law U_{NTSMC} will not result in the singularity problem as lone as the condition $q<p<2q$ holds.

  - Moreover, when s_n=0, the system dynamic $\dot{e}(t) = -\lambda e(t)^{q/p}$ is equivalent to the one of TSMC. Therefore, the finite time t_s taken to reach the equilibrium point e=0 of the NTSMC system is the same as the one of the TSMC system.

Precise Tracking Control of TAMB System—Using RNTSMC

- *C. MISO RHNN Estimator*
  - In the proposed RNTSMC, the MISO RHNN with two inputs and one output is proposed as the uncertainty estimator.
  - For ease of discussion, the output of the RHNN are rewritten as follows:

    $\hat{y}(e \mid \hat{\boldsymbol{W}}) = \hat{\boldsymbol{W}}^{\boldsymbol{T}} \boldsymbol{\Gamma}$

    where $\boldsymbol{\Gamma} = [\Gamma_1 \;\; \Gamma_2 \cdots \Gamma_n]^T \;\; \hat{\boldsymbol{W}} = [w_1 \; w_2 \cdots w_n]^T$
  - By universal approximation theorem,

    $L = y^*(e \mid \boldsymbol{W}^*) + \varepsilon = \boldsymbol{W}^{*\boldsymbol{T}} \boldsymbol{\Gamma} + \varepsilon$

    optimal weighting vectors

    minimum approximated errors
  - The MISO RHNN uncertainty estimator with superior approximated ability is employed to directly estimate the lumped uncertainty of the TAMB on-line.
  - Thus, the exact value of the bound of the lumped uncertainty is unnecessary.

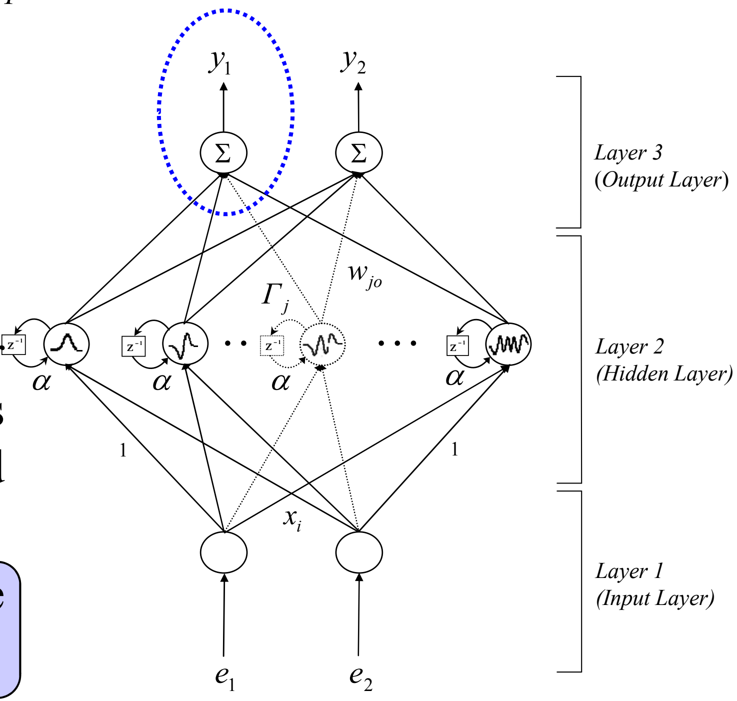

Precise Tracking Control of TAMB System—Using RNTSMC

- *D. Robust Non-Singular Terminal Sliding-Mode Control (RNTSMC)*
  - Comparing with the TSMC and NTSMC systems, the RNTSMC system possesses no chattering and maintains asymptotic stability due to the switching function and the saturation function are not used, respectively.
  - ***Theorem 5.1***: Considering the TAMB system represented by (4.2), if the proposed RNTSMC control law $U_{RNTSMC}(t)$, which is composed of the equivalent control law $U_{eq}(t)$, the MISO RHNN uncertainty estimator $U_{RHNN}(t)$ with estimation law and the robust controller $U_r(t)$ with adaptive law, is adopted as the control effort , then the asymptotic stability of the proposed RNTSMC system can be guaranteed.

$$U_{RNTSMC}(t) = U_{eq}(t) + U_{RHNN}(t) + U_r(t)$$

$$U_{eq}(t) = G_n^{-1}\left[\ddot{z}_m(t) - A_n\dot{z}(t) - B_n z(t) + \lambda\frac{q}{p}\dot{e}(t)^{2-\frac{p}{q}}\right]$$

$U_{RHNN}(t) = -G_n^{-1}\hat{y}(t)$ using estimation law $\dot{\hat{\boldsymbol{W}}} = -\eta_W \frac{s_n(t)}{\lambda}\frac{p}{q}\dot{e}(t)^{\frac{p}{q}-1}\boldsymbol{\Gamma}$

$U_r(t) = -G_n^{-1}\left[\hat{\varepsilon} - \zeta s_n(t)\right]$ using adaptive law $\dot{\hat{\varepsilon}} = -\eta_\varepsilon \frac{s_n(t)}{\lambda}\frac{p}{q}\dot{e}(t)^{\frac{p}{q}-1}$

$\dot{V}_{RNTSMC}(s_n(t), \tilde{\boldsymbol{W}}, \tilde{\varepsilon}) = -\zeta s_n(t)^2$ $\quad \lim_{t\to\infty}\xi s_n(t)^2 = 0$ asymptotic stability is guaranteed

Precise Tracking Control of TAMB System—Using RNTSMC

- The configuration of the TAMB control system using RNTSMC system with MISO RHNN estimator is shown as follows:

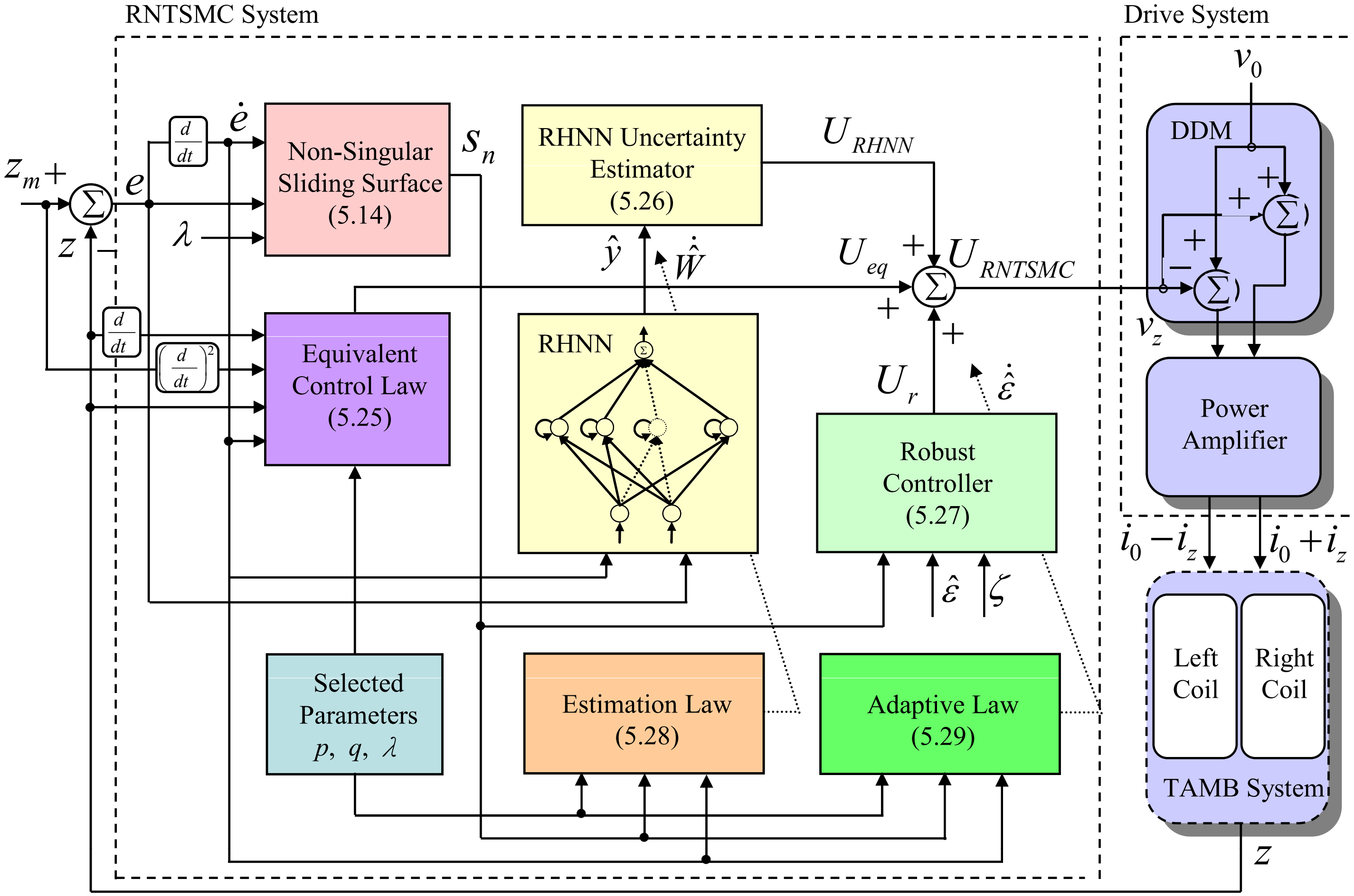

Precise Tracking Control of TAMB System—Using RNTSMC

- The solution of the actual complex problem in the programming of the implementation.
  - The terminal sliding surface s_m and the non-singular terminal sliding surface s_n:

$$s_m(t) = \dot{e}(t) + \lambda e(t)^{\frac{q}{p}}$$

Complex value
ex: e=-2, p=5, q=3

$$s_n(t) = e(t) + \frac{1}{\lambda}\dot{e}(t)^{\frac{p}{q}}$$

Complex value
ex: $\dot{e}$=-2, p=5, q=3

  - The powers q/p of terminal sliding surface when e<0, and p/q of non-singular terminal sliding surface when $\dot{e}$ <0 may lead the terms to the complex values. Therefore, the new form is adopted as the following new form:

$$s_m(t) = \dot{e}(t) + \lambda \left|e(t)\right|^{\frac{q}{p}} sign(e(t))$$

$$s_n(t) = e(t) + \frac{1}{\lambda}\left|\dot{e}(t)\right|^{\frac{p}{q}} sign(\dot{e}(t))$$

  - Both of the above forms are continuous and differentiable although the absolute value and signum operators are involved. Moreover, their derivatives can be expressed as

$$\dot{s}_m(t) = \ddot{e}(t) + \lambda \frac{q}{p}\left|e(t)\right|^{\frac{q}{p}-1}\dot{e}(t)$$

$$\dot{s}_n(t) = \dot{e}(t) + \frac{1}{\lambda}\frac{p}{q}\left|\dot{e}(t)\right|^{\frac{p}{q}-1}\ddot{e}(t)$$

Precise Tracking Control of TAMB System— Using Robust Non-Singular Terminal SMC

- *A. Experimental results of TAMB control system using TSMC system*
  - From the experimental results, the rotor position can not track the reference commands precisely and immediately.
  - Moreover, the unstable control efforts which are cause by the singular problem, result in the vibratory tracking performance and terminal sliding surface.

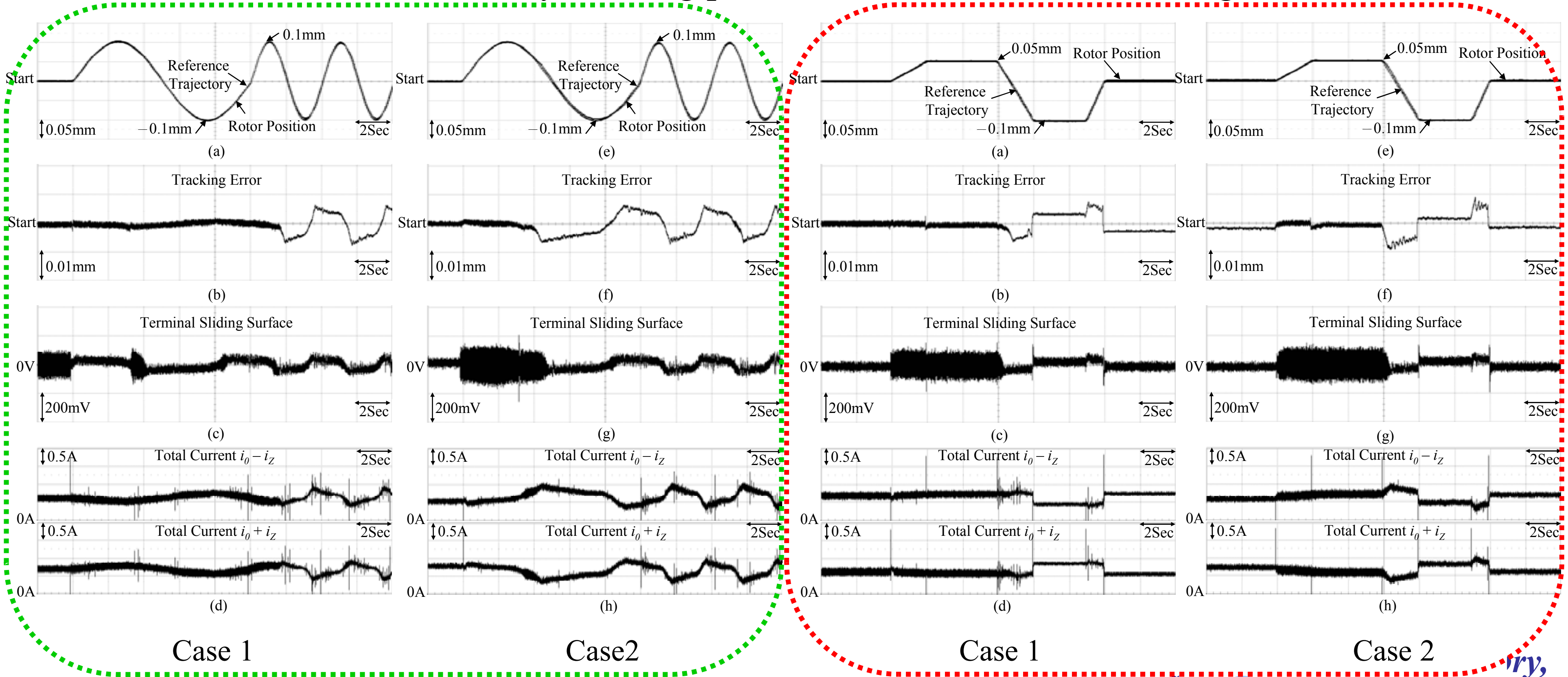

Precise Tracking Control of TAMB System—Using Robust Non-Singular Terminal SMC

- *B.Experimental results of TAMB control system using NTSMC system*
  - One can observe that the tracking responses obtained from the NTSMC system are much degraded compared with the ones obtained from the TSMC system.
  - Though NTSMC solve the singular problem of TSMC, the steady-state errors become worse (the proof will be discussed in conclusion).

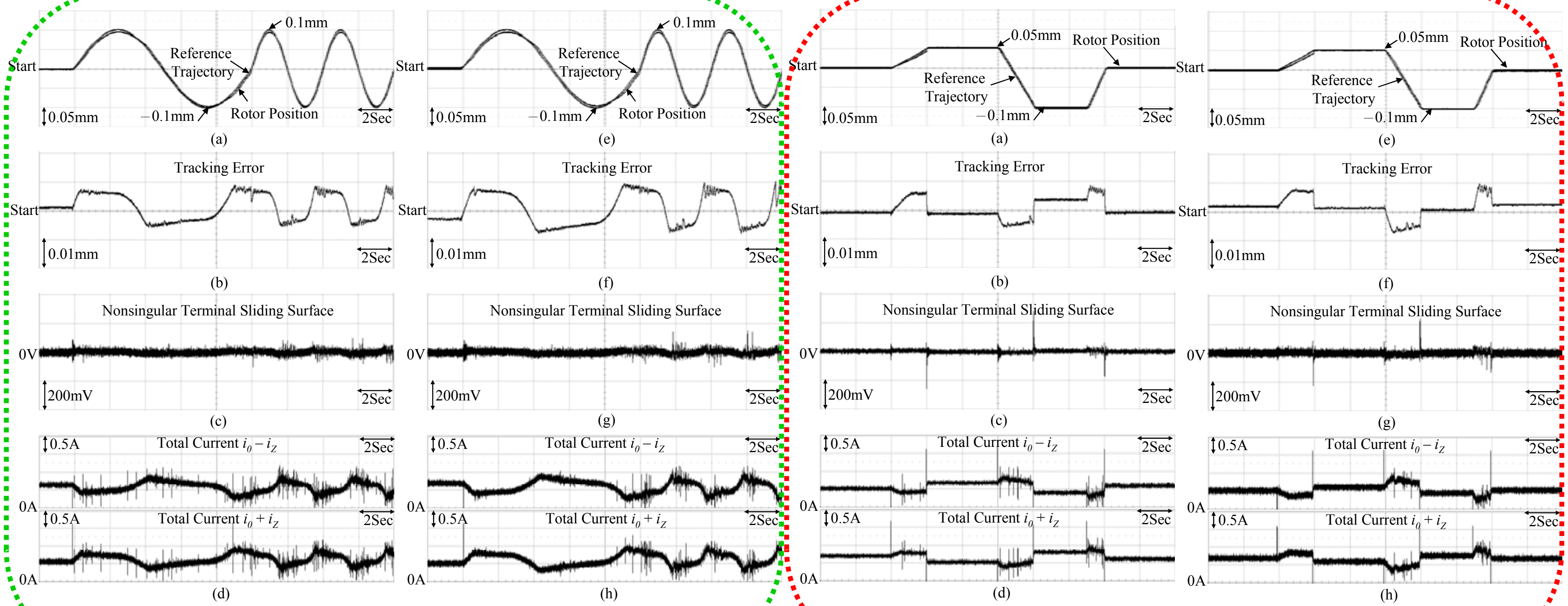

Case 1 Case2 Case 1 Case 2

Precise Tracking Control of TAMB System—Using Robust Non-Singular Terminal SMC

- The reasons of the unbounded control efforts for TSMC and NTSMC systems are:
  - The control law of TSMC system:

$$U_{TSMC}(t)=G_n^{-1}\left[\ddot{z}_m(t)-A_n\dot{z}(t)-B_n z(t)+\lambda\frac{q}{p}e(t)^{\frac{q}{p}-1}\dot{e}(t)+\delta\operatorname{sgn}(s_m(t))\right]$$

  - The control law of NTSMC system:

$$U_{NTSMC}(t)=G_n^{-1}\left[\ddot{z}_m(t)-A_n\dot{z}(t)-B_n z(t)+\lambda\frac{q}{p}\dot{e}(t)^{\frac{2q-p}{q}}+\delta\operatorname{sgn}(s_n(t))\right]$$

  - If p=5, q=3, then

$$e(t)^{\frac{q}{p}-1}\dot{e}(t)=\frac{1}{\sqrt[5]{e^2(t)}}\dot{e}(t)$$ singular problem

$$\dot{e}(t)^{\frac{2q-p}{q}}=\dot{e}(t)^{\frac{1}{3}}$$ enlarged control effort

Ex: 0.02^(1/3)=0.2714

More frequently

Precise Tracking Control of TAMB System—Using Robust Non-Singular Terminal SMC

- *C.Experimental results of TAMB control system using RNTSMC system*
  - According to the on-line lumped uncertainty estimation via MISO RHNN estimator, the best control performance and robustness are obtained.

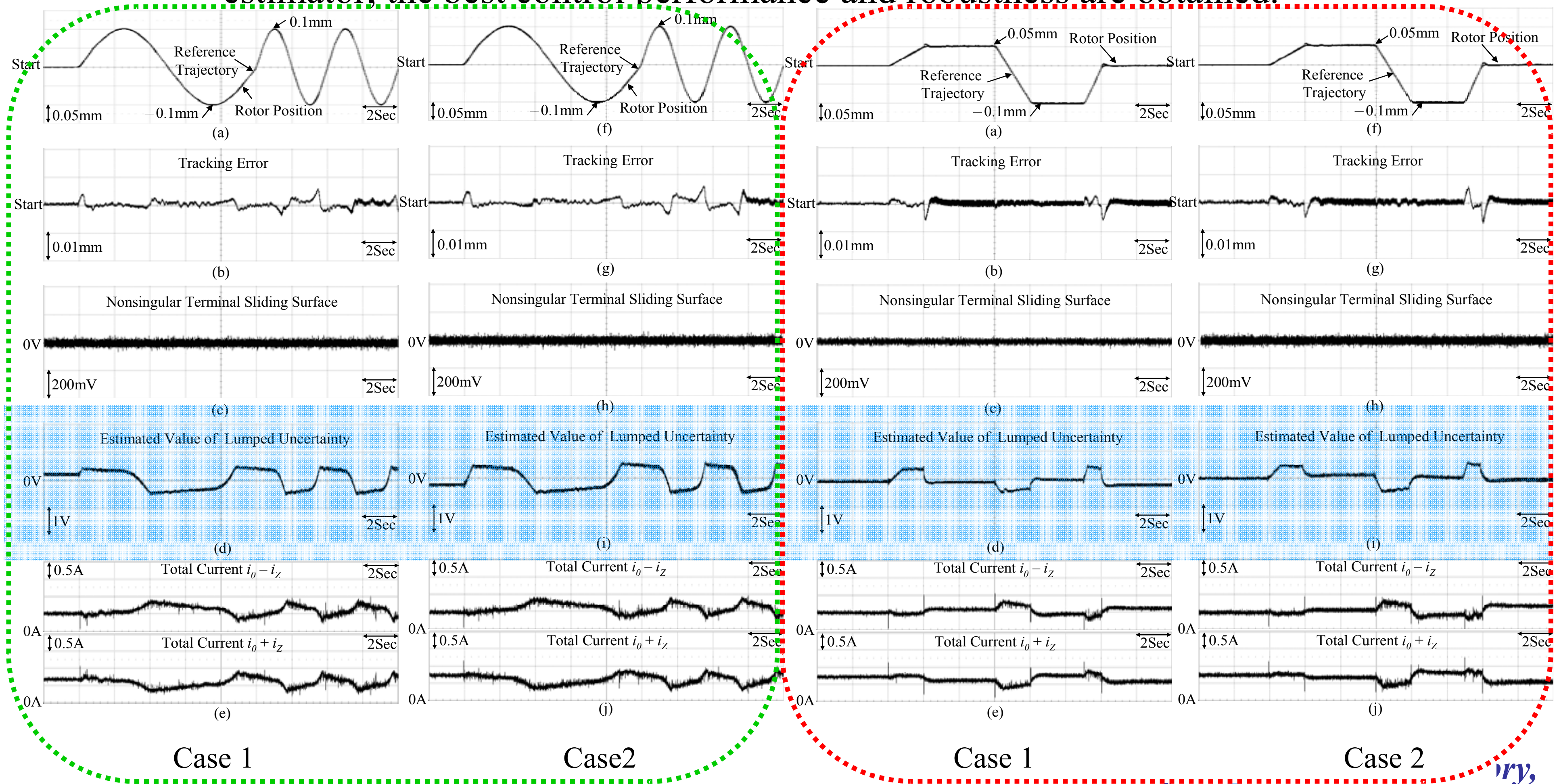

Precise Tracking Control of TAMB System—Using Robust Non-Singular Terminal SMC

- The performance measures of the TSMC, NTSMC and RNTSMC systems are shown in Table 5.1 and Table 5.2, respectively.
- Obviously, the proposed RNTSMC possesses the best robust control performance and can control the TAMB system effectively.

Table 5.1 Performance measures of TAMB control system using TSMC, NTSMC, and RNTSMC systems at Case 1.

Tracking Errors, μm	TSMC		NTSMC		RNTSMC	
	Sinusoid	Trapezoid	Sinusoid	Trapezoid	Sinusoid	Trapezoid
Maximum	7.697	6.997	8.448	7.834	5.303	5.963
Average	2.086	1.984	4.161	2.376	0.826	0.561
Standard Deviation	1.885	1.540	2.099	1.743	0.797	0.760

Table 5.2 Performance measures of TAMB control system using TSMC, NTSMC, and RNTSMC systems at Case 2.

Tracking Errors, μm	TSMC		NTSMC		RNTSMC	
	Sinusoid	Trapezoid	Sinusoid	Trapezoid	Sinusoid	Trapezoid
Maximum	7.260	9.140	9.541	9.355	5.666	7.372
Average	2.866	2.127	4.114	2.533	0.908	0.626
Standard Deviation	2.035	1.864	2.039	2.203	0.964	0.875

Outline

- Abstract
- Introduction
- System Dissection, Dynamic Analyses, and Experimental Designs of Five-DOF AMB System
  - TAMB System
  - Five-DOF AMB System
- Precise Tracking Control of TAMB System
  - Using Model-Free Control Methods
  - Using Adaptive Complementary Sliding-Mode Control
  - Using Robust Non-Singular Terminal Sliding-Mode Control
- Robust Control of Fully Suspended Five-DOF AMB System
  - Using Decentralized PID Neural Network Control
  - Using Decentralized Intelligent Double Integral Sliding-Mode Control
- Discussions and Conclusions

Robust Control of Fully Suspended Five-DOF AMB System Using Decentralized PIDNN Control

- The network structure of the PIDNN controller used for φ-axis of the five-DOF AMB system is shown as:

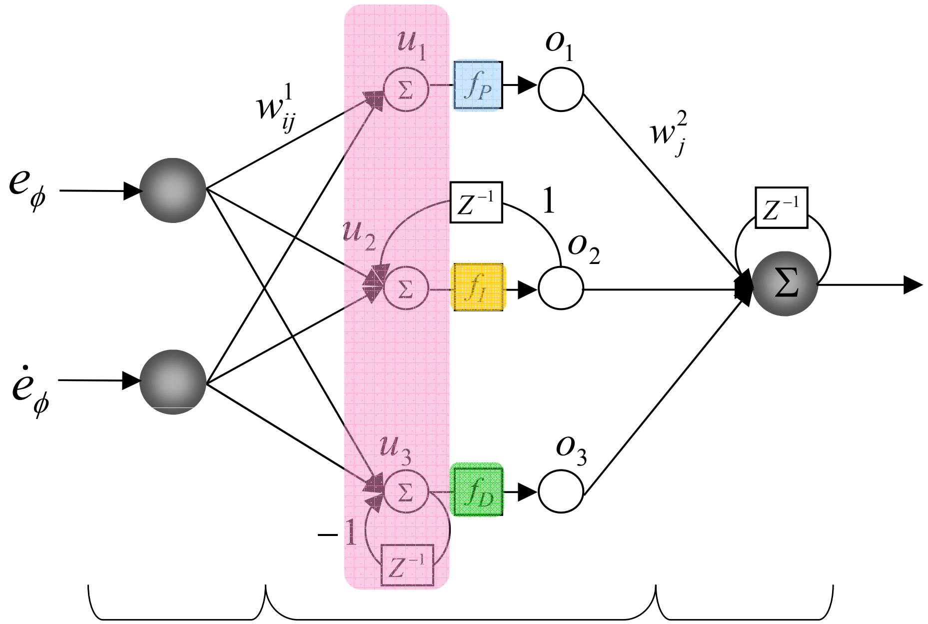

P control

$$o_1(N) = f_P\big(u_1(N)\big) = \sum_{i=1}^{2} w_{i1}^1(N)\phi_i(N)$$

I control

$$o_2(N) = f_I\big(u_2(N) + o_2(N-1)\big) = \sum_{i=1}^{2} w_{i2}^1(N)\phi_i(N) + o_2(N-1)$$

D control

$$o_3(N) = f_D\big(u_3(N) - u_3(N-1)\big) = \sum_{i=1}^{2} w_{i3}^1(N)\phi_i(N) - \sum_{i=1}^{2} w_{i3}^1(N-1)\phi_i(N-1)$$

Robust Control of Fully Suspended Five-DOF AMB System Using Decentralized PIDNN Control

- Te on-line learning algorithm of the PIDNN using supervised gradient decent method:

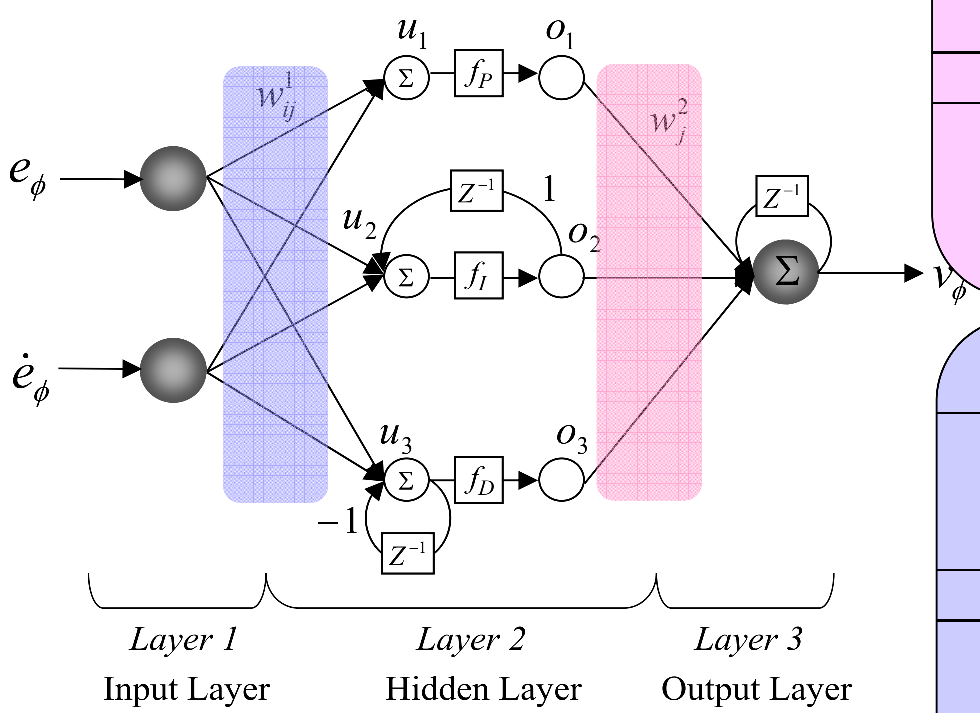

Connective Weight Between Hidden and Output Layers

$$\Delta w_j^2(N) = -\eta_{W^2}\frac{\partial E(N)}{\partial w_j^2(N)} = \eta_{W^2}\delta_\phi(N)o_j(N)$$

$$w_j^2(N+1) = w_j^2(N) + \Delta w_j^2(N)$$

Optimal Learning Rate

$$\eta_{W^2} = \frac{E(N)}{2\left\{\sum_{j=1}^{3}\left[\frac{\partial E(N)}{\partial w_j^2}\right]^2 + \varepsilon\right\}}$$

Connective Weight Between Input and Hidden Layers

$$\Delta w_{ij}^1(N) = -\eta_{W^1}\frac{\partial E(N)}{\partial w_{ij}^1(N)} = \eta_{W^1}\delta_\phi(N)w_j^2(N)\phi_i(N)$$

$$w_{ij}^1(N+1) = w_{ij}^1(N) + \Delta w_{ij}^1(N)$$

Optimal Learning Rate

$$\eta_{W^1} = \frac{E(N)}{2\left\{\sum_{i=1}^{2}\sum_{j=1}^{3}\left[\frac{\partial E(N)}{\partial w_{ij}^1}\right]^2 + \varepsilon\right\}}$$

$$E(N+1) = \frac{1}{2}e_\phi{}^2(N+1) < E(N)$$

Robust Control of Fully Suspended Five-DOF AMB System Using Decentralized PIDNN Control

- The configuration of the ψ-axis AMB control subsystem using PIDNN controller with on-line learning algorithm and adaptive learning rates is shown as follows:

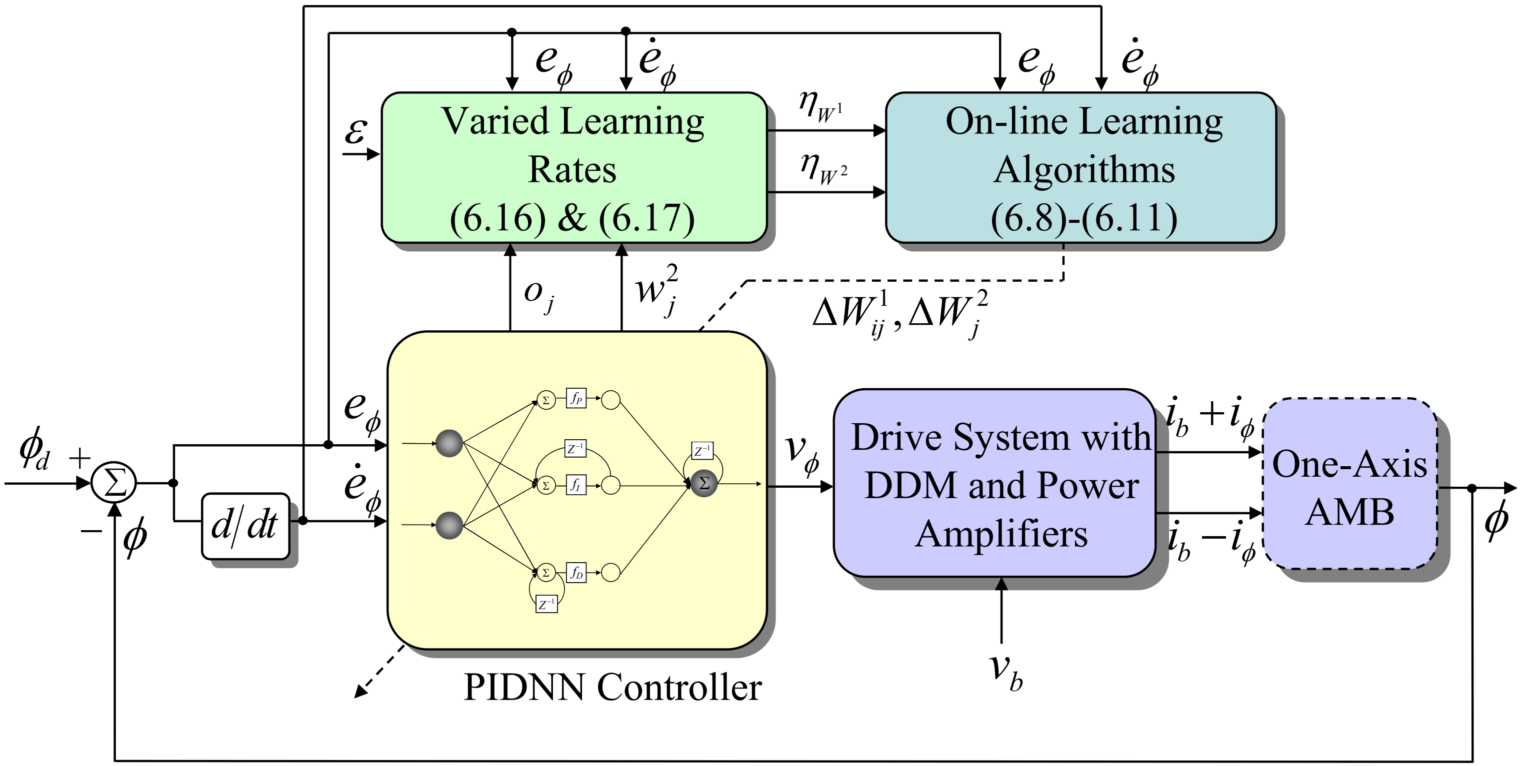

Robust Control of Fully Suspended Five-DOF AMB System Using Decentralized PIDNN Control

- *A. Experimental results of fully suspended five-DOF AMB control system using decentralized PID controller*
  - Five conventional PID controllers are also used to construct a decentralized PID controller for the comparison of control performances.

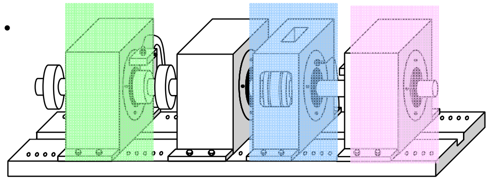

$$u_{\phi} = K_{P\phi} e_{\phi} + K_{I\phi} \int_0^t e_{\phi} dt + K_{D\phi} \dot{e}_{\phi}$$

maximum run outs: 0.2 mm

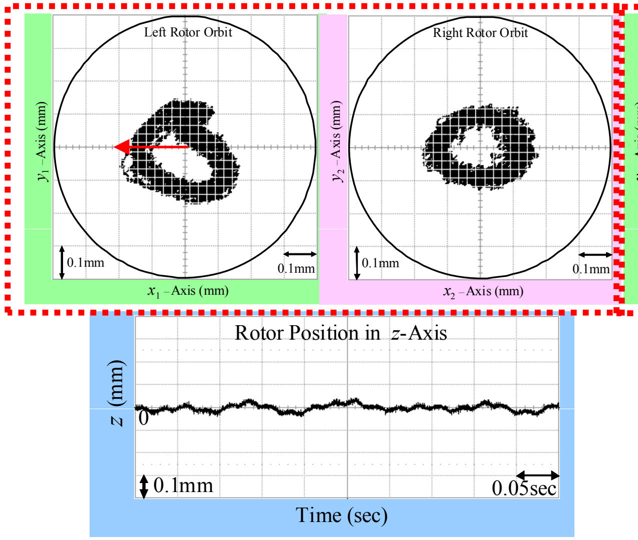

Case 1
2400RPM

maximum run outs: 0.238 mm

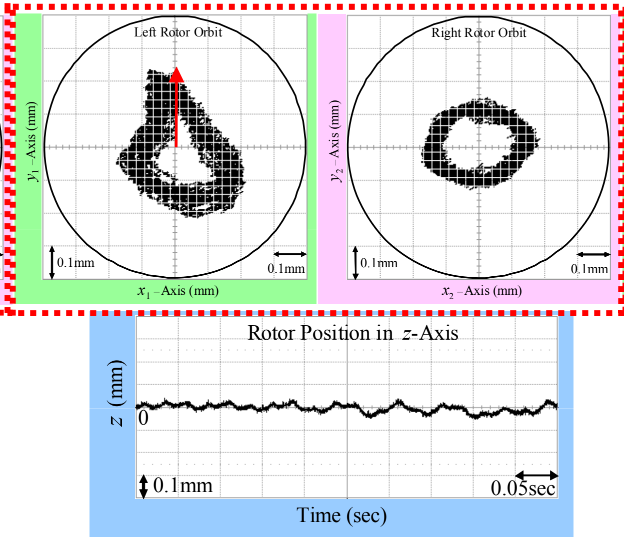

Case2
2400RPM with Load

maximum run outs: 0.282 mm

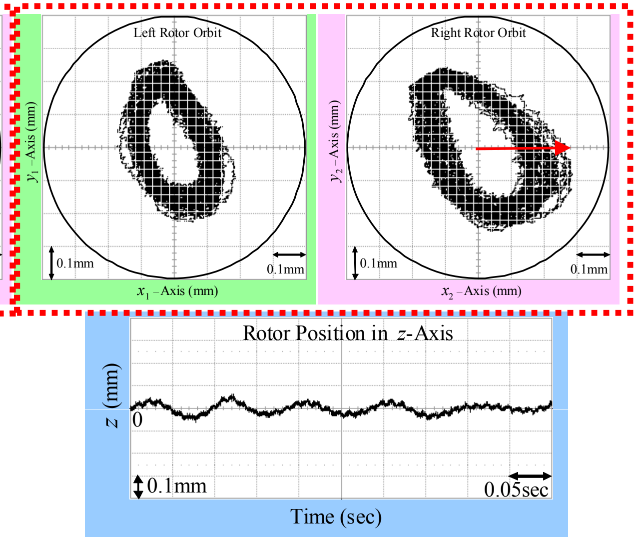

Case 3
4800RPM

Robust Control of Fully Suspended Five-DOF AMB System Using Decentralized PIDNN Control

- *A. Experimental results of fully suspended five-DOF AMB control system using decentralized PIDNN controller*
  - Five proposed PIDNN controllers are used to construct a decentralized PIDNN controller to achieve the regulating and stabilizing purposes for the fully suspended five-DOF AMB control system.

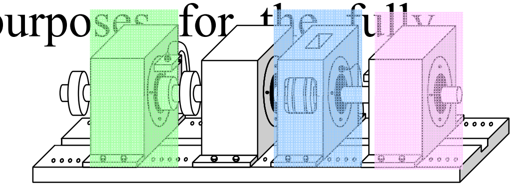

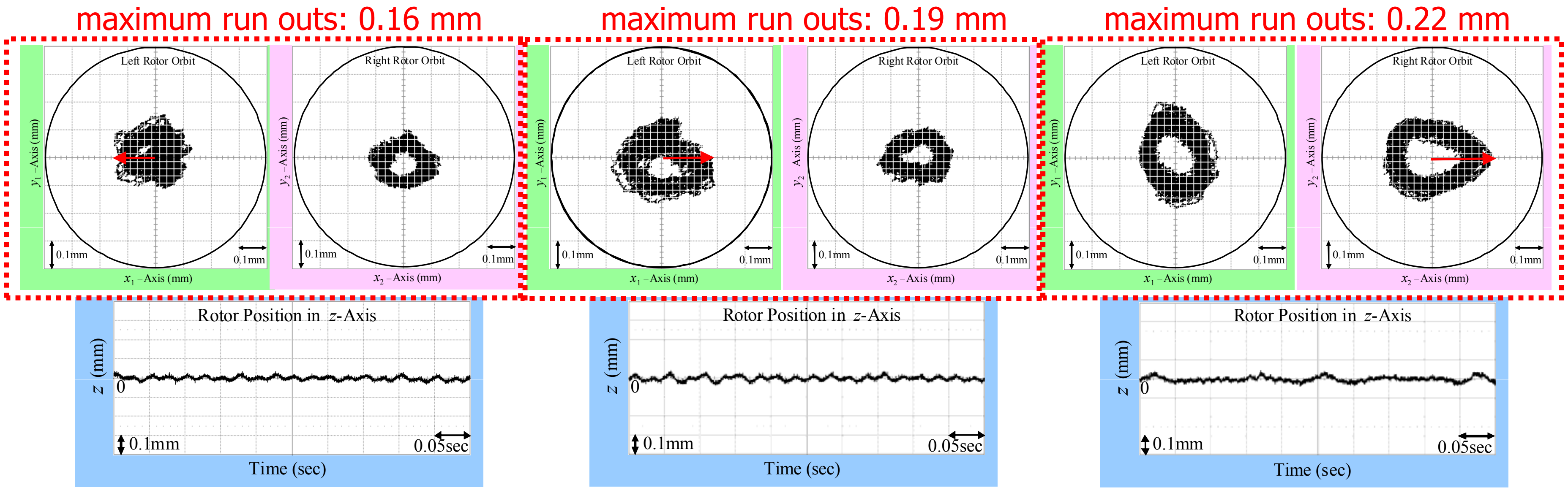

Case 1
2400RPM

Case2
2400RPM with Load

Case 3
4800RPM

Robust Control of Fully Suspended Five-DOF AMB System Using Decentralized PIDNN Control

- The performance measures of the decentralized PID controller, decentralized PIDNN controller are shown in the following.
- Obviously, the proposed decentralized PIDNN controller possesses the better robust control performance.

Axes	Regulating Errors (μm)	Case 1		Case 2		Case 3	
		PID	PIDNN	PID	PIDNN	PID	PIDNN
x_1	RMS Values	79.02	60.68	92.94	77.64	82.72	73.81
	Peak to Peak Values	359.1	278.7	390.5	373.3	356.0	286.5
y_1	RMS Values	88.39	50.85	114.09	72.38	130.60	87.62
	Peak to Peak Values	315.9	265.9	447.5	307.7	486.7	377.9
x_2	RMS Values	90.23	59.95	102.98	70.86	125.87	104.42
	Peak to Peak Values	351.1	259.8	358.8	276.4	495.1	389.0
y_2	RMS Values	66.54	52.00	73.29	46.71	148.03	74.75
	Peak to Peak Values	259.8	215.1	277.7	213.2	495.0	302.7
z	RMS Values	14.42	9.45	17.01	11.30	21.45	12.34
	Peak to Peak Values	84.7	66.3	93.7	75.6	126.8	83.2

Outline

- Abstract
- Introduction
- System Dissection, Dynamic Analyses, and Experimental Designs of Five-DOF AMB System
  - TAMB System
  - Five-DOF AMB System
- Precise Tracking Control of TAMB System
  - Using Model-Free Control Methods
  - Using Adaptive Complementary Sliding-Mode Control
  - Using Robust Non-Singular Terminal Sliding-Mode Control
- Robust Control of Fully Suspended Five-DOF AMB System
  - Using Decentralized PID Neural Network Control
  - Using Decentralized Intelligent Double Integral Sliding-Mode Control
- Discussions and Conclusions

Robust Control of Fully Suspended Five-DOF AMB System Using Decentralized IDISMC System

- From the developed decoupled dynamic model, the standard second order state equation of the one-axis AMB subsystem is:

$$\underline{M}\ddot{X} = \underline{A}X + \underline{B}U + \underline{M}H$$

$$\ddot{x}(t) = Ax(t) + BU(t) + h(t)$$

- Considering the separation of the nominal parameters and parameter variations as follows:

$$\ddot{x}(t) = [A_n + \Delta A(\boldsymbol{x};t)]x(t) + [B_n + \Delta B(\boldsymbol{x};t)]U(t) + h(t)$$
$$= A_n x(t) + B_n U(t) + \boxed{L(\boldsymbol{x};t)}$$

$$\begin{bmatrix} h_{x_1} \\ h_{x_2} \\ h_{y_1} \\ h_{y_2} \\ h_z \end{bmatrix} = \begin{bmatrix} -\alpha_1\dot{y}_1 + \alpha_1\dot{y}_2 + 2k_{rp}\beta_2 x_2 + 2k_{ri}\beta_2 i_{x_2} + \gamma_1 f_{dx} \\ \alpha_2\dot{y}_1 - \alpha_2\dot{y}_2 + 2k_{rp}\beta_2 x_1 + 2k_{ri}\beta_2 i_{x_1} + \gamma_2 f_{dx} \\ \alpha_1\dot{x}_1 - \alpha_1\dot{x}_2 + 2k_{rp}\beta_2 y_2 + 2k_{ri}\beta_2 i_{y_2} + \gamma_1 f_{dy} - g \\ -\alpha_2\dot{x}_1 + \alpha_2\dot{x}_2 + 2k_{rp}\beta_2 y_1 + 2k_{ri}\beta_2 i_{y_1} + \gamma_2 f_{dy} - g \\ \gamma_3 f_{dz} \end{bmatrix}$$

- $L(\boldsymbol{x};t)$ is called the lumped uncertainty and defined as

$$\boxed{L(\boldsymbol{x};t) = \Delta A(\boldsymbol{x};t)x(t) + \Delta B(\boldsymbol{x};t)U(t) + h(t)}$$

- The bound of the lumped uncertainty is necessary to be known in advance and satisfies the inequality as follows:

$$|L(\boldsymbol{x};t)| < \delta$$

Robust Control of Fully Suspended Five-DOF AMB System Using Decentralized ISMC System

- *A. Decentralized Integral Sliding-Mode Control (ISMC)*
  - First, the regulating error $e \equiv x_d - x$ is defined where e represents the reference position and is designed as zero in the AMB applications.
  - Then, a conventional integral sliding surface s_1 is defined as follows:

    $$s_1(t) = \dot{e}(t) + c_1 e(t) + c_2 \int_0^t e(\tau) d\tau$$

  - The GUUB stability is guaranteed if the control effort $U(t)$ is using the control law $U_{ISMC}(t)$ of ISMC designed as:

    $$U_{ISMC}(t) = B_n^{-1}\left[\ddot{x}_d(t) - A_n x(t) + c_1 \dot{e}(t) + c_2 e(t) + \delta \mathrm{sat}(s_1(t))\right]$$

  - Therefore, the control law of ISMC ensures that any initial states outside the boundary layer ($s_1(0)>\Phi$) will reach the boundary layer in finite time and remain inside thereafter ($s_1(t) \leqq \Phi$).
  - Five ISMC systems are used to construct a decentralized ISMC system for the comparison of control performances.

Robust Control of Fully Suspended Five-DOF AMB System Using Decentralized Ideal IDISMC System

- *B. Decentralized Intelligent Double Integral Sliding-Mode Control*
- (a) *Ideal IDISMC*
  - To improve the steady-state control performance, a double integral sliding surface s_2 is defined as follows:

$$s_2(t) = \dot{e}(t) + c_1 e(t) + c_2 \int_0^t e(\tau)d\tau + \boxed{c_3 \int_0^t \int_0^t e(\tau)d\tau d\tau}$$

  - Differentiating $s_2(t)$ with respect to time, one can obtain

$$\begin{aligned} \dot{s}_2(t) &= \ddot{e}(t) + c_1\dot{e}(t) + c_2 e(t) + c_3 \int_0^t e(\tau)d\tau \\ &= \ddot{x}_d(t) - A_n x(t) - B_n U(t) - L(\boldsymbol{x};t) + c_1\dot{e}(t) + c_2 e(t) + c_3 \int_0^t e(\tau)d\tau \end{aligned}$$

  - In order to achieve the GUUB stability of the AMB subsystem, the control law of the ideal IDISMC is designed as follows:

$$\boxed{\overline{U}_{IDISMC}(t) = B_n^{-1}\left[\ddot{x}_d(t) - A_n x(t) + c_1\dot{e}(t) + c_2 e(t) + c_3 \int_0^t e(\tau)d\tau + \delta \text{sat}(s_2(t))\right]}$$

Robust Control of Fully Suspended Five-DOF AMB System Using Decentralized Ideal IDISMC System

- Observing the ISMC and ideal IDISMC, the integral term is embedded in both the integral and double integral sliding surfaces but reflected only in the IDISMC control law.

$$s_1(t) = \dot{e}(t) + c_1 e(t) + c_2 \int_0^t e(\tau)d\tau$$

$$U_{ISMC}(t) = B_n^{-1}\left[\ddot{x}_d(t) - A_n x(t) + c_1\dot{e}(t) + c_2 e(t) + \delta \mathrm{sat}(s_1(t))\right]$$

$$s_2(t) = \dot{e}(t) + c_1 e(t) + c_2 \int_0^t e(\tau)d\tau + c_3 \int_0^t \int_0^t e(\tau)d\tau d\tau$$

PID Controller

$$\overline{U}_{IDISMC}(t) = B_n^{-1}\left[\ddot{x}_d(t) - A_n x(t) + c_1\dot{e}(t) + c_2 e(t) + c_3 \int_0^t e(\tau)d\tau + \delta \mathrm{sat}(s_2(t))\right]$$

- Therefore, the ideal IDISMC with integral control features results in improved steady-state error performance compared with the ISMC.
- However, it will cause saturated control effort easily and the control parameters c_1, c_2, c_3, δ, and Φ are very difficult to design overall.
- Hence, the optimal output of the MPIDNN observer also named as the observation target, is defined as follows:

$$y(t) = c_1\dot{e}(t) + c_2 e(t) + c_3 \int_0^t e(\tau)d\tau - L(\boldsymbol{x};t)$$

Robust Control of Fully Suspended Five-DOF AMB System Using Decentralized IDISMC System

- (b) *MPIDNN observer*
  - The well-designed MPIDNN observer results in ingenious mapping between the network architecture and observation target.
  - According to the on-line tuning, not only the PID control gains K_P, K_I, and K_D are adaptive real time but also the lumped uncertainty $L(\boldsymbol{x};t)$ is observed on-line.

$$\overline{U}_{IDISMC}(t) = B_n^{-1}\left[\ddot{x}_d(t) - A_n x(t) + \underbrace{c_1\dot{e}(t) + c_2 e(t) + c_3\int_0^t e(\tau)\,d\tau + \delta\,\mathrm{sat}(s_2(t))}_{\hat{y}(t)}\right]$$

$$\hat{y}(t) = K_P(t)o_1 + K_I(t)o_2 + K_D(t)o_3 + K_L(t)o_4$$

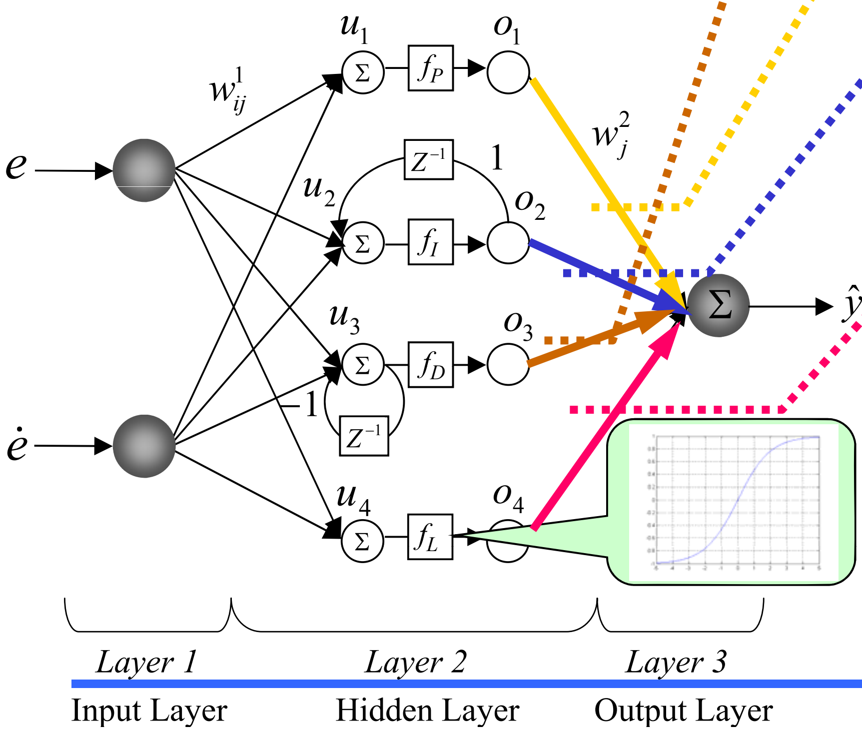

$$o_1(N) = f_P\left(u_1(N)\right)$$

$$o_2(N) = f_I\left(u_2(N) + o_2(N-1)\right)$$

$$o_3(N) = f_D\left(u_3(N) - u_3(N-1)\right)$$

$$o_4(N) = f_L\left(u_4(N)\right) = \frac{1-\exp\left[-\sum_{i=1}^{2} w_{i4}^1(N)e_i(N)\right]}{1+\exp\left[-\sum_{i=1}^{2} w_{i4}^1(N)e_i(N)\right]}$$

$$\hat{y}(N) = \sum_{j=1}^{4} w_j^2(N)o_j(N)$$

$$\hat{y}(e\,|\,\hat{\boldsymbol{W}}) = \hat{\boldsymbol{W}}^T\boldsymbol{O}$$

$$y = y^*(e\,|\,\boldsymbol{W}^*) + \varepsilon$$

$$= \boldsymbol{W}^{*T}\boldsymbol{O} + \varepsilon$$

Robust Control of Fully Suspended Five-DOF AMB System Using Decentralized IDISMC System

- (c) *IDISMC system*
  - ***Theorem 7.1***: Considering the AMB subsystem represented by (7.2), if the proposed control law U_{IDISMC} of IDISMC, which is composed of a robust controller U_r with adaptive law, and the MPIDNN observer U_y with learning algorithm, is adopted as the control effort , then the asymptotic stability of the AMB subsystem is guaranteed.

$$U_{IDISMC}(t) = U_r(t) + U_y(t)$$

$$U_r(t) = B_n^{-1}\left[\ddot{x}_d(t) - A_n x(t) + \hat{\varepsilon} + \xi s_2(t)\right] \quad \text{using adaptive law} \quad \dot{\hat{\varepsilon}} = \eta_\varepsilon s_2(t)$$

$$U_y(t) = B_n^{-1}\hat{y}(t) \quad \text{using estimation law} \quad \dot{\hat{\boldsymbol{W}}} = \eta_W s_2(t)\boldsymbol{O}$$

  - ***Proof:*** Choose the Lyapunov function as

$$V(s_2(t), \tilde{\boldsymbol{W}}, \tilde{\varepsilon}) = \frac{1}{2}s_2{}^2(t) + \frac{B_n}{2\eta_W}\tilde{\boldsymbol{W}}^T\tilde{\boldsymbol{W}} + \frac{B_n}{2\eta_\varepsilon}\tilde{\varepsilon}^2 \quad \text{where } \tilde{\boldsymbol{W}} = \boldsymbol{W}^* - \hat{\boldsymbol{W}} \text{ and } \tilde{\varepsilon} = \varepsilon - \hat{\varepsilon}$$

  - Taking the time derivative of the Lyapunov function, one can obtain

$$\dot{V}(s_2(t), \tilde{\boldsymbol{W}}, \tilde{\varepsilon}) = s_2(t)\dot{s}_2(t) - \frac{1}{\eta_W}\tilde{\boldsymbol{W}}^T\dot{\hat{\boldsymbol{W}}} - \frac{1}{\eta_\varepsilon}\tilde{\varepsilon}\dot{\hat{\varepsilon}} = -\xi s_2{}^2(t)$$

By using Barbalat's Lemma, it can be shown that $s_2(t)$ will converge to zero as $t \to \infty$, therefore, asymptotic stability is guaranteed.

Robust Control of Fully Suspended Five-DOF AMB System Using Decentralized IDISMC System

- The configuration of the one-axis AMB control subsystem using IDISMC system with MISO MPIDNN RHNN observer is shown as follows:

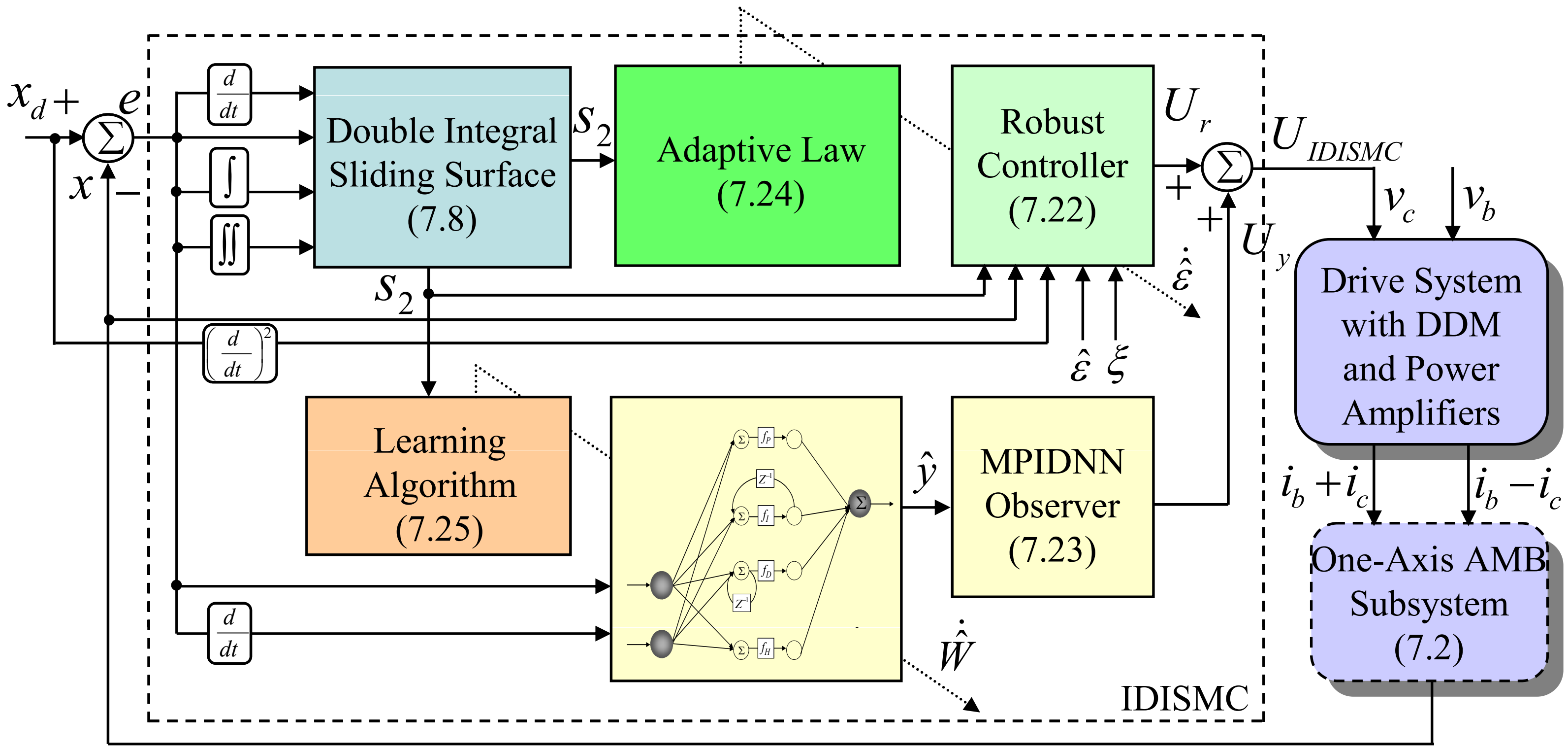

Robust Control of Fully Suspended Five-DOF AMB System Using Decentralized IDISMC System

- *A. Experimental results of fully suspended five-DOF AMB control system using decentralized ISMC system*
  - Five ISMC systems are used to construct a decentralized ISMC system for the comparison of control performances.

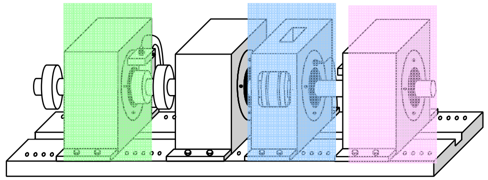

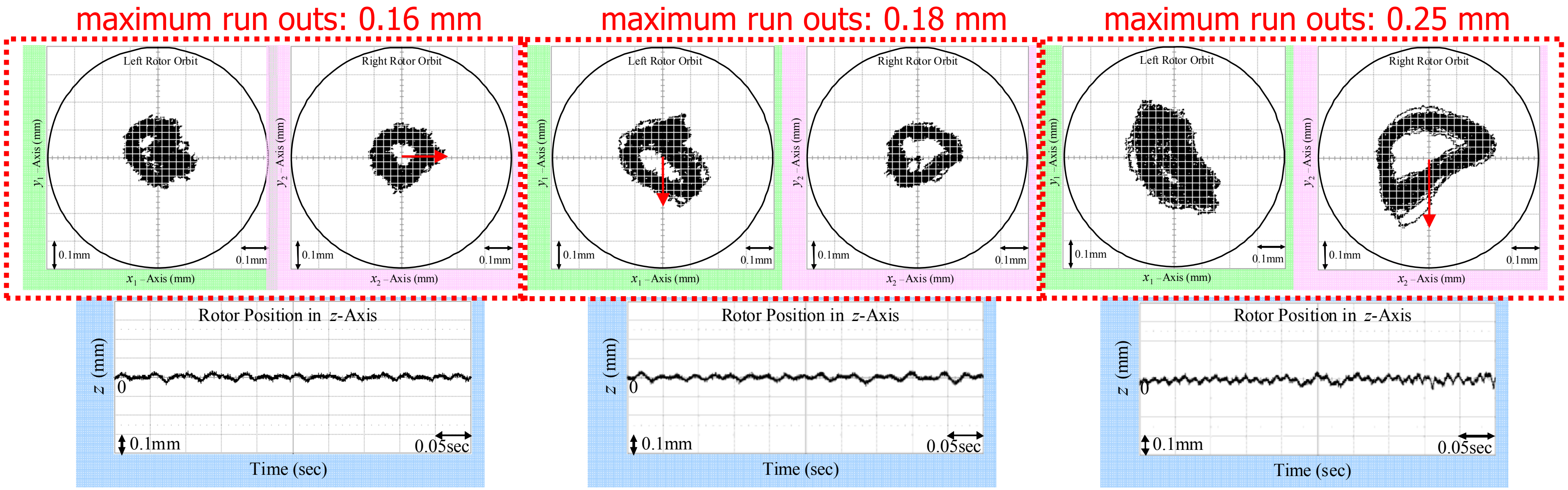

Case 1
2400RPM

Case2
2400RPM with Load

Case 3
4800RPM

Robust Control of Fully Suspended Five-DOF AMB System Using Decentralized IDISMC System

- *A. Experimental results of fully suspended five-DOF AMB control system using decentralized IDISMC system*
  - Five proposed IDISMC systems are used to construct a decentralized IDISMC system to achieve the regulating and stabilizing purposes for the fully suspended five-DOF AMB control system.

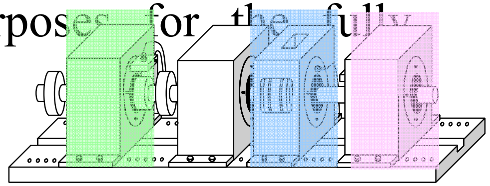

maximum run outs: 0.14 mm　　maximum run outs: 0.15 mm　　maximum run outs: 0.19 mm

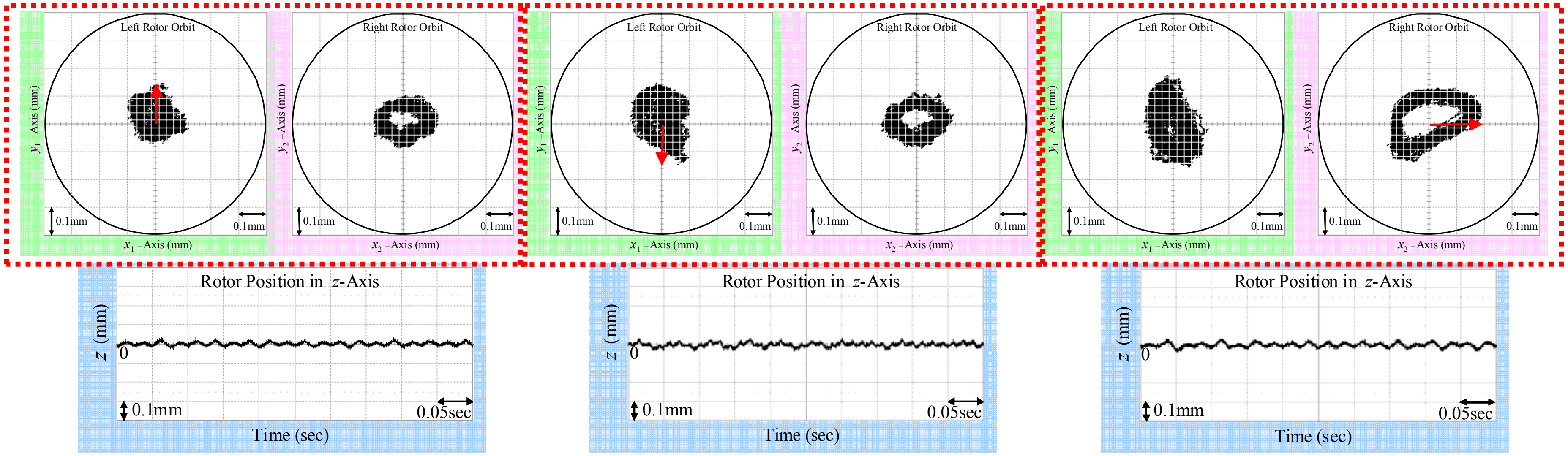

Case 1	Case2	Case 3
2400RPM	2400RPM with Load	4800RPM

Robust Control of Fully Suspended Five-DOF AMB System Using Decentralized IDISMC System

- The performance measures of the decentralized ISMC system, decentralized IDISMC system are shown in the following.
- Obviously, the proposed decentralized IDISMC system possesses the better robust control performance.

Axes	Regulating Errors (μm)	Case 1		Case 2		Case 3	
		ISMC	IDISMC	ISMC	IDISMC	ISMC	IDISMC
x_1	RMS Values	56.27	45.04	69.93	45.55	76.90	45.81
	Peak to Peak Values	269.3	218.4	328.2	212.6	341.7	230.7
y_1	RMS Values	59.87	45.29	82.39	62.94	102.34	77.54
	Peak to Peak Values	267.2	211.7	335.0	290.2	408.6	326.6
x_2	RMS Values	66.32	58.48	79.50	61.28	125.34	97.27
	Peak to Peak Values	276.0	233.2	283.0	262.6	438.6	338.3
y_2	RMS Values	50.94	44.20	59.20	45.27	95.10	68.53
	Peak to Peak Values	255.1	190.7	236.2	204.3	435.7	265.6
z	RMS Values	10.43	8.93	11.70	10.43	14.06	10.93
	Peak to Peak Values	75.6	60.3	80.8	68.3	96.8	74.4

Outline

- Abstract
- Introduction
- System Dissection, Dynamic Analyses, and Experimental Designs of Five-DOF AMB System
  - TAMB System
  - Five-DOF AMB System
- Precise Tracking Control of TAMB System
  - Using Model-Free Control Methods
  - Using Adaptive Complementary Sliding-Mode Control
  - Using Robust Non-Singular Terminal Sliding-Mode Control
- Robust Control of Fully Suspended Five-DOF AMB System
  - Using Decentralized PID Neural Network Control
  - Using Decentralized Intelligent Double Integral Sliding-Mode Control
- Discussions and Conclusions

Discussions

- This dissertation had developed various PC-based control systems to control the rotor position in the axial direction of the TAMB system for the tracking of various reference trajectories.
  - *Therefore, the moveable controlled rotor of the TAMB system can be applied to different operating demands and environments.*

- On the other hand, several PC-based decentralized control systems were developed based on the proposed decoupled dynamic model to regulate and stabilize the five-axes of the rotor of the five-DOF AMB system in the centers considering the existences of the serious uncertainties.
  - *According to the decoupled procedure and decentralized concept, the controller design was simplified and the computational burden was reduced.*

Discussions

- Table 8.1 shows the comparison of different ultimate bounds of various SMC approaches including SMC, CSMC, ACSMC, TSMC, NTSMC, and RNTSMC.
  - Since SMC, CSMC, TSMC, and NTSMC use saturation functions for chattering reduction, only GUUB stabilities can be guaranteed.
  - Since the saturation functions are not used in the ACSMC and RNTSMC, both of them can guarantee the asymptotic stabilities through Lyapunov theorem and Barbalat's Lemma.

	SMC	CSMC	ACSMC	TSMC	NTSMC	RNTSMC
Sliding Surfaces	$s(t)=\left(\frac{d}{dt}+\lambda\right)e(t)$	$s_g(t)=\left(\frac{d}{dt}+\lambda\right)^2\Lambda(t)$ $s_c(t)=\left(\frac{d}{dt}+\lambda\right)\left(\frac{d}{dt}-\lambda\right)\Lambda(t)$ where $\Lambda(t)=\int_0^t e(\tau)d\tau$	$s_g(t)=\left(\frac{d}{dt}+\lambda\right)^2\Lambda(t)$ $s_c(t)=\left(\frac{d}{dt}+\lambda\right)\left(\frac{d}{dt}-\lambda\right)\Lambda(t)$ where $\Lambda(t)=\int_0^t e(\tau)d\tau$	$s_m(t)=\dot{e}(t)+\lambda e(t)^{\frac{q}{p}}$	$s_n(t)=e(t)+\frac{1}{\lambda}\dot{e}(t)^{\frac{p}{q}}$ where $p>q$	$s_n(t)=e(t)+\frac{1}{\lambda}\dot{e}(t)^{\frac{p}{q}}$ where $p>q$
Ultimate Bounds	$\lim_{t\to\infty}\lvert e(t)\rvert\le\frac{\Phi}{\lambda}$ $\lim_{t\to\infty}\lvert\dot{e}(t)\rvert\le 2\Phi$	$\lim_{t\to\infty}\lvert e(t)\rvert\le\frac{\Phi}{2\lambda}$ $\lim_{t\to\infty}\lvert\dot{e}(t)\rvert\le\Phi$	$\lim_{t\to\infty}\lvert e(t)\rvert=0$ $\lim_{t\to\infty}\lvert\dot{e}(t)\rvert=0$	$\lim_{t\to\infty}\lvert e(t)\rvert\le\left(\frac{\Phi}{\lambda}\right)^{\frac{p}{q}}$ $\lim_{t\to\infty}\lvert\dot{e}(t)\rvert\le 2\Phi$	$\lim_{t\to\infty}\lvert e(t)\rvert\le\Phi$ $\lim_{t\to\infty}\lvert\dot{e}(t)\rvert\le(2\lambda\Phi)^{\frac{q}{p}}$	$\lim_{t\to\infty}\lvert e(t)\rvert=0$ $\lim_{t\to\infty}\lvert\dot{e}(t)\rvert=0$

GUUB stabilities   asymptotic stabilities   GUUB stabilities   asymptotic stabilities

Discussions

- The ultimate bounds of tracking error e can be ordered as TSMC<CSMC<SMC<NTSMC.
- The ultimate bounds of tracking error's derivative $\dot{e}$ can be ordered as CSMC<TSMC=SMC<NTSMC.
- Obviously, CSMC and TSMC own the two best steady-state control performances.

	SMC	CSMC	ACSMC	TSMC	NTSMC	RNTSMC
Sliding Surfaces	$s(t)=\left(\frac{d}{dt}+\lambda\right)e(t)$	$s_g(t)=\left(\frac{d}{dt}+\lambda\right)^2\Lambda(t)$ $s_c(t)=\left(\frac{d}{dt}+\lambda\right)\left(\frac{d}{dt}-\lambda\right)\Lambda(t)$ where $\Lambda(t)=\int_0^t e(\tau)d\tau$	$s_g(t)=\left(\frac{d}{dt}+\lambda\right)^2\Lambda(t)$ $s_c(t)=\left(\frac{d}{dt}+\lambda\right)\left(\frac{d}{dt}-\lambda\right)\Lambda(t)$ where $\Lambda(t)=\int_0^t e(\tau)d\tau$	$s_m(t)=\dot{e}(t)+\lambda e(t)^{\frac{q}{p}}$	$s_n(t)=e(t)+\frac{1}{\lambda}\dot{e}(t)^{\frac{p}{q}}$ where $p>q$	$s_n(t)=e(t)+\frac{1}{\lambda}\dot{e}(t)^{\frac{p}{q}}$ where $p>q$
Ultimate Bounds	$\lim_{t\to\infty}\lvert e(t)\rvert\le\frac{\Phi}{\lambda}$ $\lim_{t\to\infty}\lvert\dot{e}(t)\rvert\le 2\Phi$	$\lim_{t\to\infty}\lvert e(t)\rvert\le\frac{\Phi}{2\lambda}$ $\lim_{t\to\infty}\lvert\dot{e}(t)\rvert\le\Phi$	$\lim_{t\to\infty}\lvert e(t)\rvert=0$ $\lim_{t\to\infty}\lvert\dot{e}(t)\rvert=0$	$\lim_{t\to\infty}\lvert e(t)\rvert\le\left(\frac{\Phi}{\lambda}\right)^{\frac{p}{q}}$ $\lim_{t\to\infty}\lvert\dot{e}(t)\rvert\le 2\Phi$	$\lim_{t\to\infty}\lvert e(t)\rvert\le\Phi$ $\lim_{t\to\infty}\lvert\dot{e}(t)\rvert\le(2\lambda\Phi)^{\frac{q}{p}}$	$\lim_{t\to\infty}\lvert e(t)\rvert=0$ $\lim_{t\to\infty}\lvert\dot{e}(t)\rvert=0$

Discussions

- The different ultimate bounds of SMC, CSMC, TSMC, and NTSMC systems due to various values of λ are depicted in Fig. 8.1.
  - The larger values of λ result in the smaller ultimate bounds of tracking error e for SMC, and CSMC, and TSMC systems;
  - The larger values of λ result in the larger ultimate bounds of tracking error's derivative $\dot{e}$ for NTSMC system.

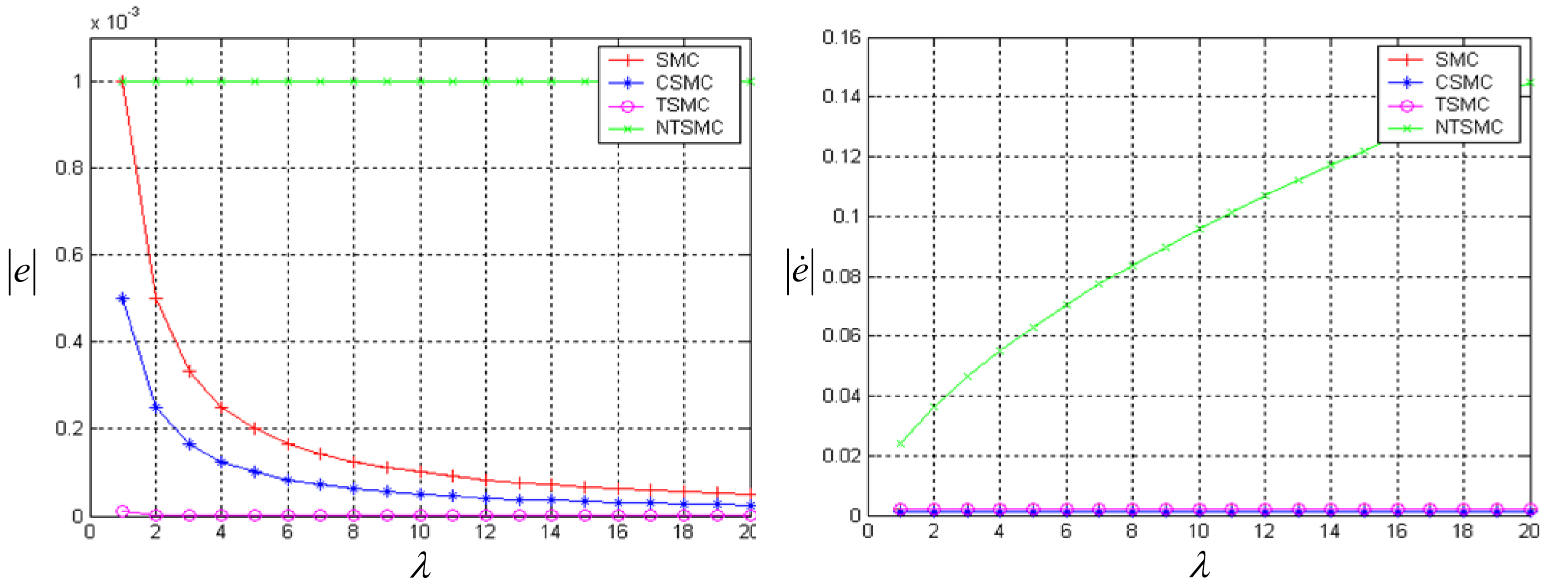

(a) (b)

Fig. 8.1 Different ultimate bounds of SMC, CSMC, TSMC, and NTSMC systems due to Φ=0.001, p=5, q=3, and various values of λ. (a) Ultimate bounds of tracking error. (b) Ultimate bounds of tracking error's derivative.

Discussions

- Comparisons of different control methods for TAMB control system
  - From the bar charts, the ACSMC and RNTSMC systems result in better control performances comparing with the others.

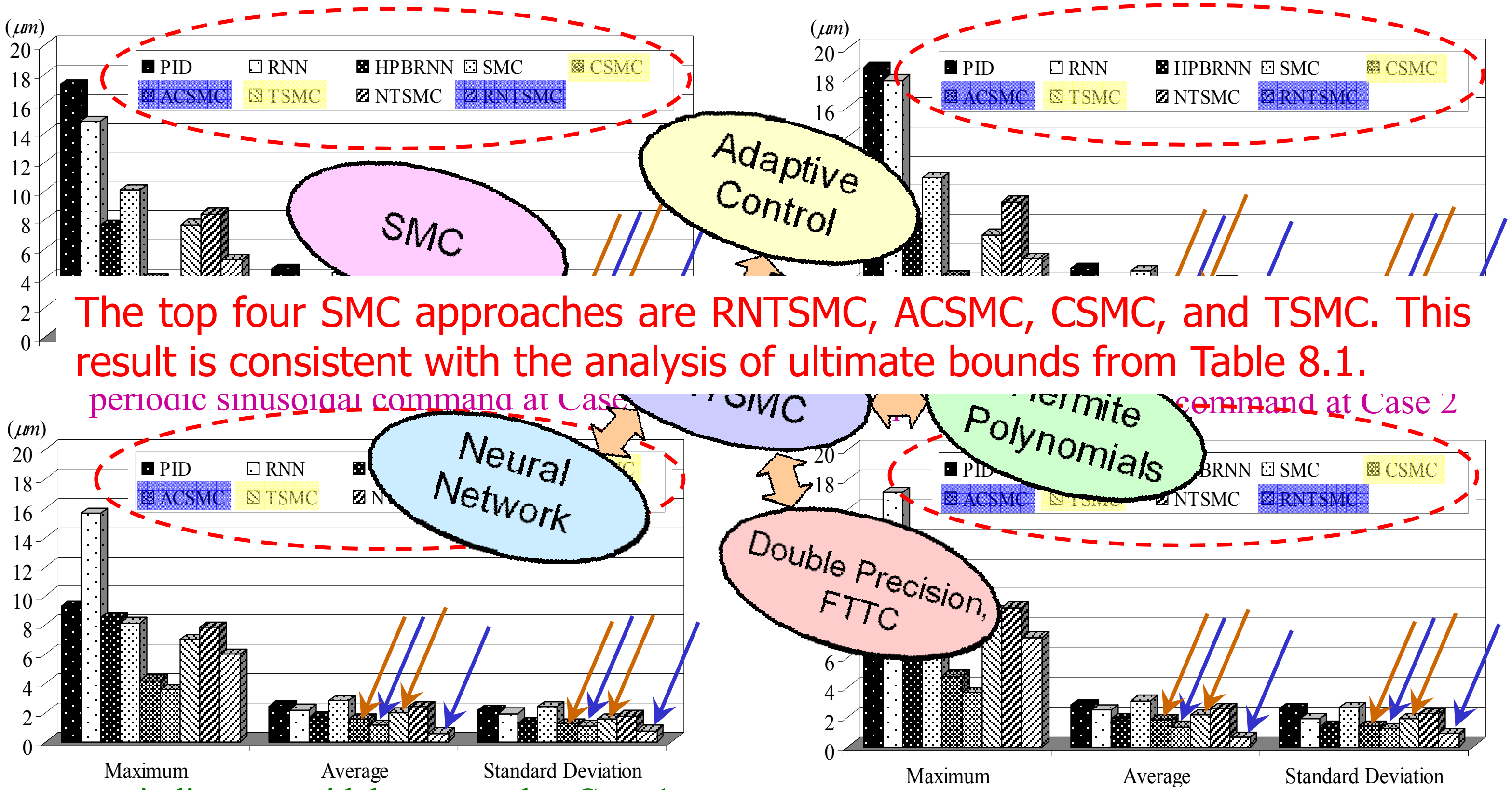

non-periodic trapezoidal command at Case 1

non-periodic trapezoidal command at Case 2

Discussions

- The comparison of control performance measures including RMS and peak to peak values of respective axes at Cases 1-3:
  - The control performance behaviors in accordance with the descending order are decentralized IDISMC system, decentralized PIDNN controller, decentralized ISMC system, and decentralized PID controller

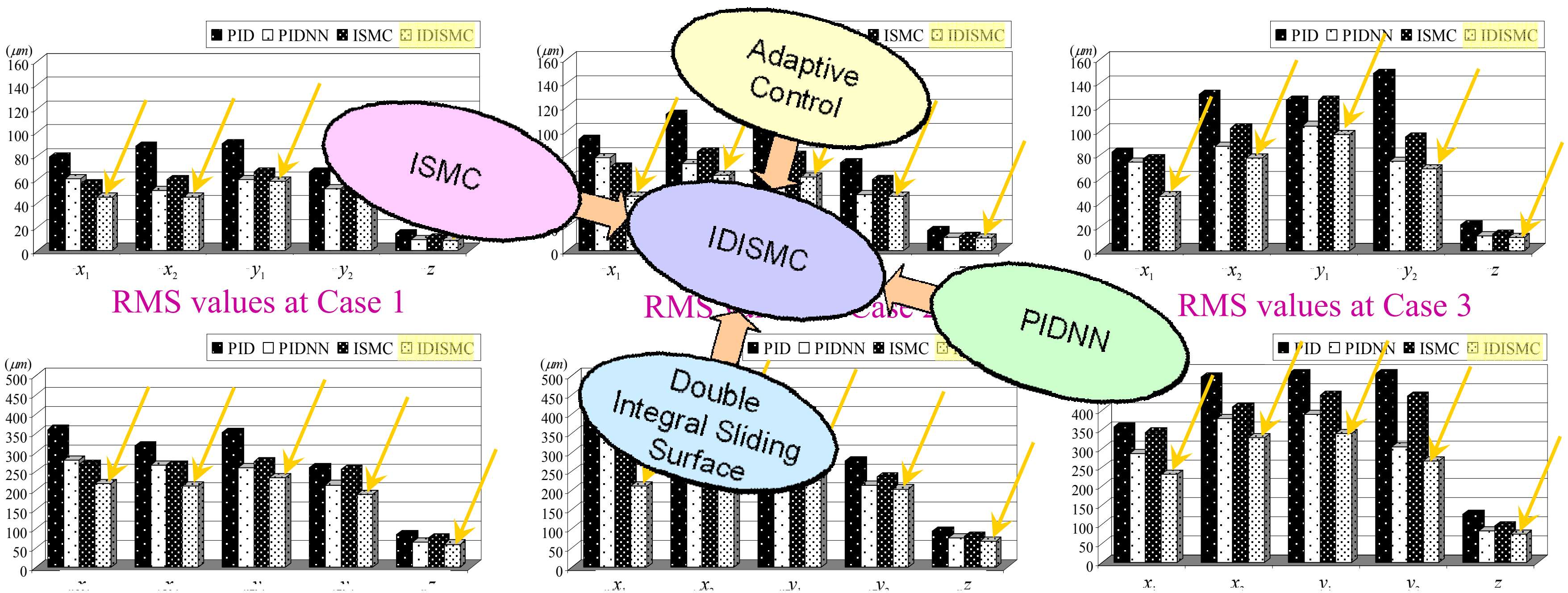

RMS values at Case 1

RMS values at Case 2

RMS values at Case 3

Peak-to-peak values at Case 1

Peak-to-peak values at Case 2

Peak-to-peak values at Case 3

Conclusions

- The major contributions of this dissertation are concluded as follows:
  1) the complete analyses of the dynamics and the detailed discussions of the drive systems for TAMB and RAMB systems;
  2) the successful developments of the various tracking controllers for the TAMB control system;
  3) the complete comparison of guaranteed ultimate bounds of various SMC approaches while using saturation functions;
  4) the successful implementations of the TAMB control system using the developed tracking controllers;
  5) the successful derivation of the decoupled dynamic model of the five-DOF AMB system for the purpose of decentralized control;
  6) the successful developments of the various decentralized control systems for the regulation and stabilization of the fully suspended five-DOF AMB control system;
  7) the successful implementations of the five-DOF AMB control system using the developed decentralized control systems.

Thank You for Your Attention!

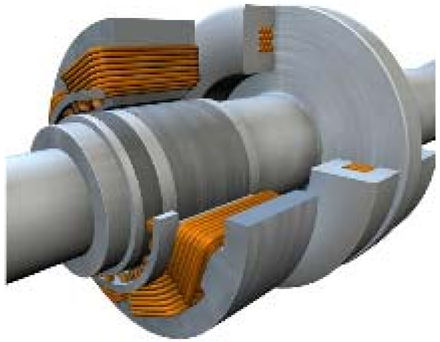

Questions?

Precise Tracking Control of TAMB System—Using TSMC

- How to calculate t_s?
  - After the terminal sliding surface is reached, the equality $\dot{e}(t) = -\lambda e(t)^{\frac{q}{p}}$ holds. Thereafter,

$$\frac{de(t)}{dt} = -\lambda e(t)^{\frac{q}{p}} \Rightarrow \frac{dt}{de(t)} = -\frac{1}{\lambda} e(t)^{-\frac{q}{p}}$$

$$dt = -\frac{1}{\lambda} e(t)^{-\frac{q}{p}} de(t) \Rightarrow \int dt = -\frac{1}{\lambda} \int e(t)^{-\frac{q}{p}} de(t)$$

$$t_s = -\frac{1}{\lambda} \int_{e(t_r)}^{0} e(t)^{-\frac{q}{p}} de = -\frac{1}{\lambda} \left[\frac{1}{1-\frac{q}{p}} e(t)^{1-\frac{q}{p}} \right]_{e(t_r)}^{0}$$

$$= -\frac{1}{\lambda} \left[0 - \frac{1}{1-\frac{q}{p}} e(t_r)^{1-\frac{q}{p}} \right] = -\frac{1}{\lambda} \left[\frac{-1}{\frac{p-q}{p}} e(t_r)^{1-\frac{q}{p}} \right] = \frac{p}{\lambda(p-q)} e(t_r)^{1-\frac{q}{p}}$$